Nonlinear X-ray-Matter interaction with X-ray Lasers

Andreas Scherz
European XFEL

Summary

Part 1 (Tuesday)

- Spectroscopy and Microscopy
- XFEL and SASE radiation
- Stimulated emission
- nonlinear response at x-ray energies

Part 2 (Wednesday)

- Nonlinear absorption
- Three-wave mixing
- Four-wave mixing

SPECTROSCOPY AND MICROSCOPY

Resonant vs non-resonant x-ray processes

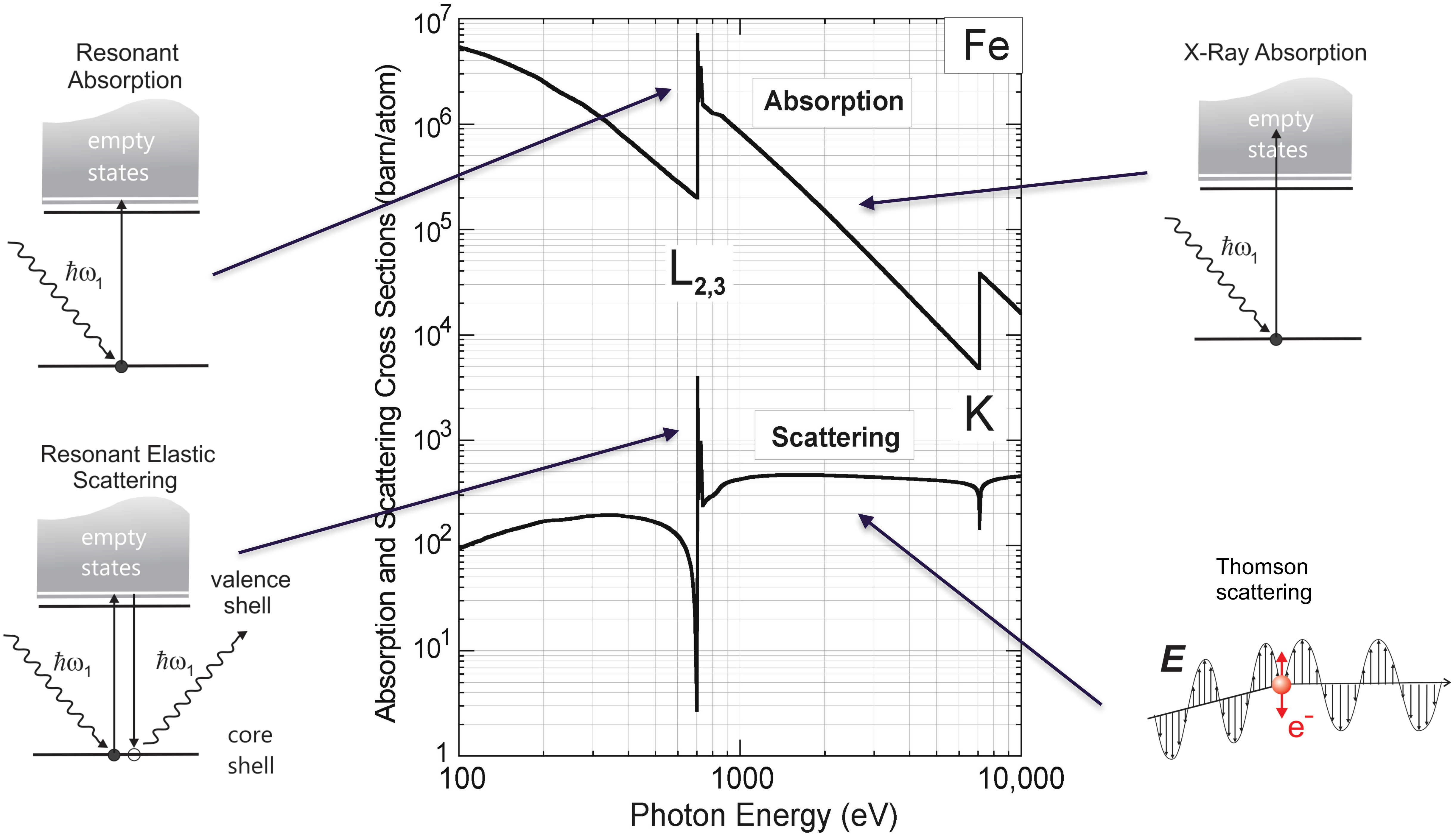

Resonant processes changes cross sections by orders of magnitude

Courtesy J. Stöhr

Transition rates of resonant X-ray Processes

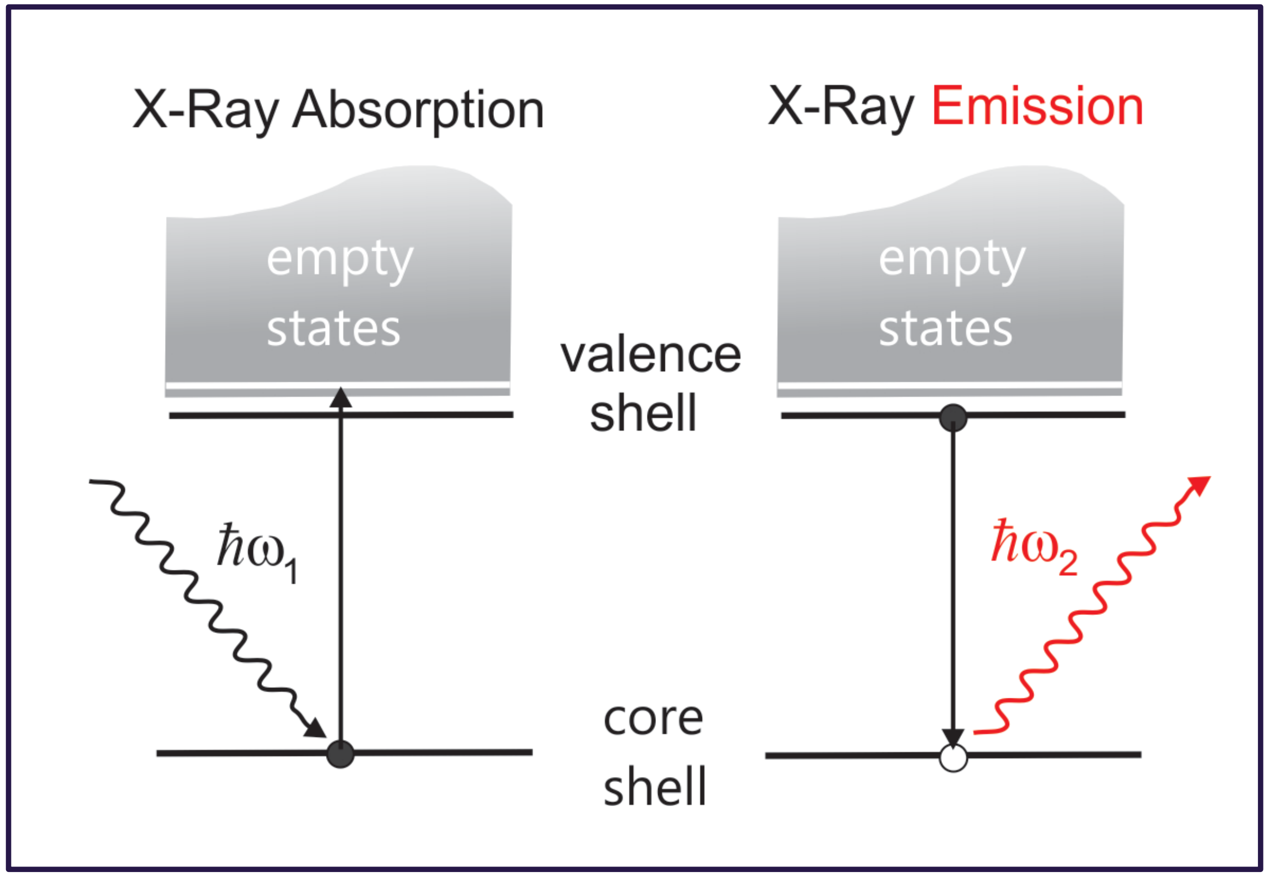

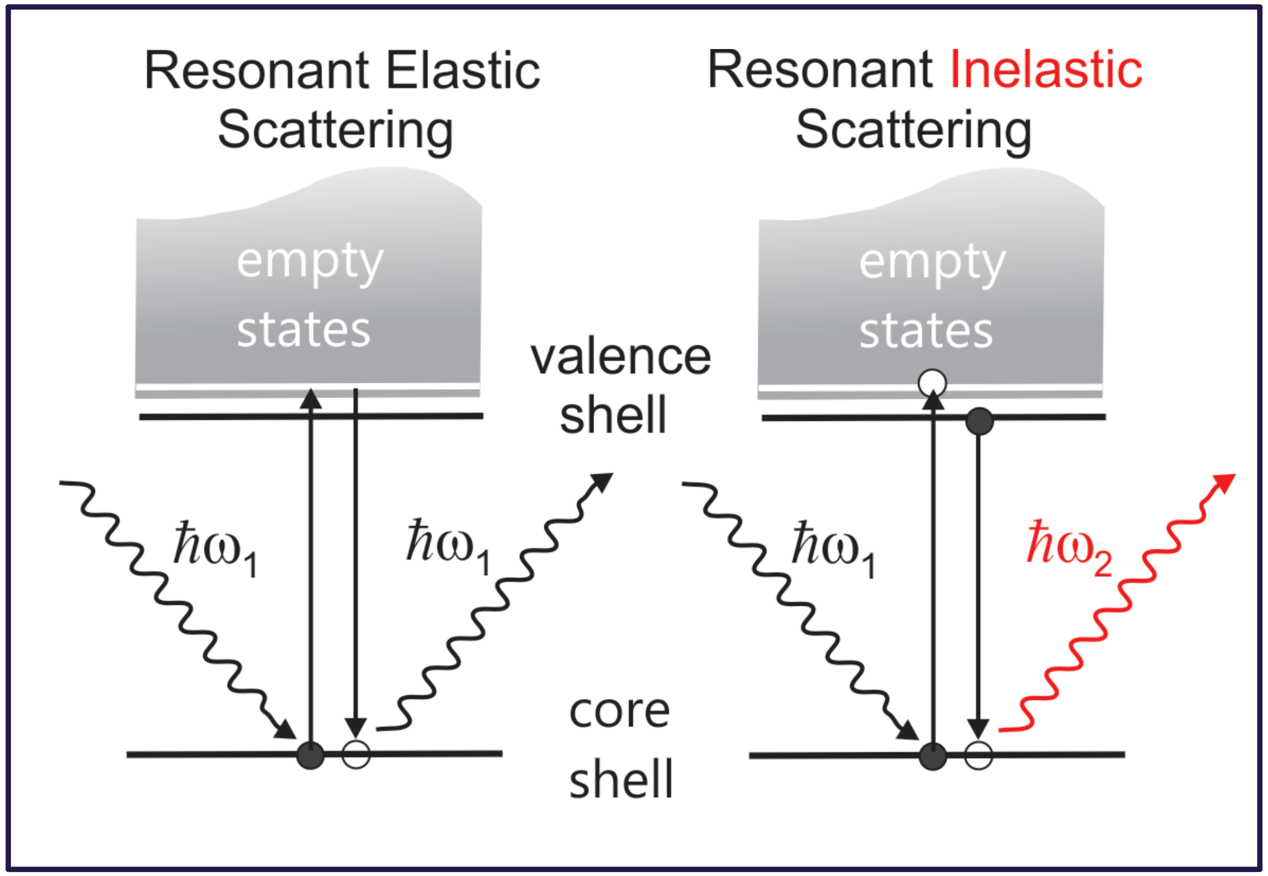

Transition rates of resonant X-ray Processes

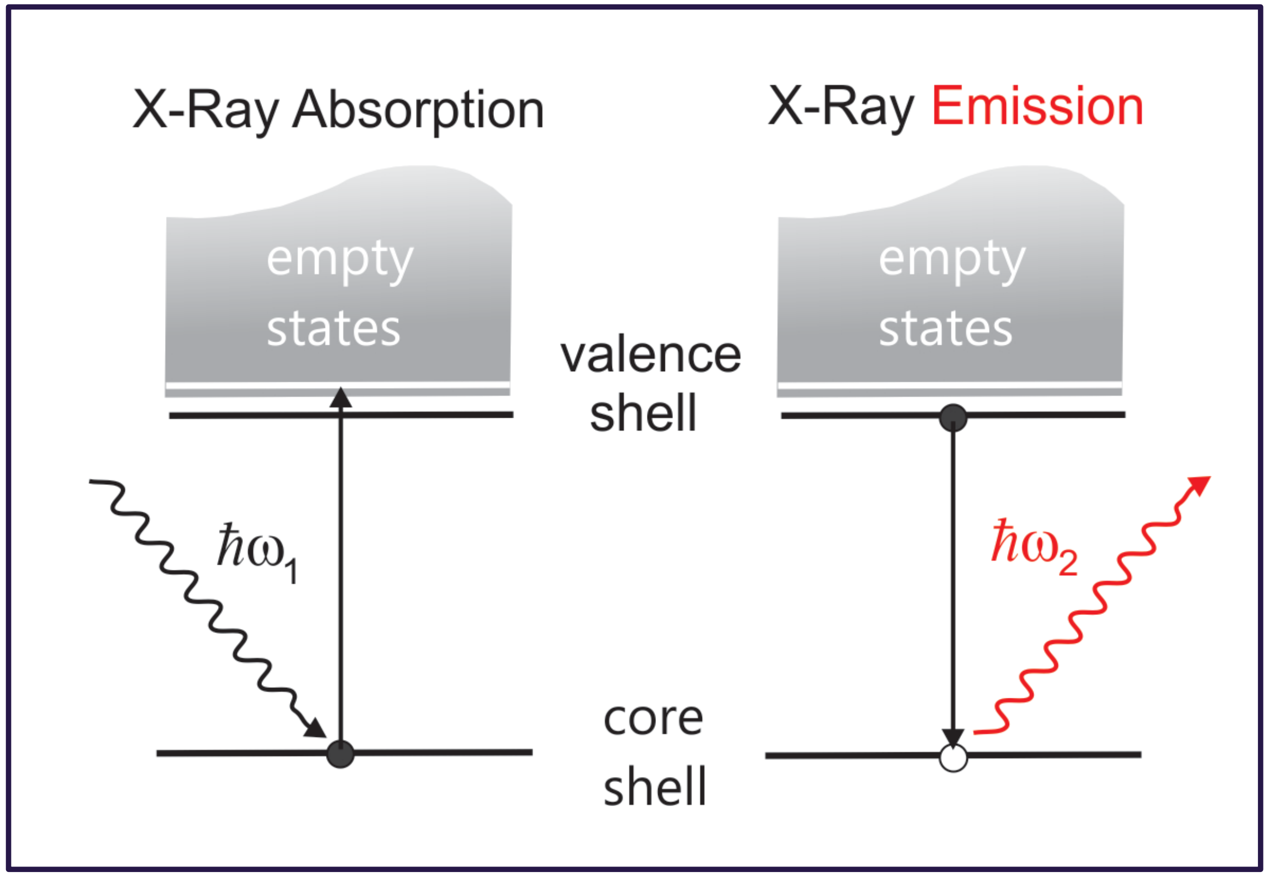

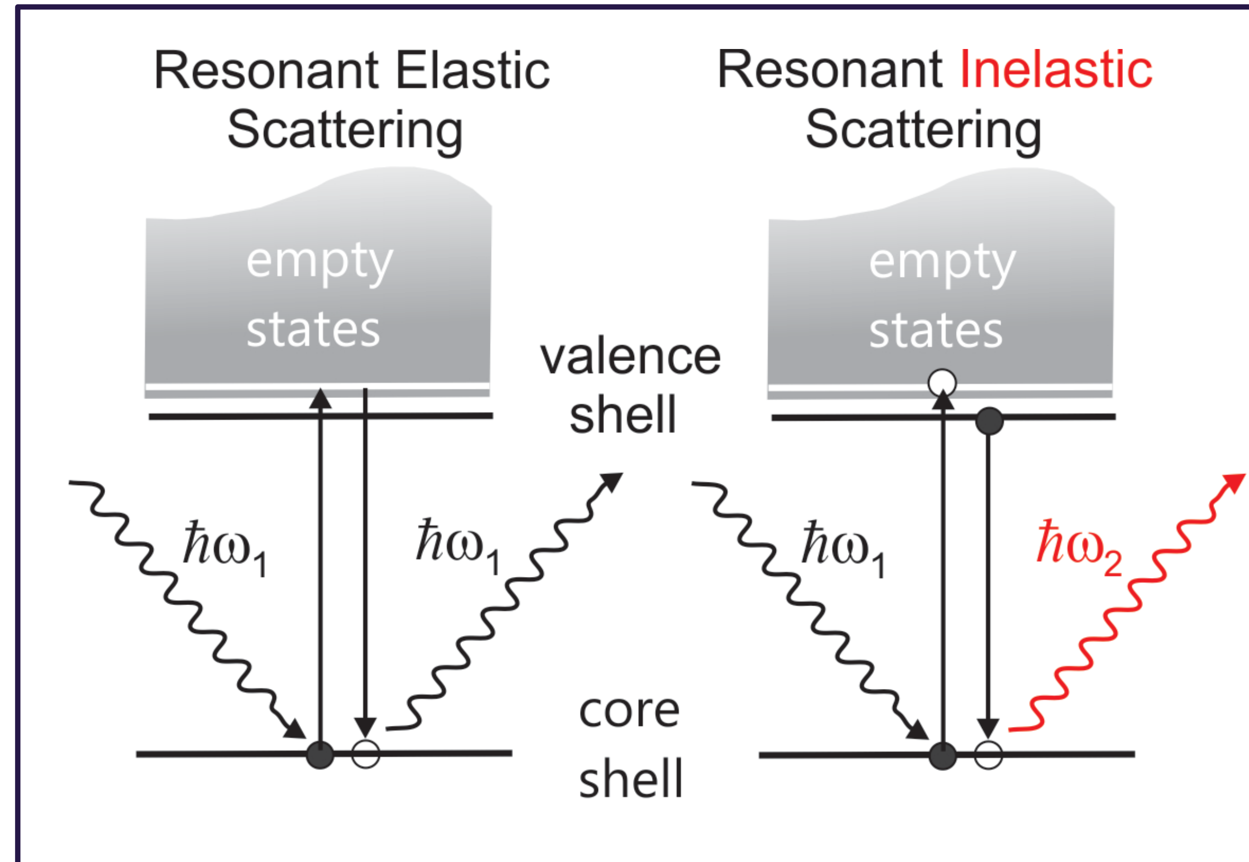

$$\mathcal{H}_{\rm int} = \frac{e}{m_{\rm e}} \boldsymbol{p} \cdot \boldsymbol{A}(\boldsymbol{r},t) = -e\,\boldsymbol{r} \cdot \boldsymbol{E}(\boldsymbol{r},t)$$

$$T_{if} = \frac{2\pi}{\hbar} \left| \langle f|\mathcal{H}_{int}|i\rangle + \sum_j \frac{\langle f|\mathcal{H}_{int}|j\rangle\langle j|\mathcal{H}_{int}|i\rangle}{\varepsilon_i - \varepsilon_j} \right|^2 \delta(\varepsilon_i - \varepsilon_f)\ \rho(\varepsilon_f)$$

Fermi's Golden rule

Kramers - Heisenberg

Measurement of resonant X-ray Processes

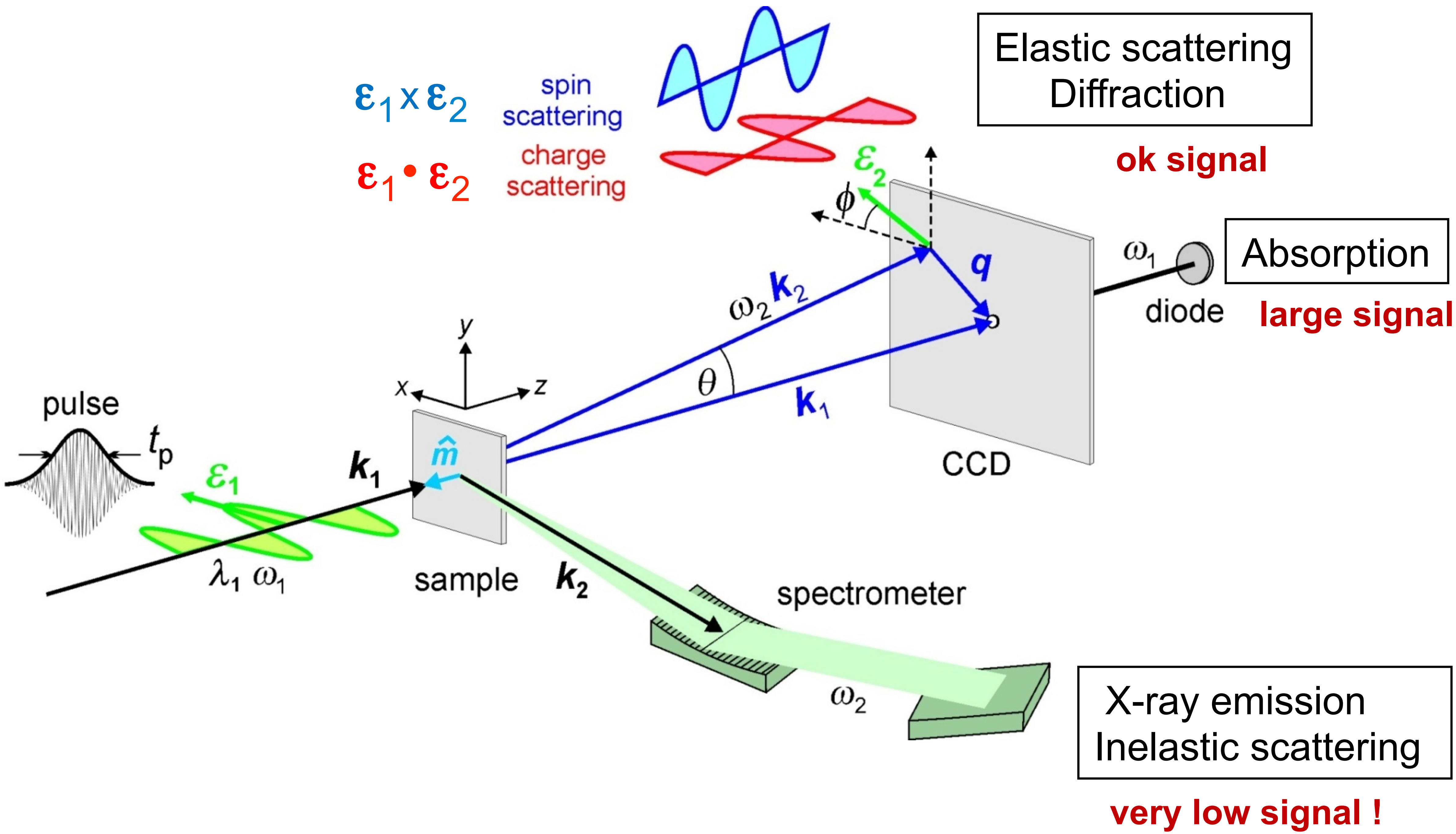

Courtesy J. Stöhr

X-ray Spectro-Microscopy

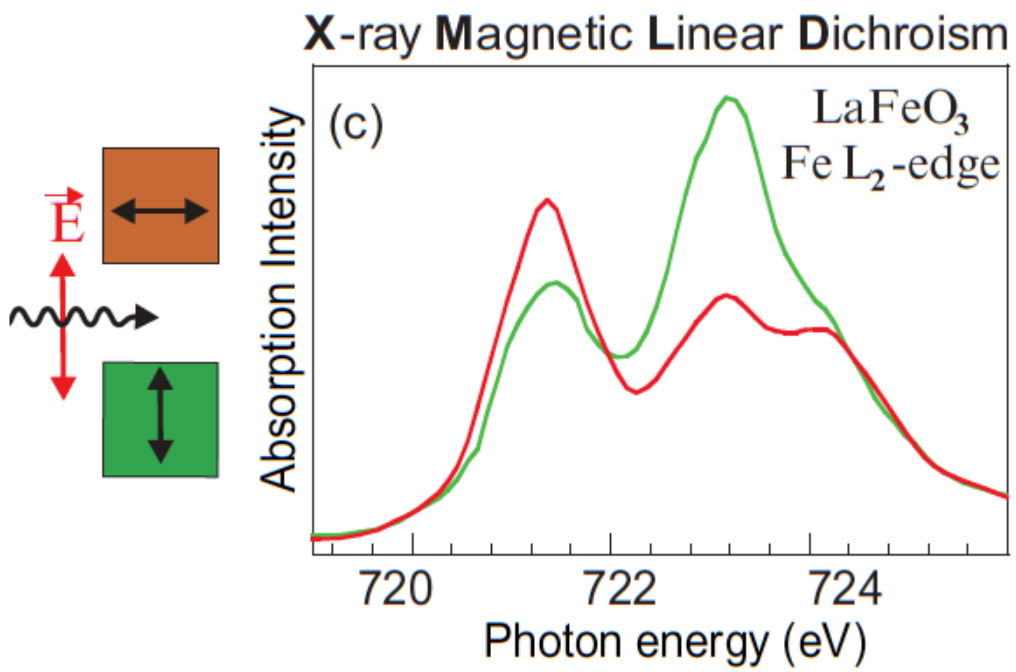

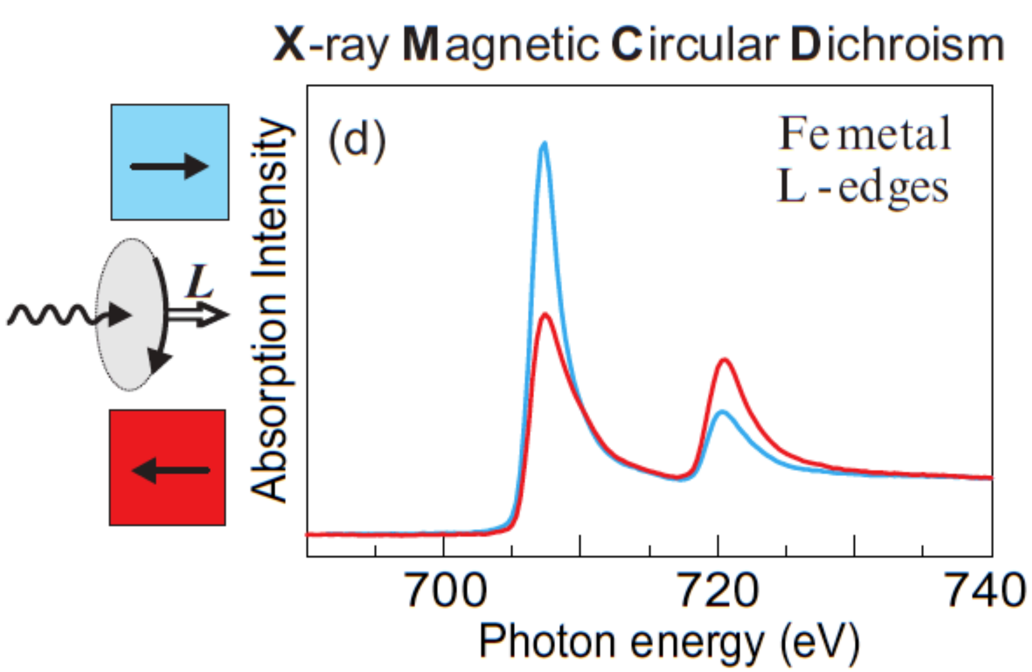

- X-ray tunability: elemental and chemical specificity
- X-ray polarization XMCD, XMLD
- Buried Structures

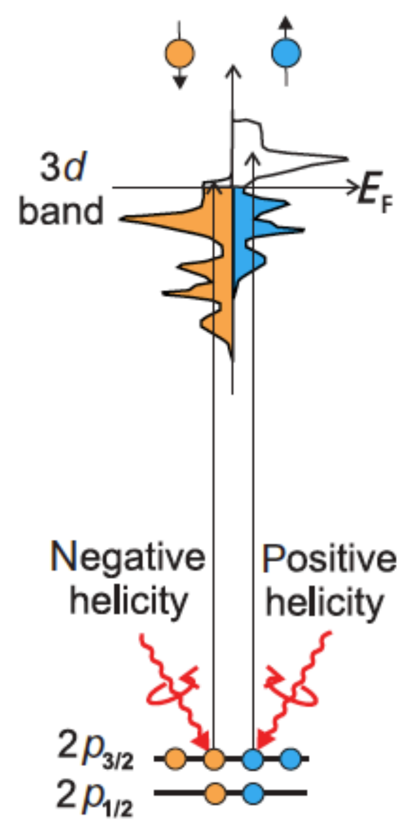

X-ray view of Exchange Bias

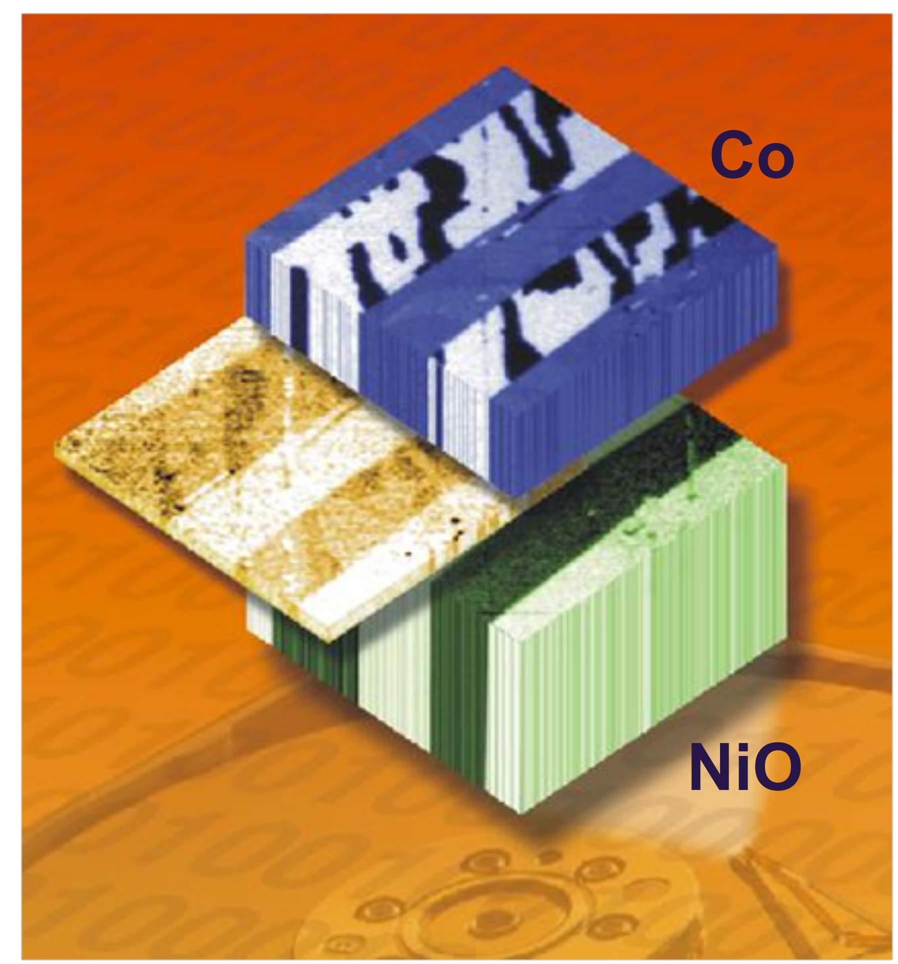

Ohldag, et al., PRL 86, 2878 (2001).

X-ray Spectro-Microscopy

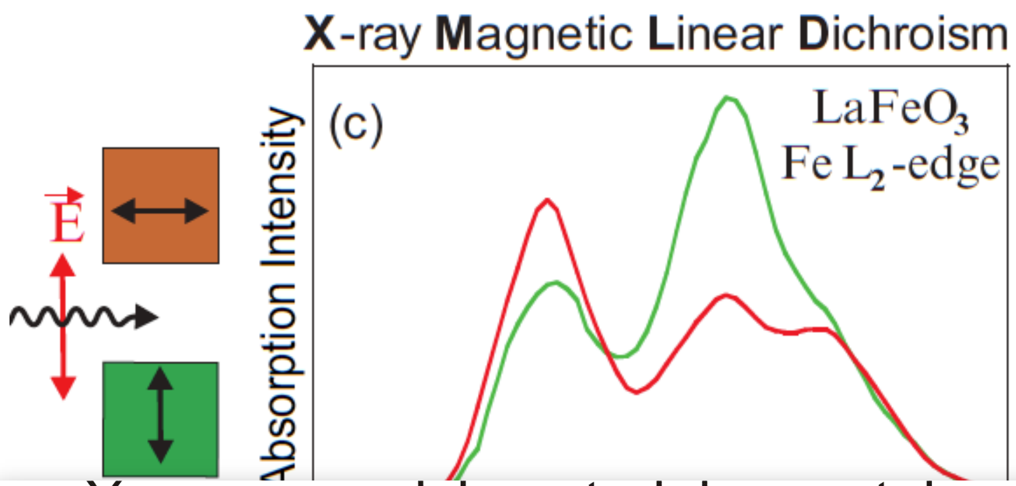

- X-ray tunability: elemental and chemical specificity
- X-ray polarization XMCD, XMLD
- Buried Structures

X-rays can pick materials apart: layer-by-layer

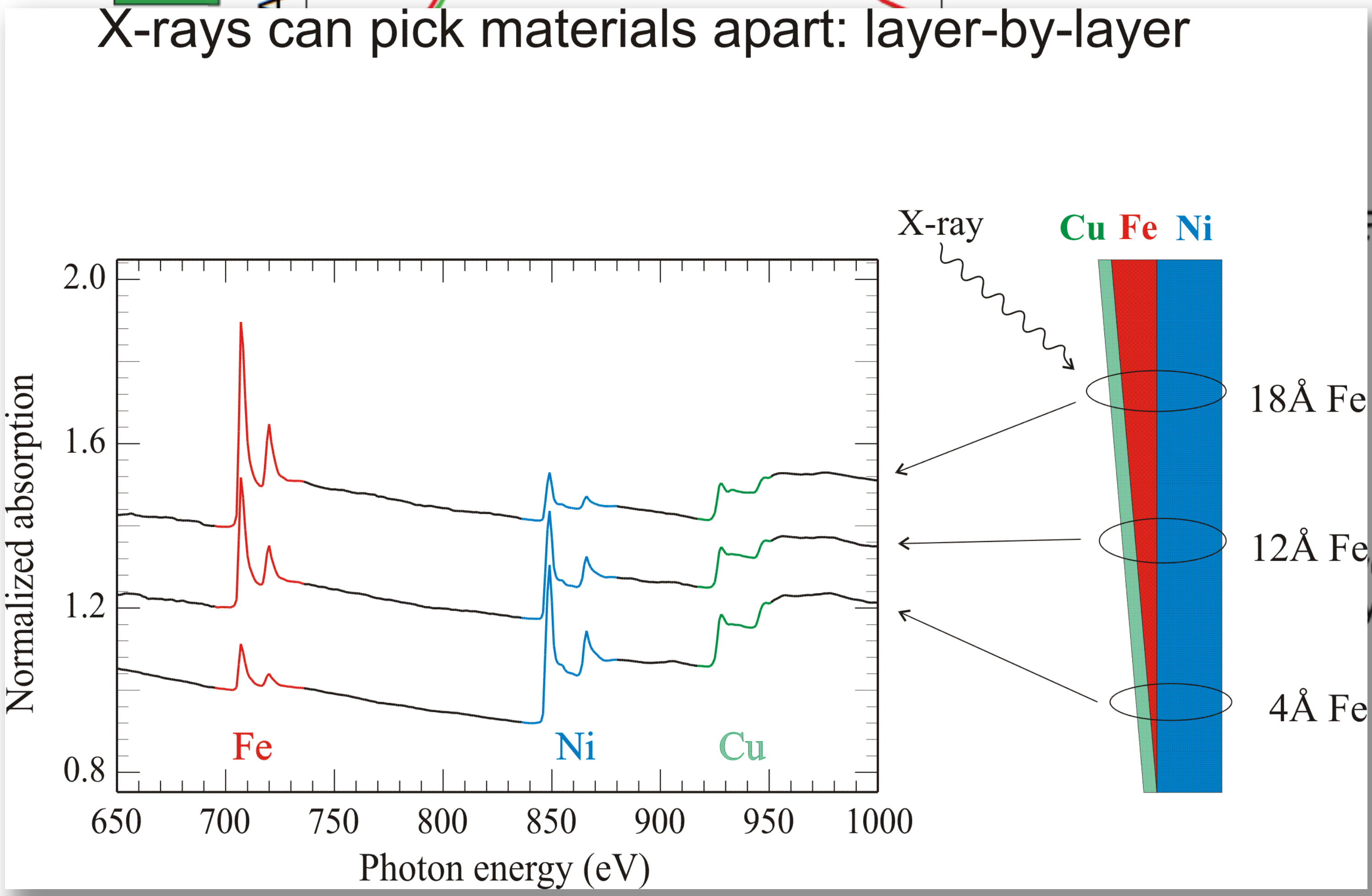

X-ray view of Exchange Bias

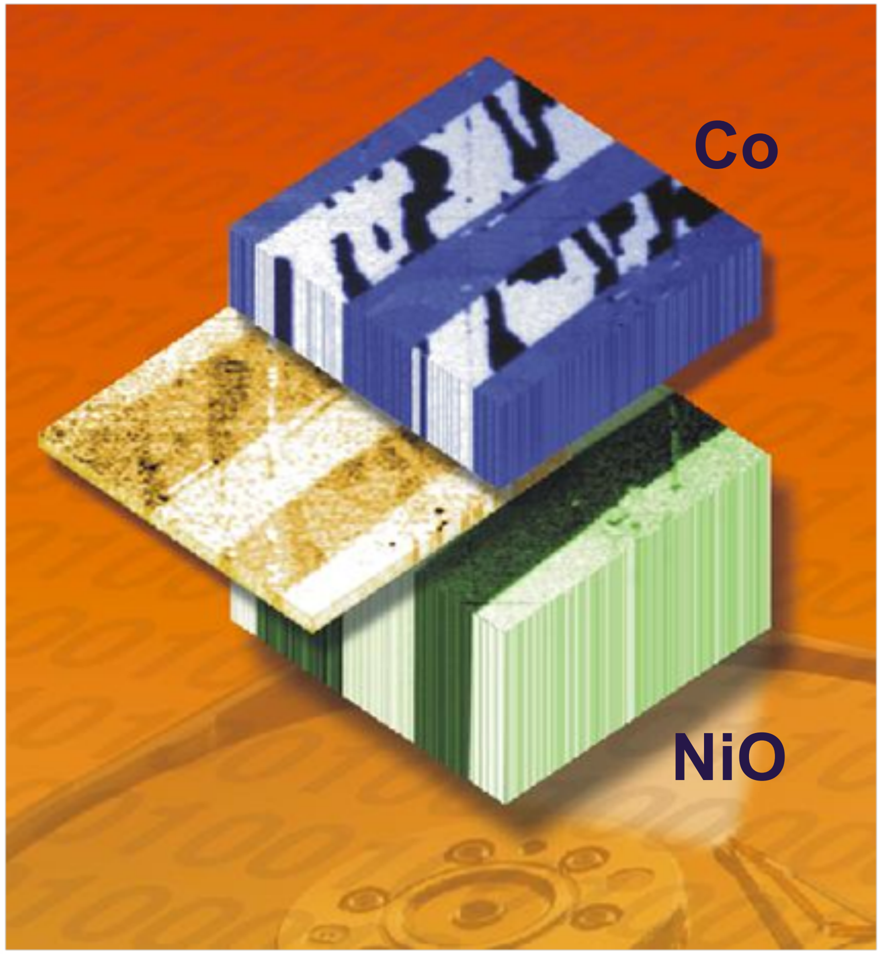

Ohldag, et al., PRL 86, 2878 (2001).

Tuning to absorption resonances

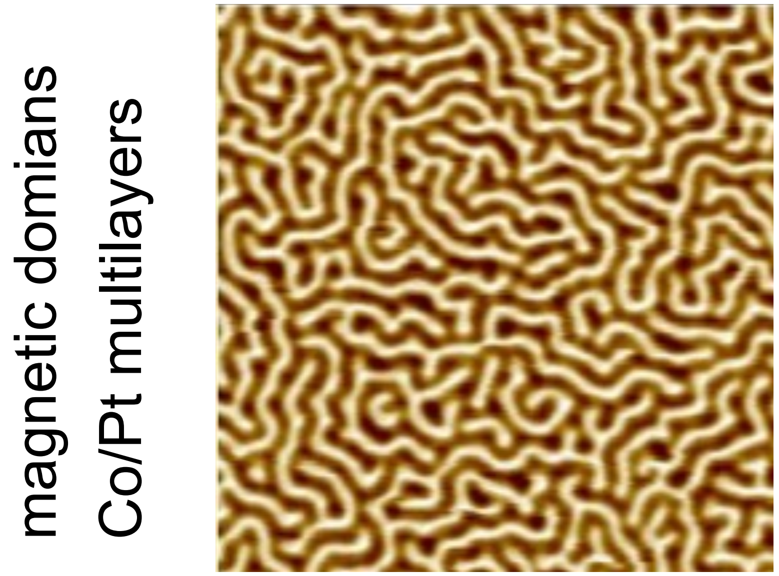

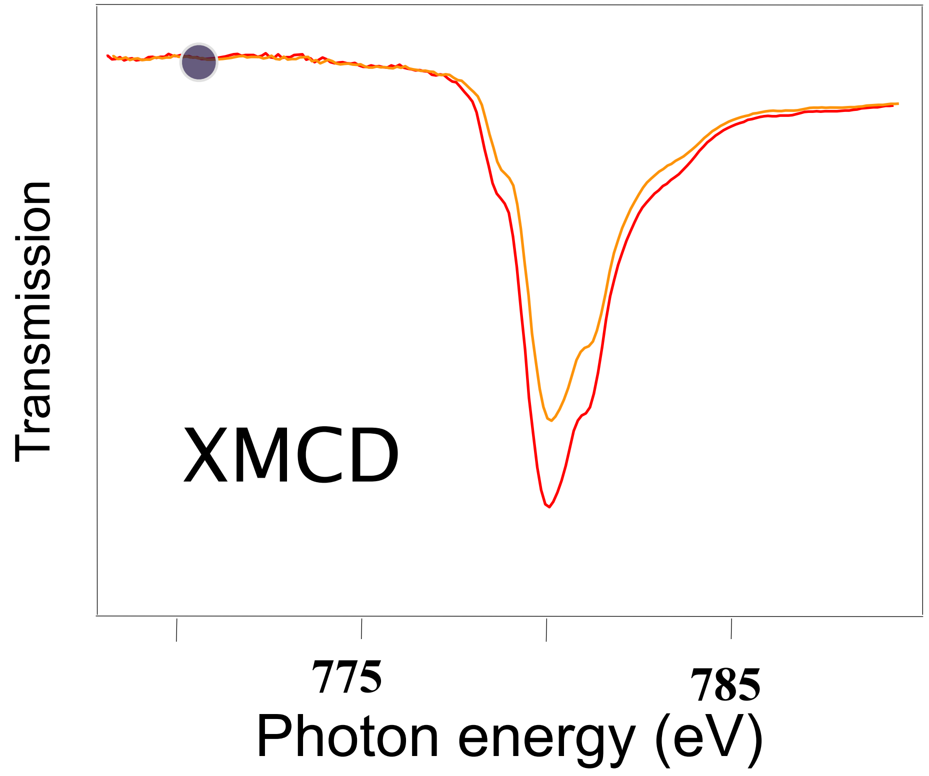

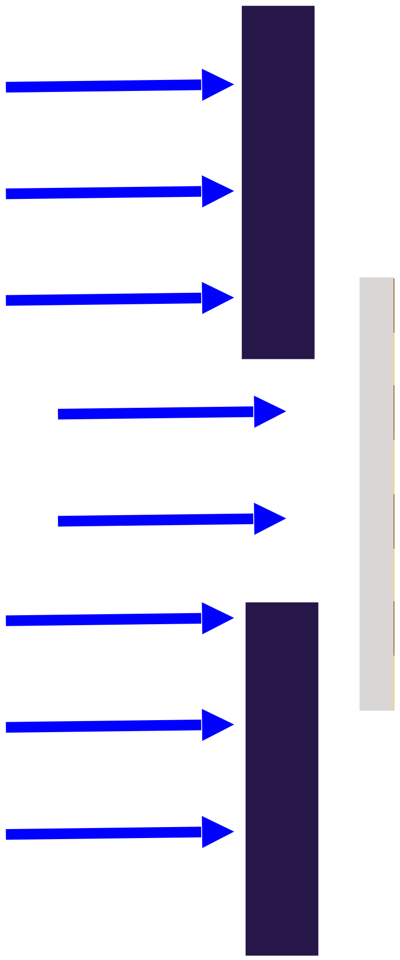

Non-Resonant

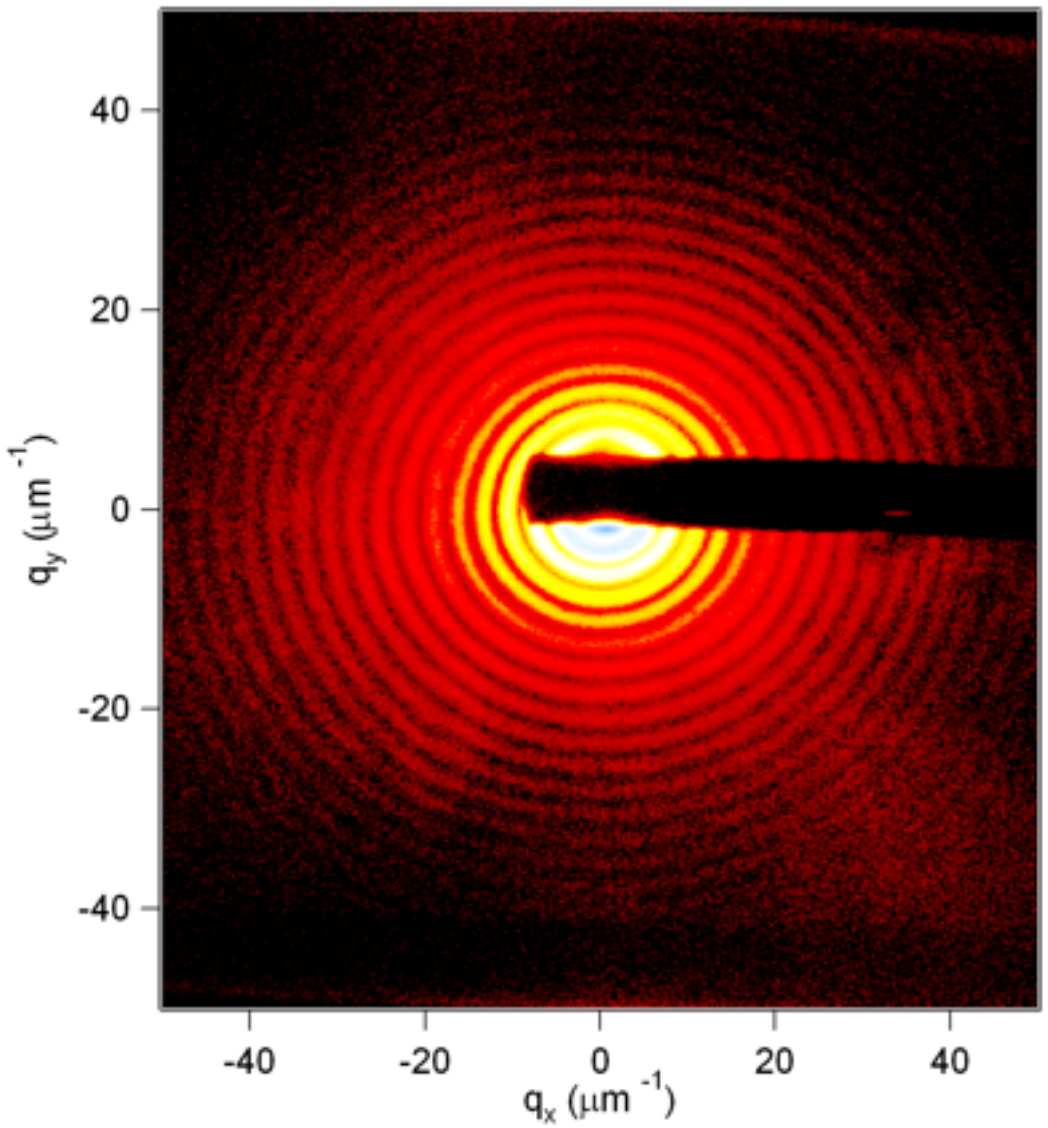

Tuning to absorption resonances

magnetic domians
Co/Pt multilayers

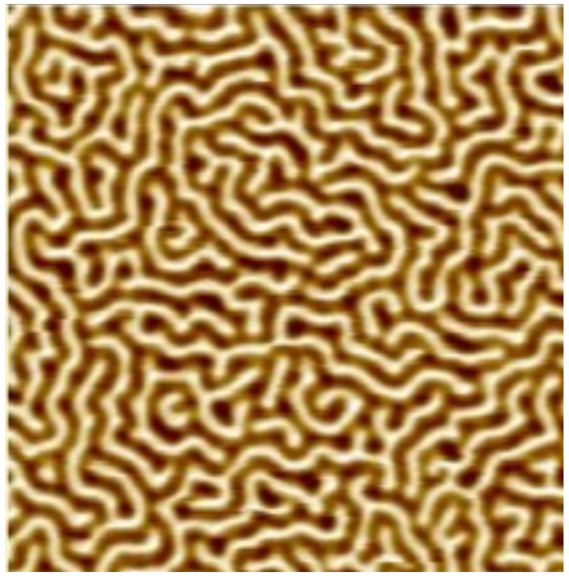

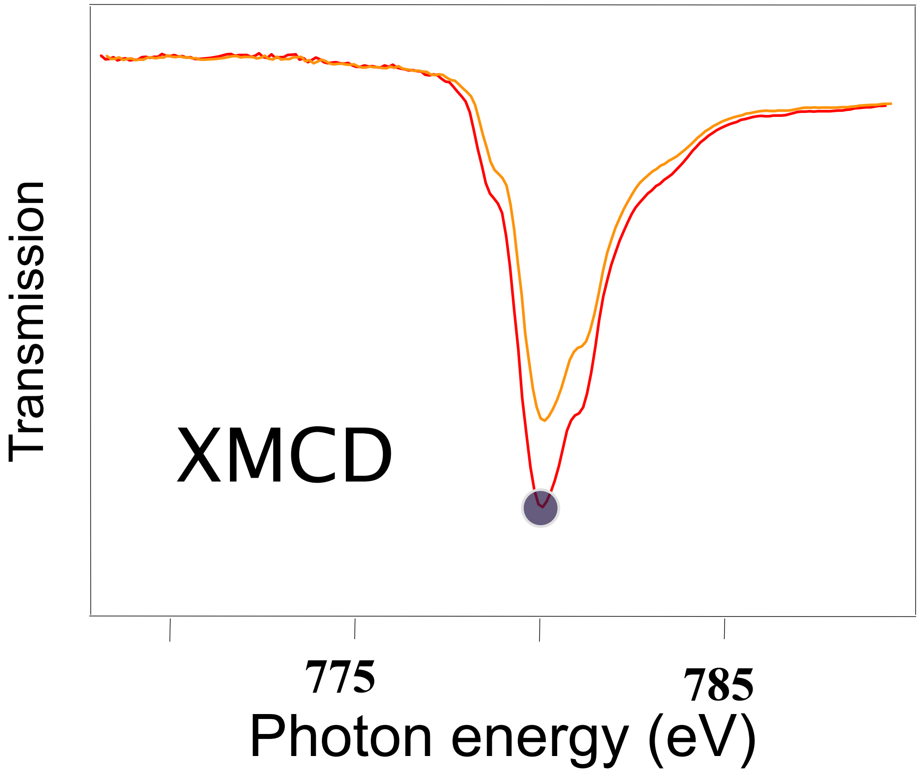

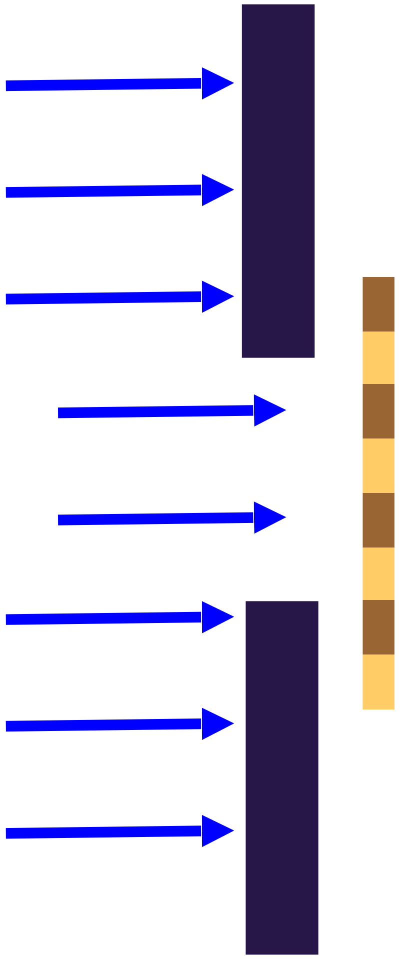

Resonant

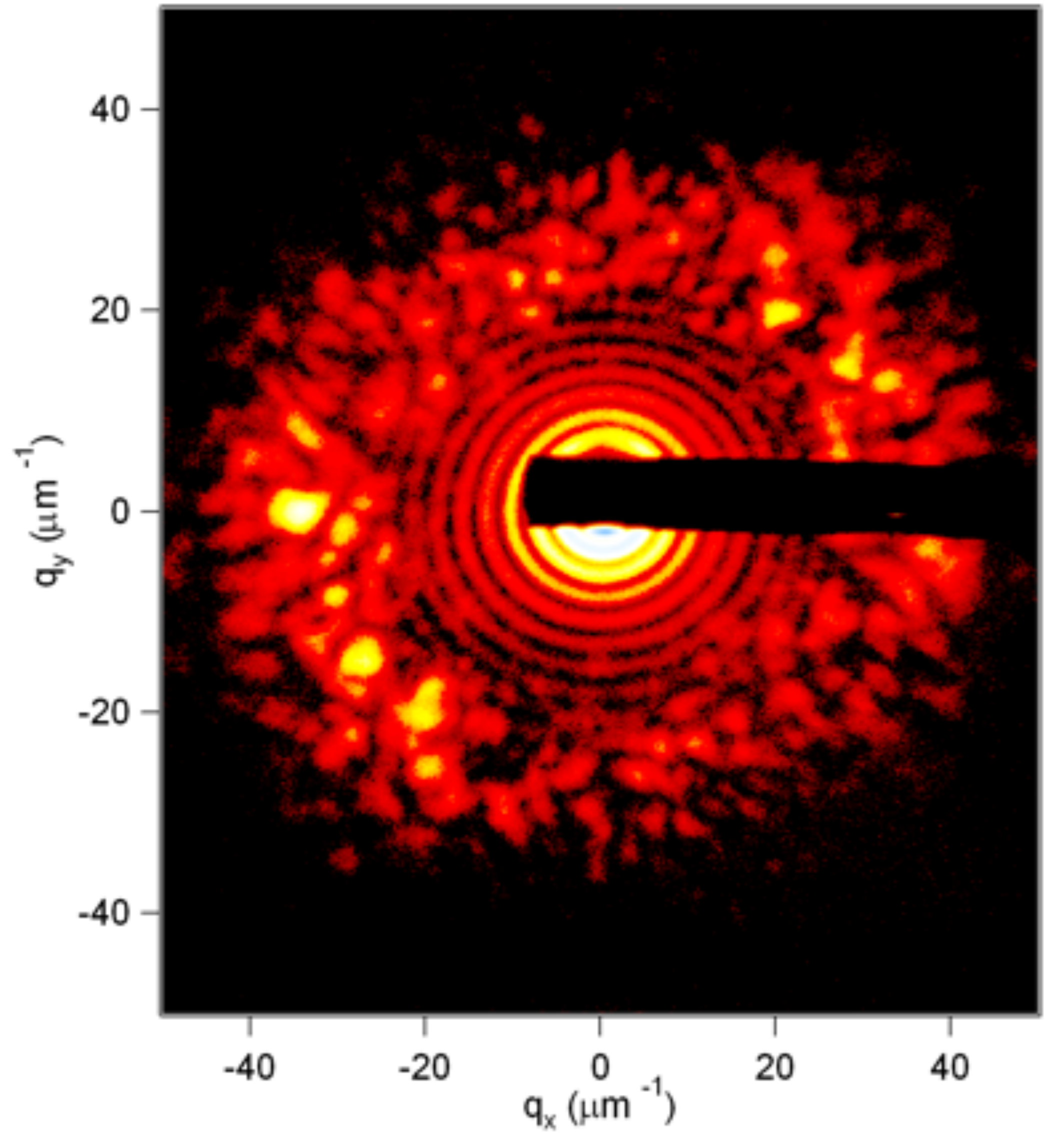

Fourier Transform Spectro-Holography

FTH Recording

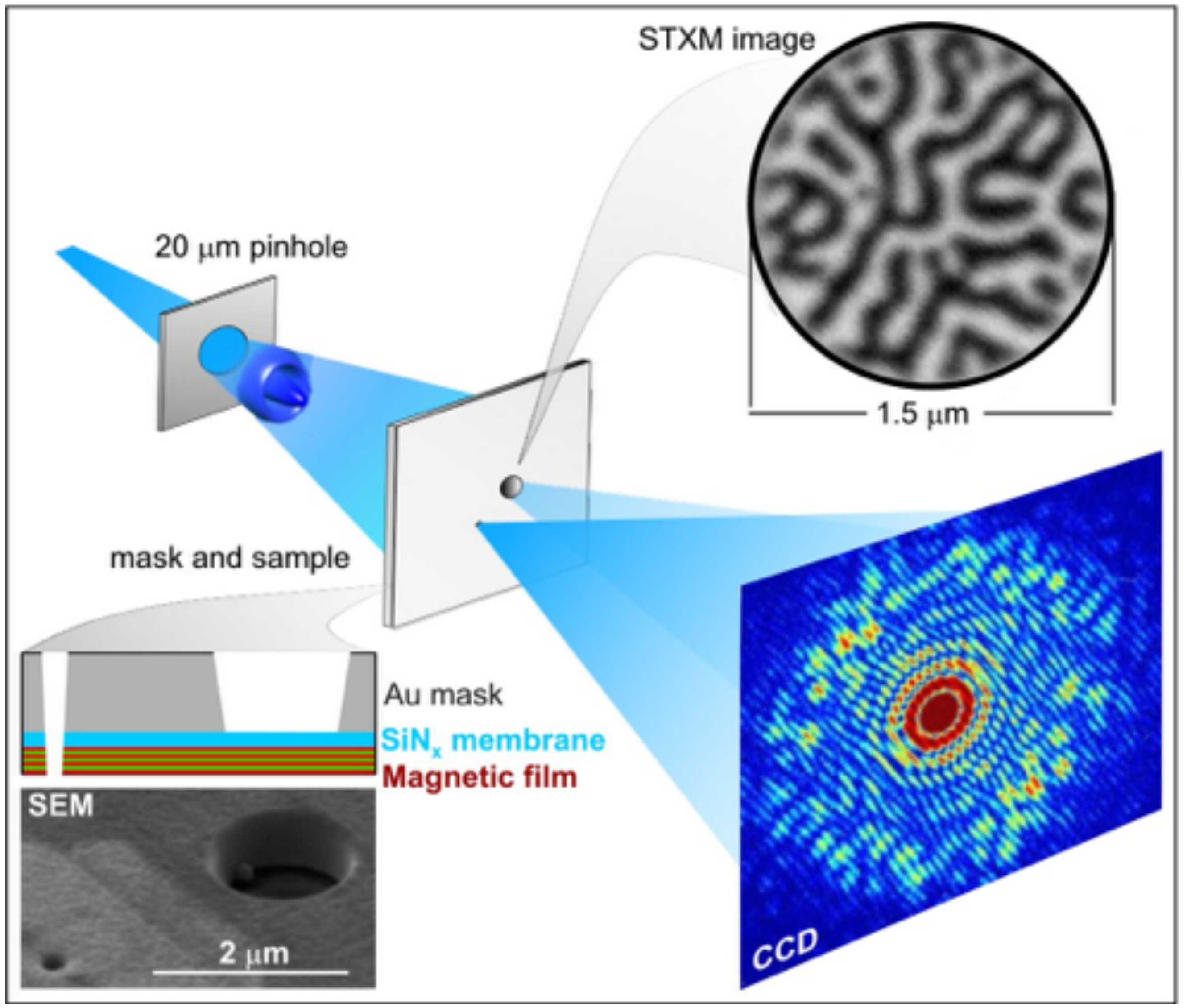

Eisebitt, Lüning, et al., Nature 432, 885 (2004).

- Using holographic mask
- exploiting XMCD to image magnetic domains
- resolution < 50nm

FTH Reconstruction

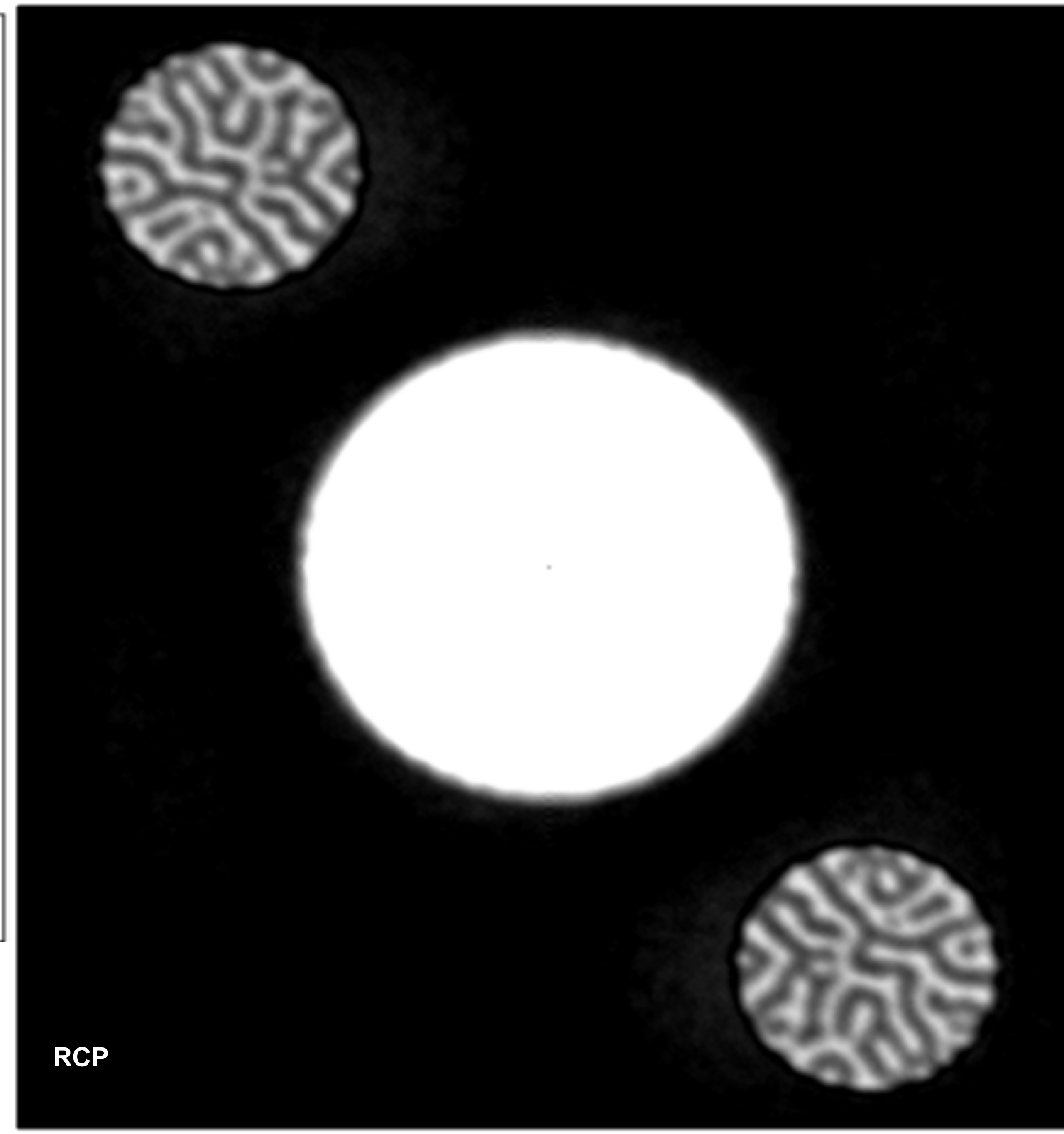

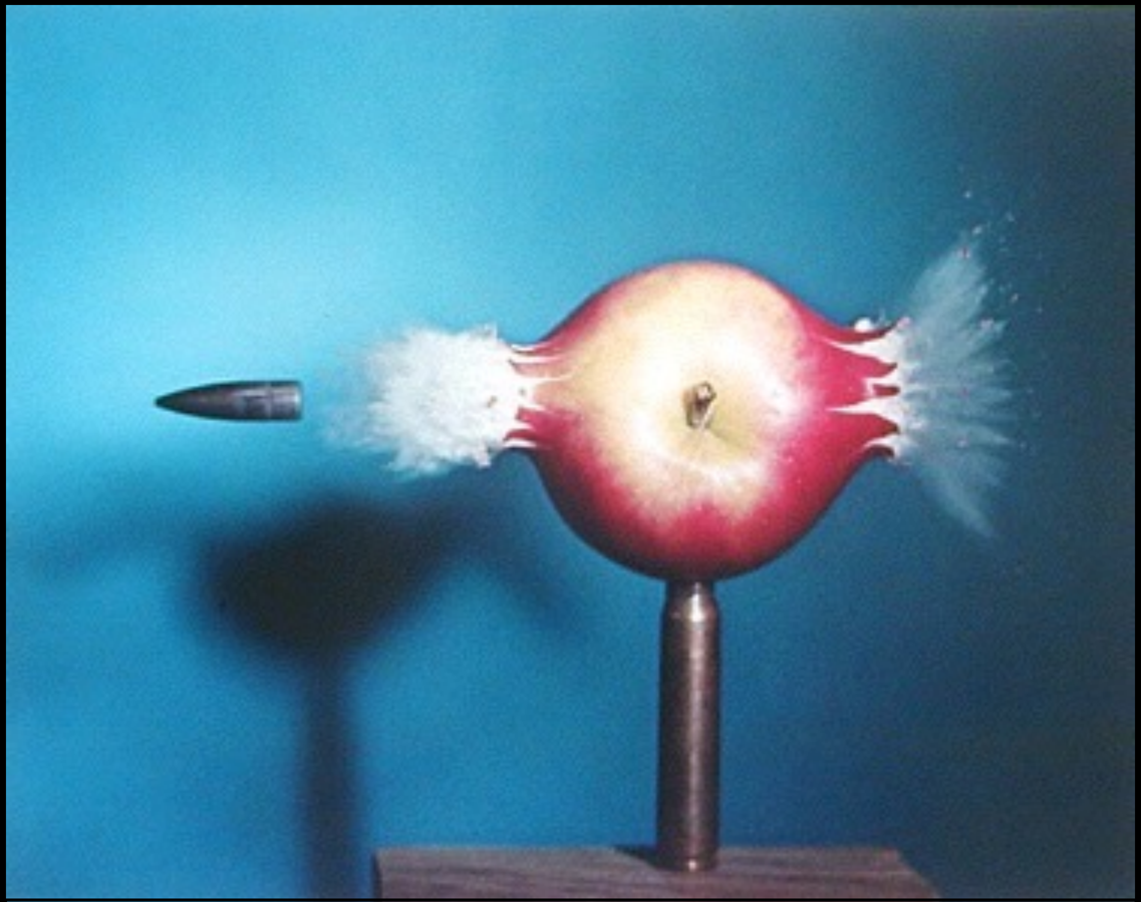

- Need a sufficient amount of photons
- Need them in a very short time
- *Nonperturbative*: Damage to the sample must occur after snap shot

XFEL and SASE radiation

X-ray Free-Electron Laser

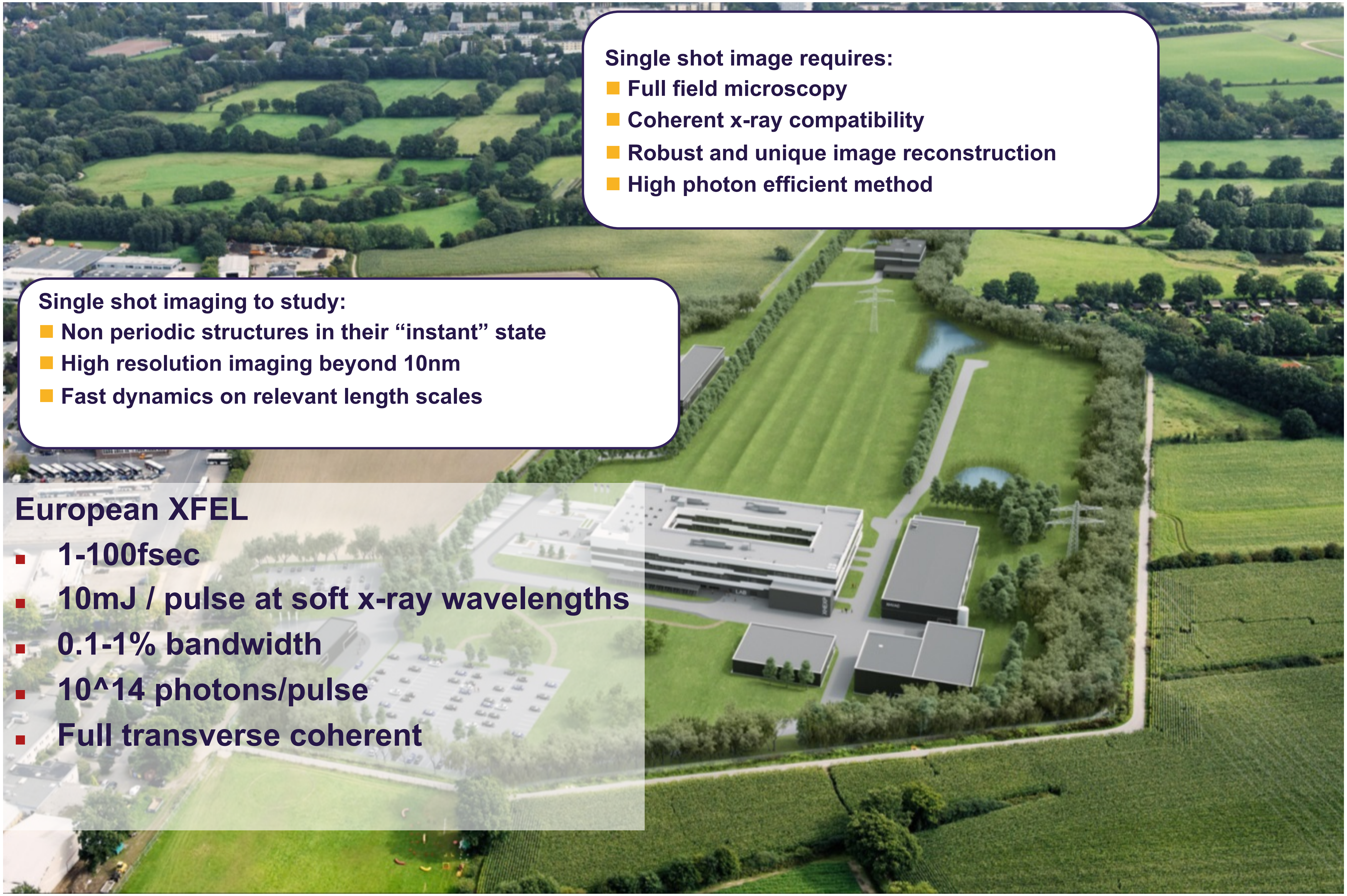

Single shot image requires:
- Full field microscopy
- Coherent x-ray compatibility
- Robust and unique image reconstruction
- High photon efficient method

Single shot imaging to study:
- Non periodic structures in their “instant” state
- High resolution imaging beyond 10nm
- Fast dynamics on relevant length scales

European XFEL
- 1-100fsec
- 10mJ / pulse at soft x-ray wavelengths
- 0.1-1% bandwidth
- 10^14 photons/pulse
- Full transverse coherent

Facility overview

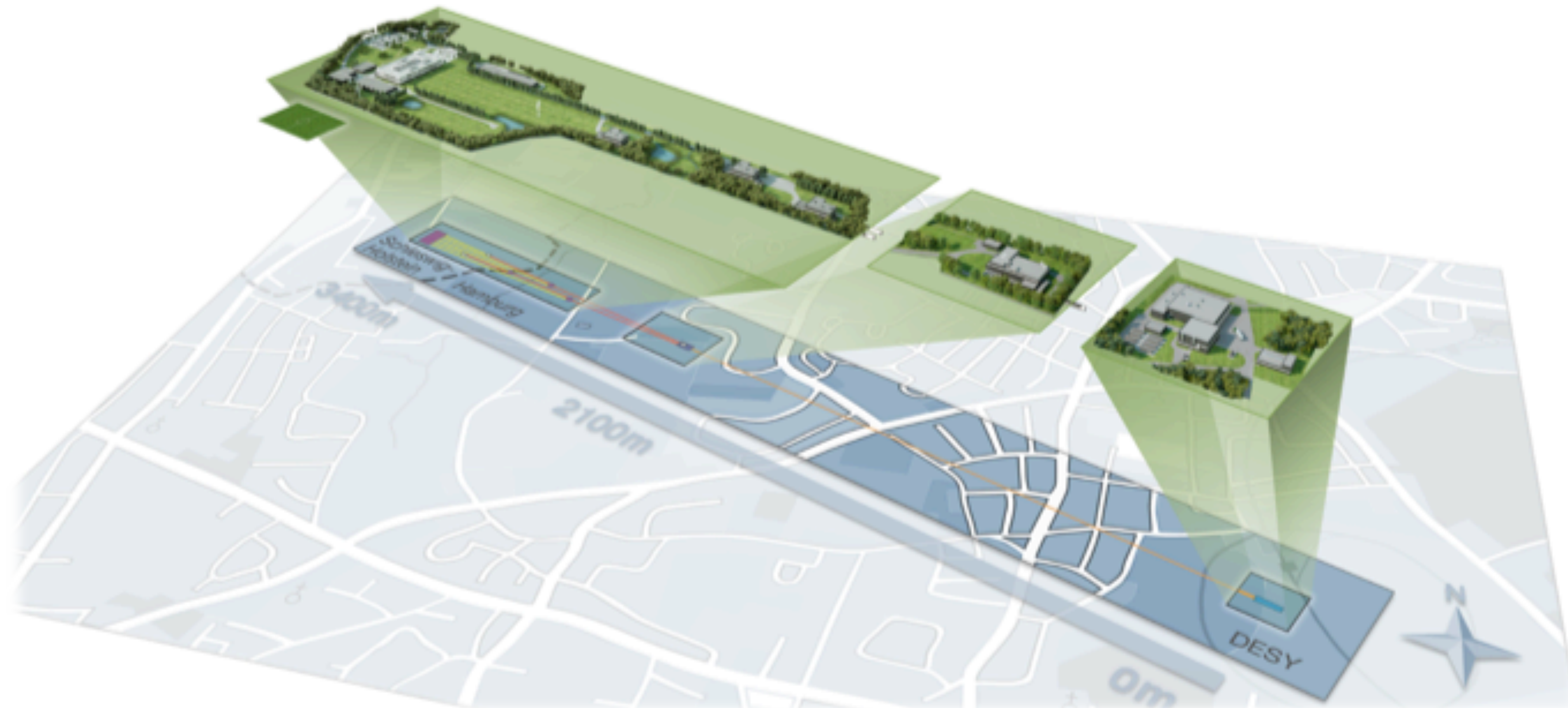

Facility overview

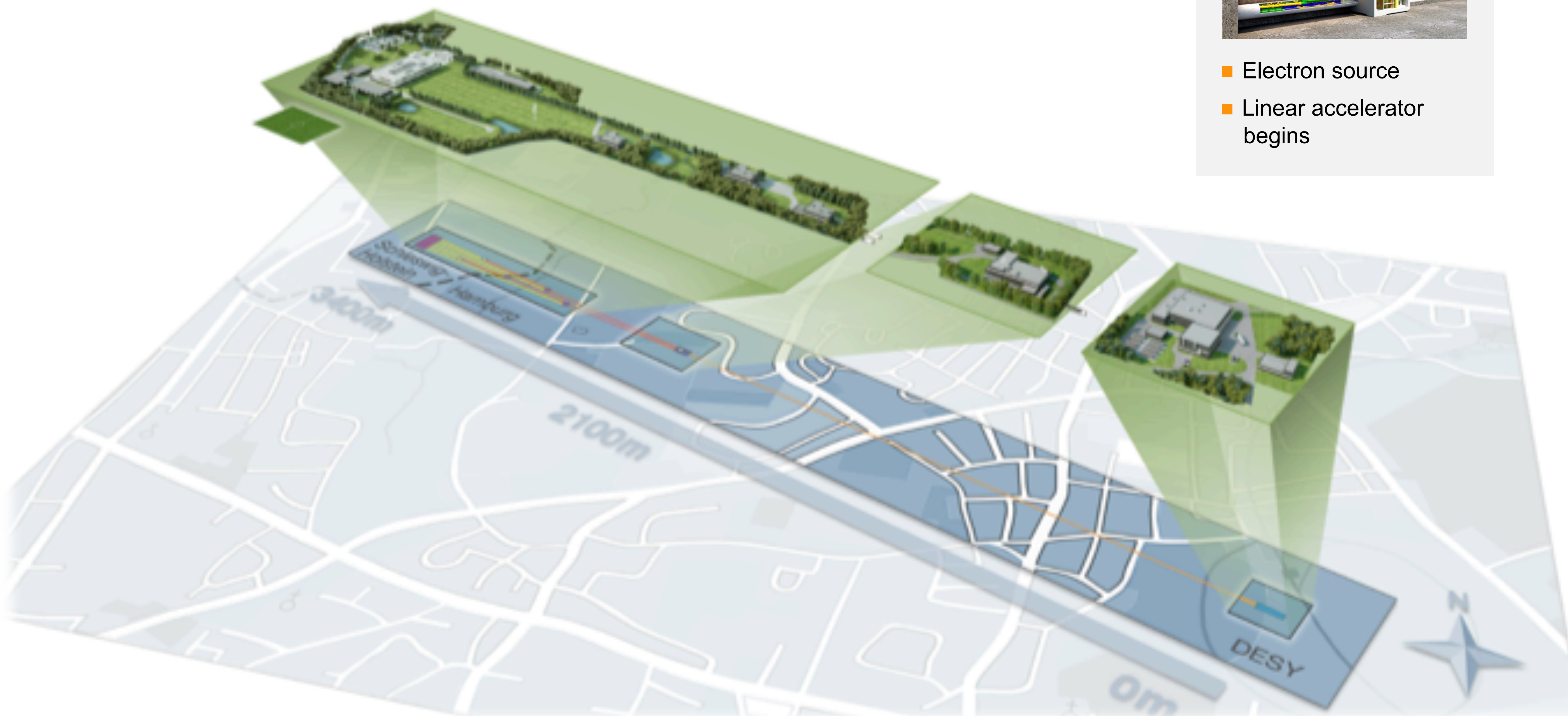

DESY-Bahrenfeld

- Electron source
- Linear accelerator begins

European XFEL

Facility overview

DESY-Bahrenfeld

- Electron source
- Linear accelerator begins

Superconducting electron accelerator

Facility overview

Osdorfer Born

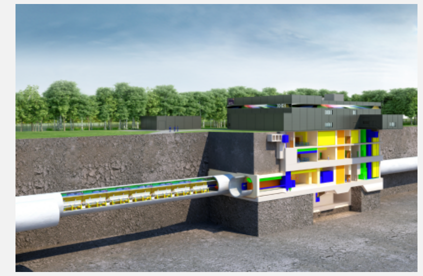

- Electron beam to photon beamlines
- Undulator systems begin

DESY-Bahrenfeld

- Electron source
- Linear accelerator begins

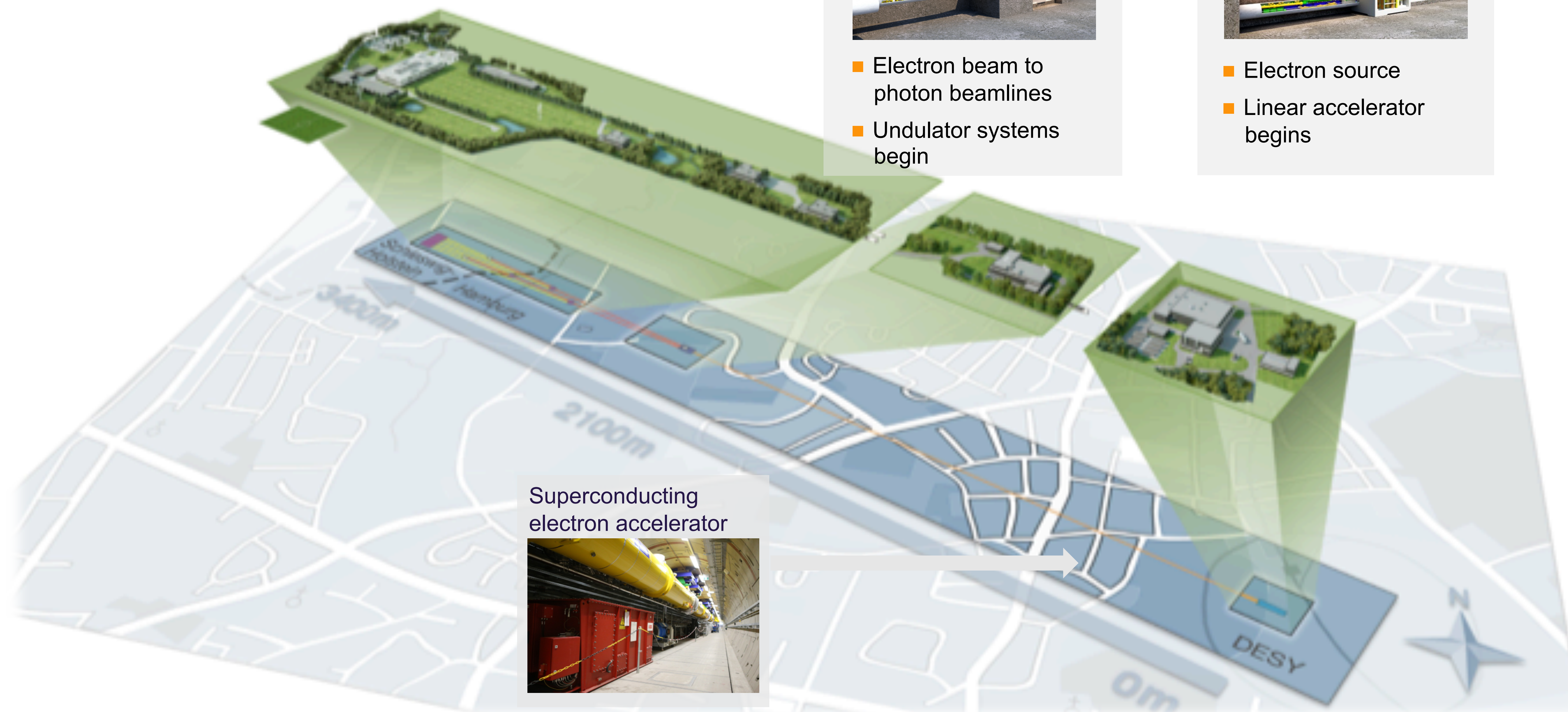

Superconducting electron accelerator

Facility overview

Schenefeld

- Experiment hall
- Laboratories
- Offices

Osdorfer Born

- Electron beam to photon beamlines
- Undulator systems begin

DESY-Bahrenfeld

- Electron source
- Linear accelerator begins

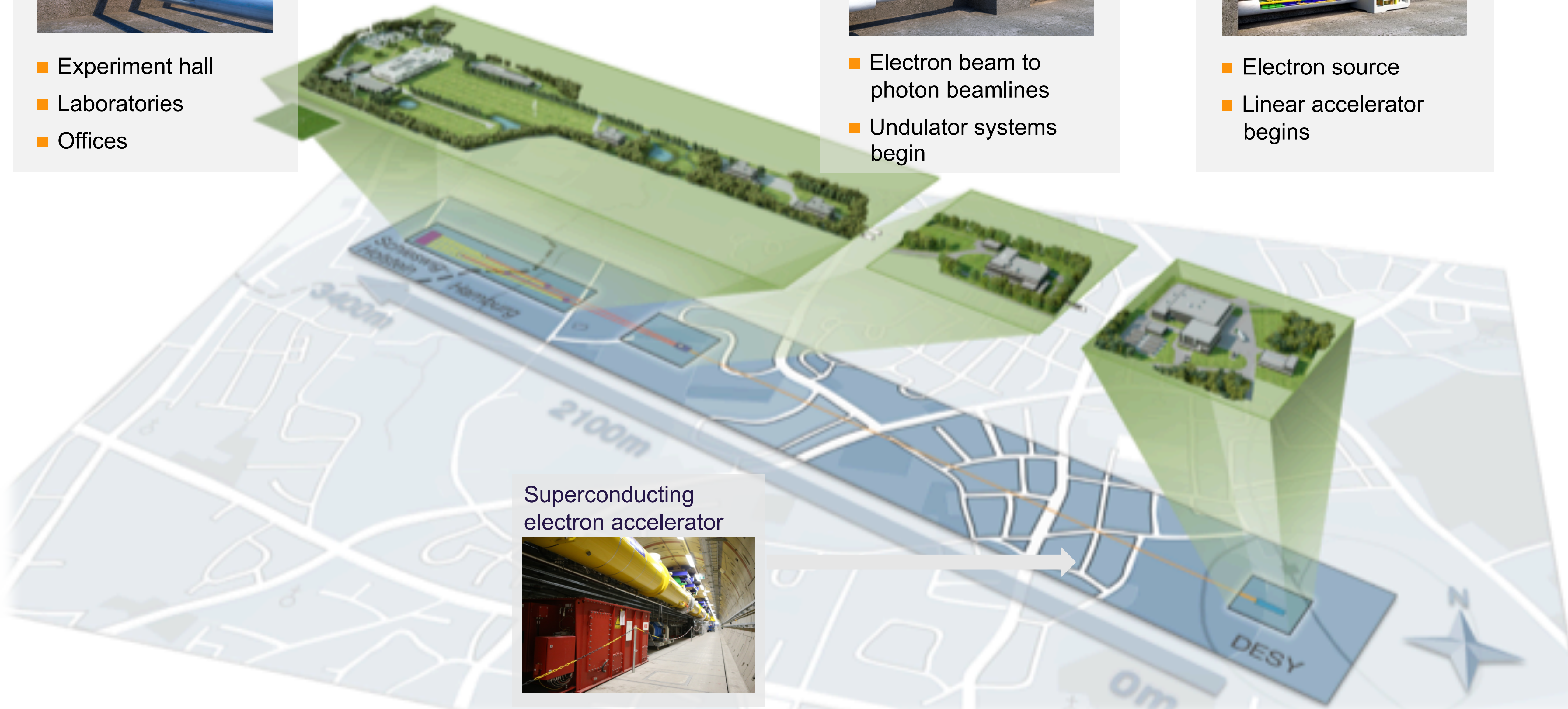

Superconducting electron accelerator

Optical beam transport and instruments

Undulator Segment	FEL radiation energy [keV]	Wavelength [nm]
SASE 1	3 - over 24	0.4 - 0.05
SASE 2	3 - over 24	0.4 - 0.05
SASE 3	0.27 - 3	4.6 – 0.4

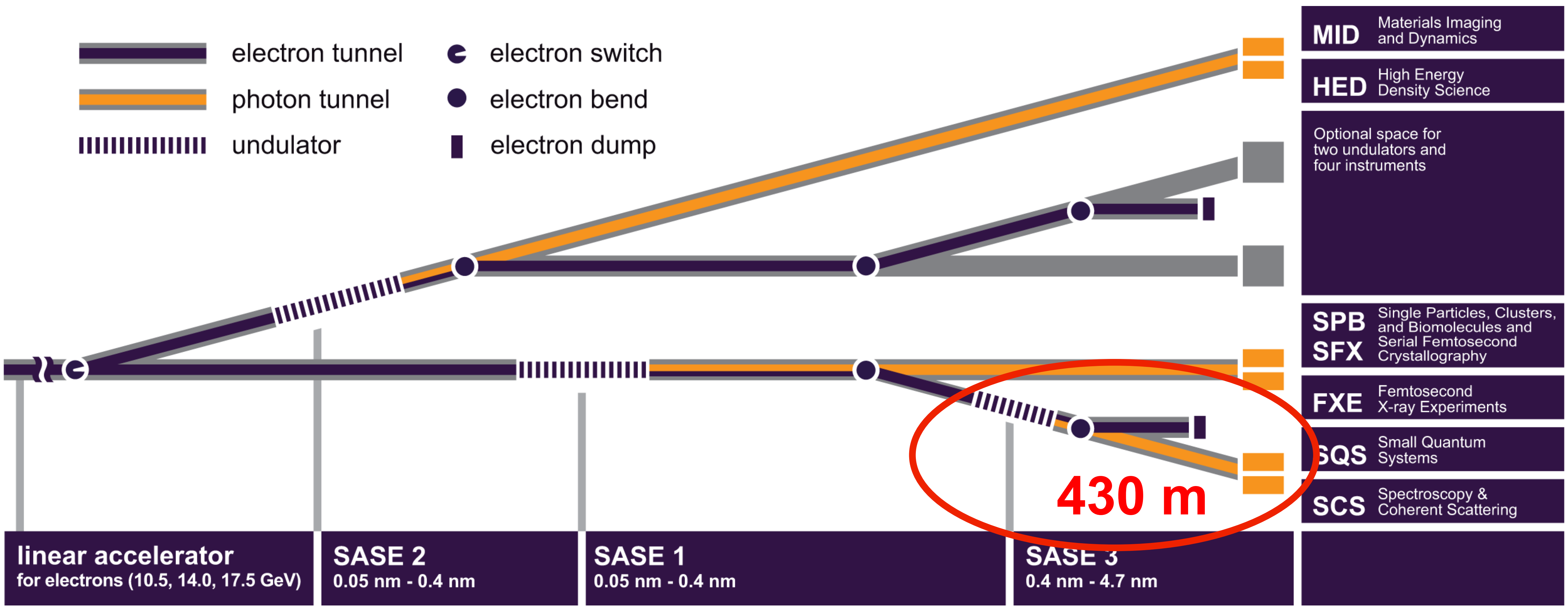

Orange color: X-ray optics & Beam Transport

Scientific Instruments

Hard X-rays

SPB/SFX: Single Particles, Clusters, and Biomolecules and Serial Femtosecond Crystallography

- Will determine the structure of single particles, such as atomic clusters, viruses, and biomolecules

MID: Materials Imaging and Dynamics

- Will be able to image and analyze nano-sized devices and materials used in engineering

FXE: Femtosecond X-Ray Experiments

- Will investigate chemical reactions at the atomic scale in short time scales—molecular movies

HED: High Energy Density Physics

- Will look into some of the most extreme states of matter in the universe, such as the conditions at the center of planets

Soft X-rays

SQS: Small Quantum Systems

- Will examine the quantum mechanical properties of atoms and molecules.

SCS: Spectroscopy and Coherent Scattering

- Will determine the structure and properties of complex materials and nano-sized structures.

Statistical properties of SASE radiation and bandpass effects

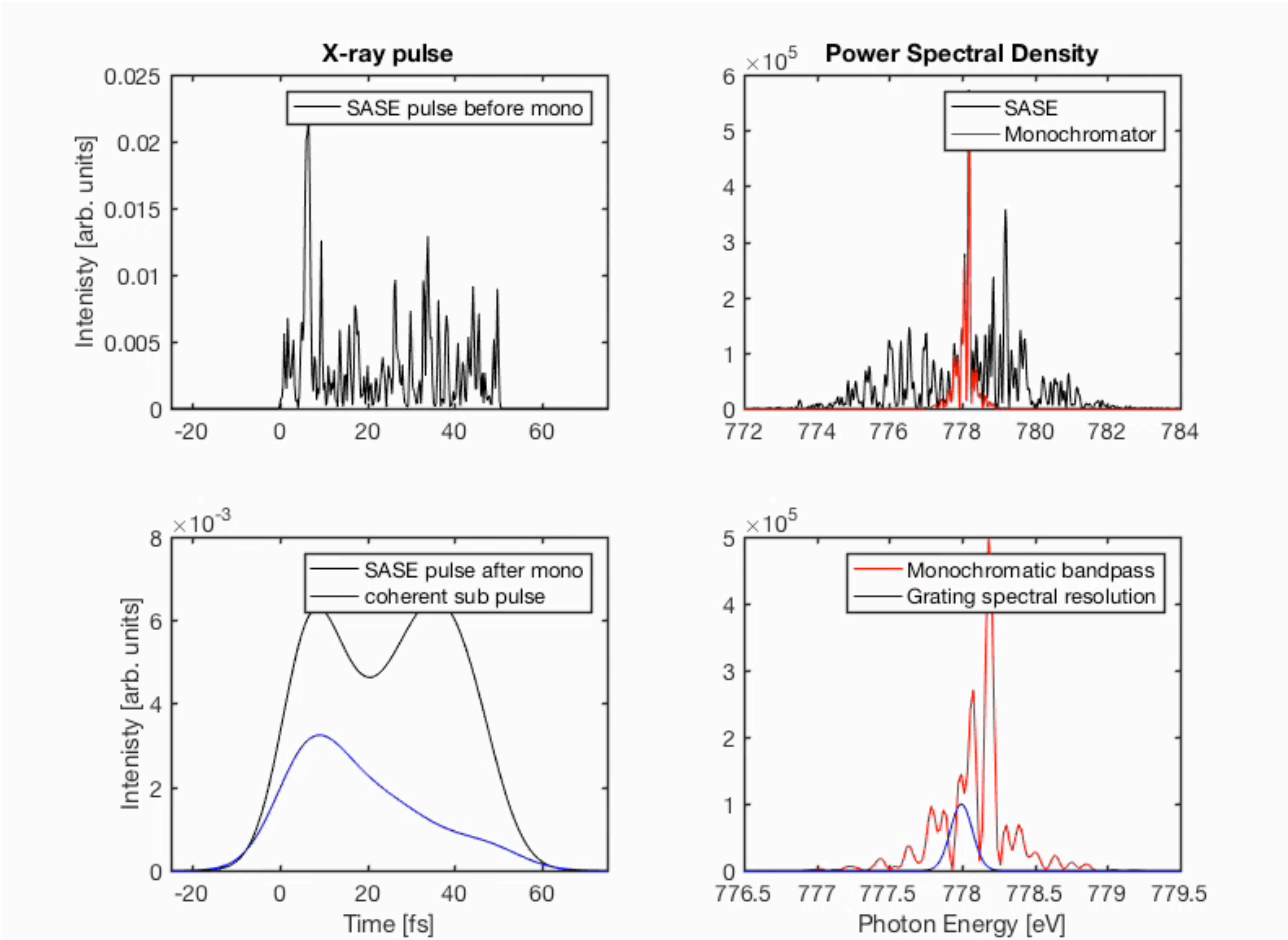

Pulse duration > τ_{coh}

Model: Saldin, Schneidmiller, Yurkov, NIMPRA 407, 291, 1998

SASE pulses after monochromator close to transform limit

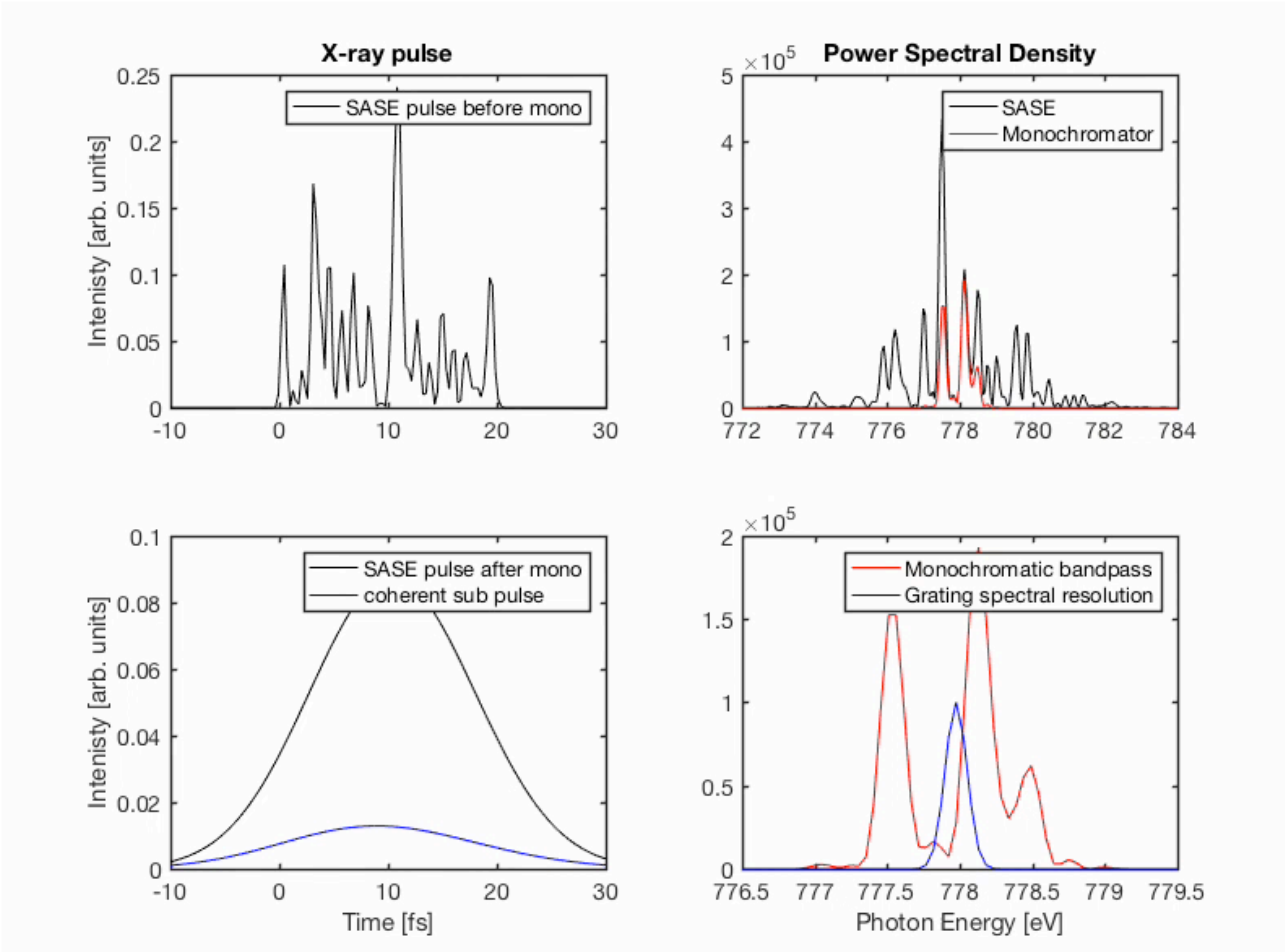

Pulse duration ≈ τ_{coh}

Model: Saldin, Schneidmiller, Yurkov, NIMPRA 407, 291, 1998

SCS X-ray beam delivery using monochromator for time-resolved spectroscopy (100x100µm2)

(PINK BEAM: up to 10^{14} photons per pulse up to 10^{18}-10^{20} W/cm2)

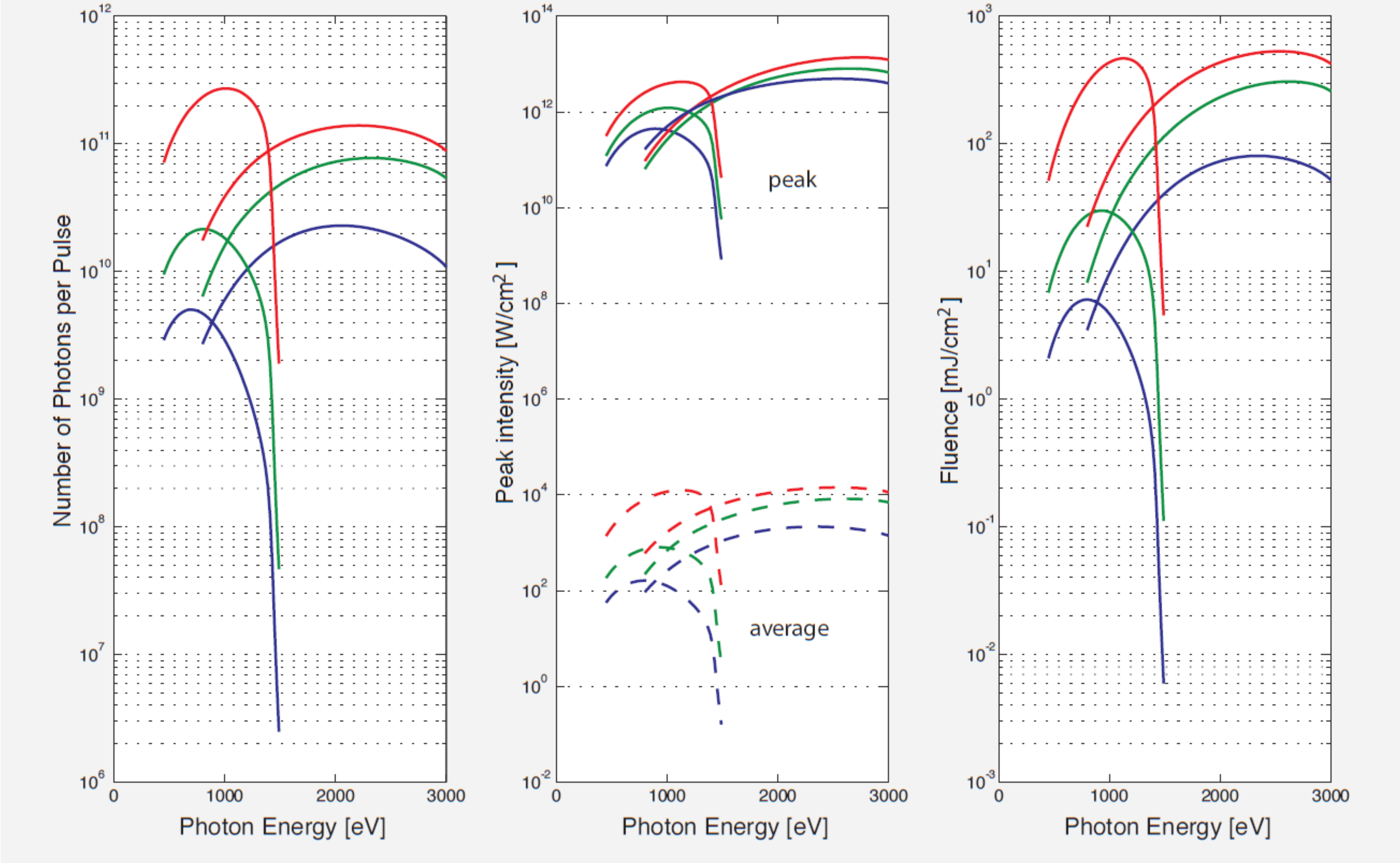

Degeneracy parameter

Number of photons in coherence volume

source	photon energy	δ
Hg lamp	4.9 eV	3×10^{-3}
synchrotron undulator	6.4 keV	2×10^{-3}
He-Ne laser	1.96 eV	2×10^{7}
XFEL	6.4 keV	2×10^{9}

number of simultaneous coherent x-rays

"simultaneous" is defined by atomic decay clock ~ 1 fs

Storage ring:

10^{14} phot./eV/**s** ⇨ 10^{-1} phot./eV/**fs** "one photon at a time"

number of simultaneous coherent x-rays

"simultaneous" is defined by atomic decay clock ~ 1 fs

Storage ring:

10^{14} phot./eV/**s** → 10^{-1} phot./eV/**fs** "one photon at a time"

X-Ray lasers 10^{9} phot./ **fs**

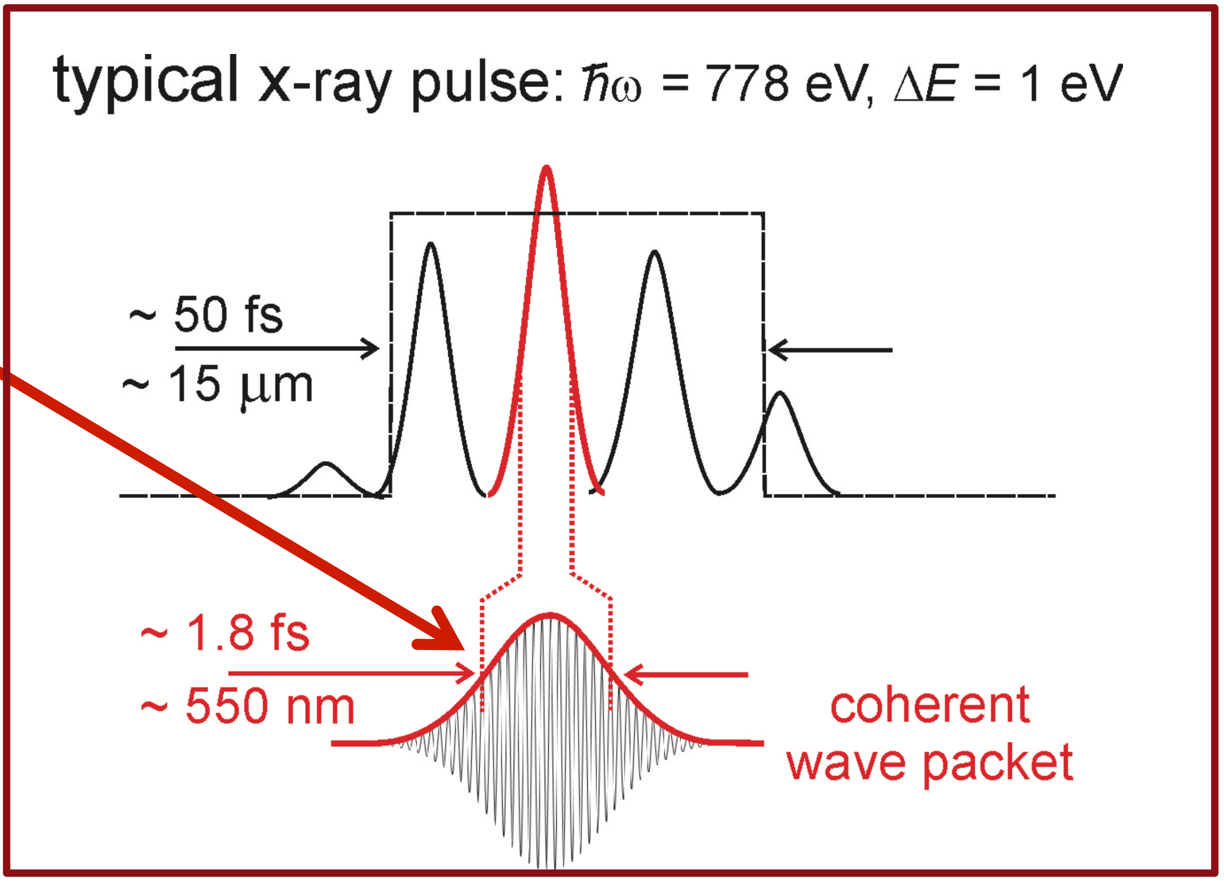

SINGLE SHOT IMAGING AND STIMULATED EMISSION

Single-shot FTH

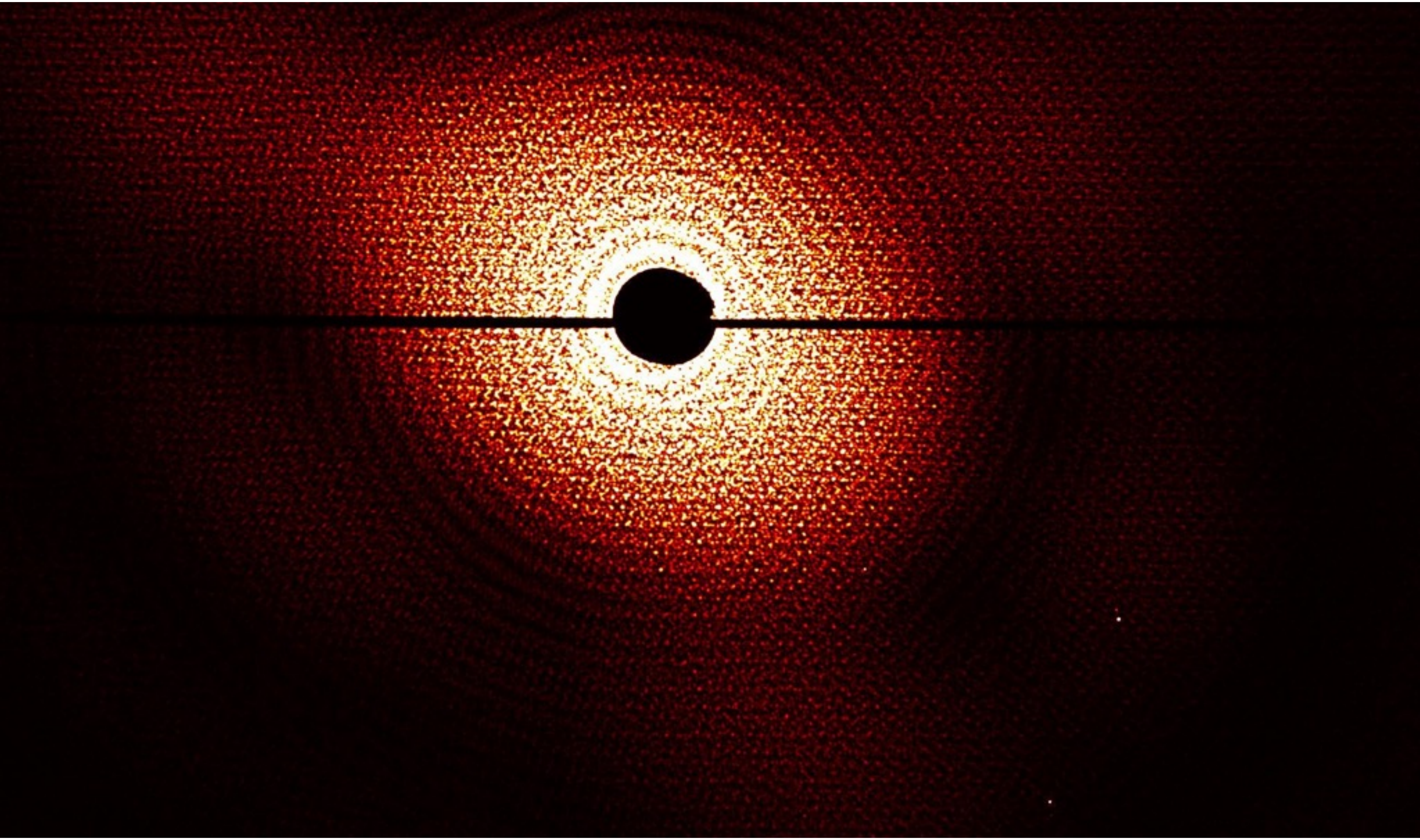

Single-shot FTH

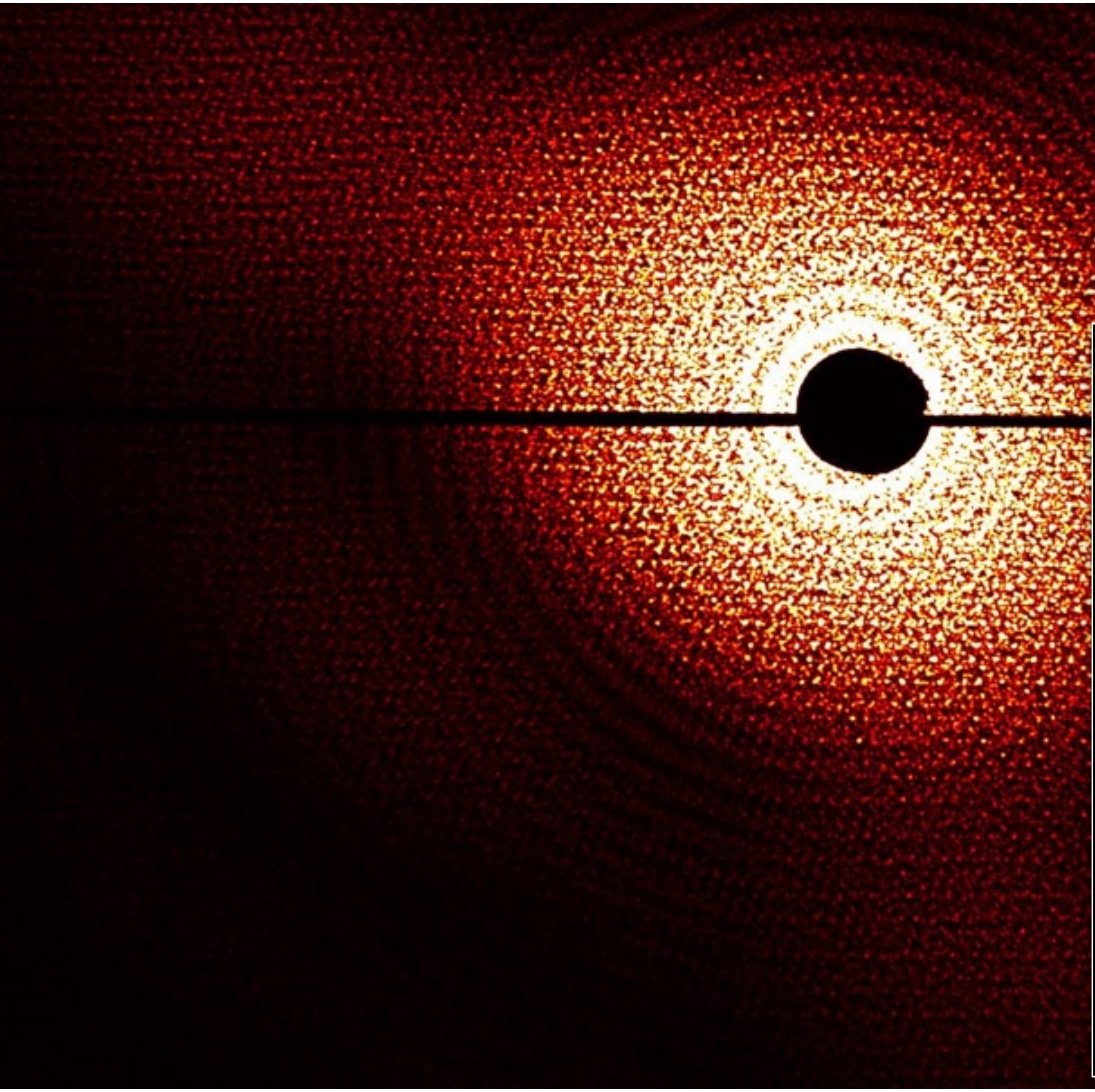

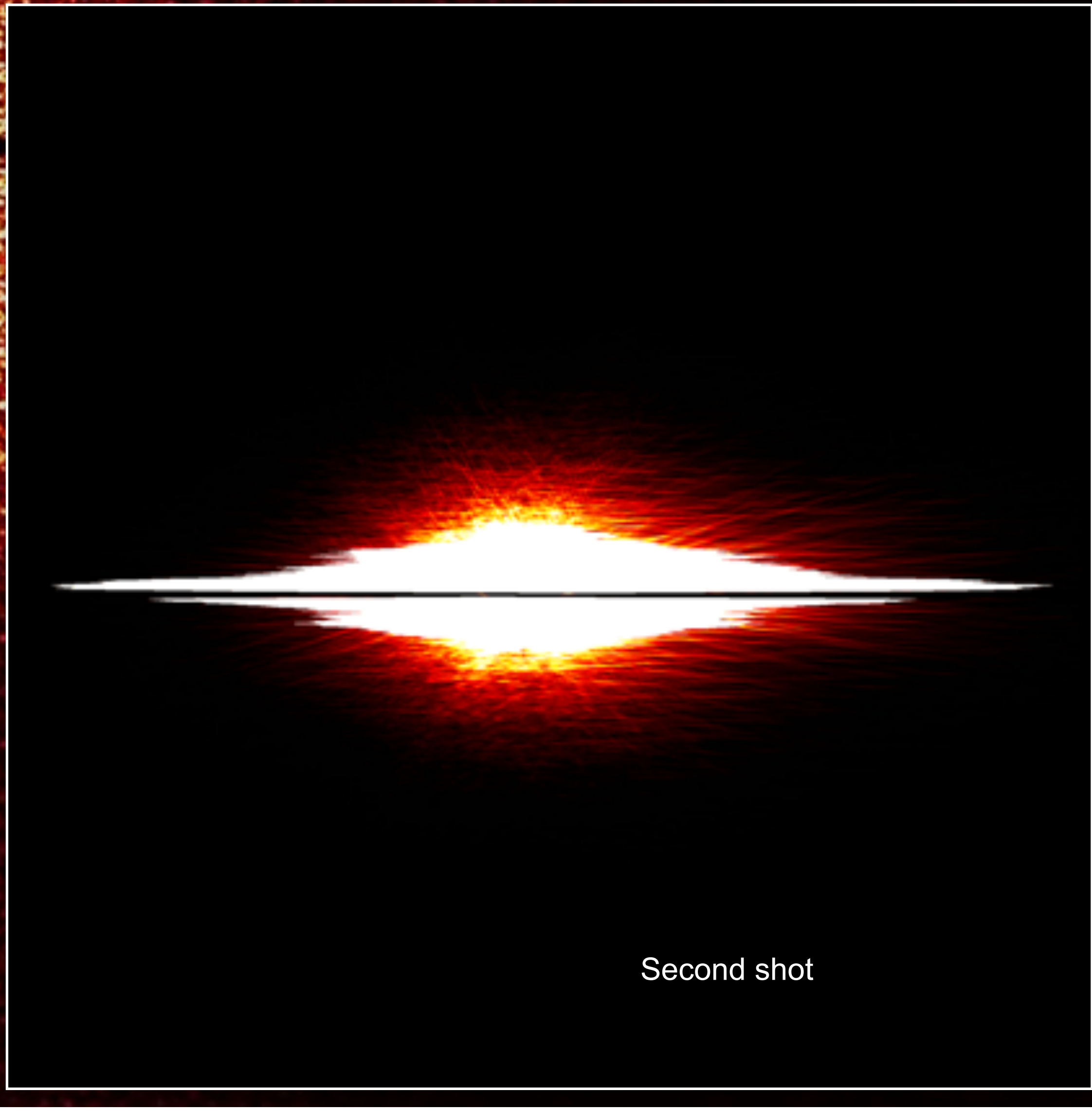

Single shot imaging of magnetic nanostructure

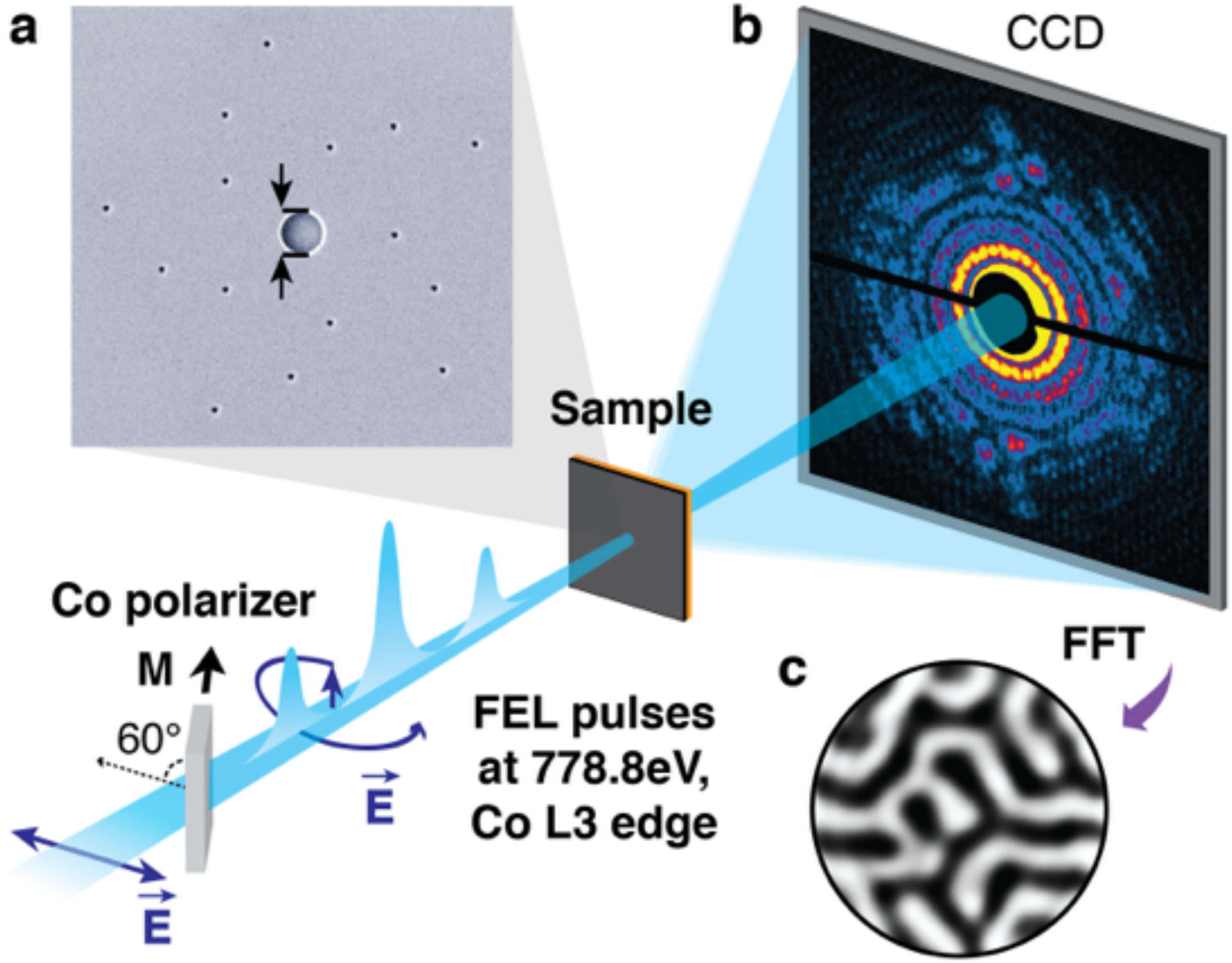

Monochromator: Co L3 edge (778.8eV) with 0.5eV bandwidth
Photons after the polarizer: 1×10^9 photons/pulse
Focus at sample: $10 \times 30 \mu m^2$
Shot-shot intensity jitter: Fluences from 1 to $30 mJ/cm^2$
Nominal pulse durations: 80fs and 360fs

Wang, Zhu, Wu *et al.* PRL **108**, 267403 (2012)

European XFEL

Imaging threshold

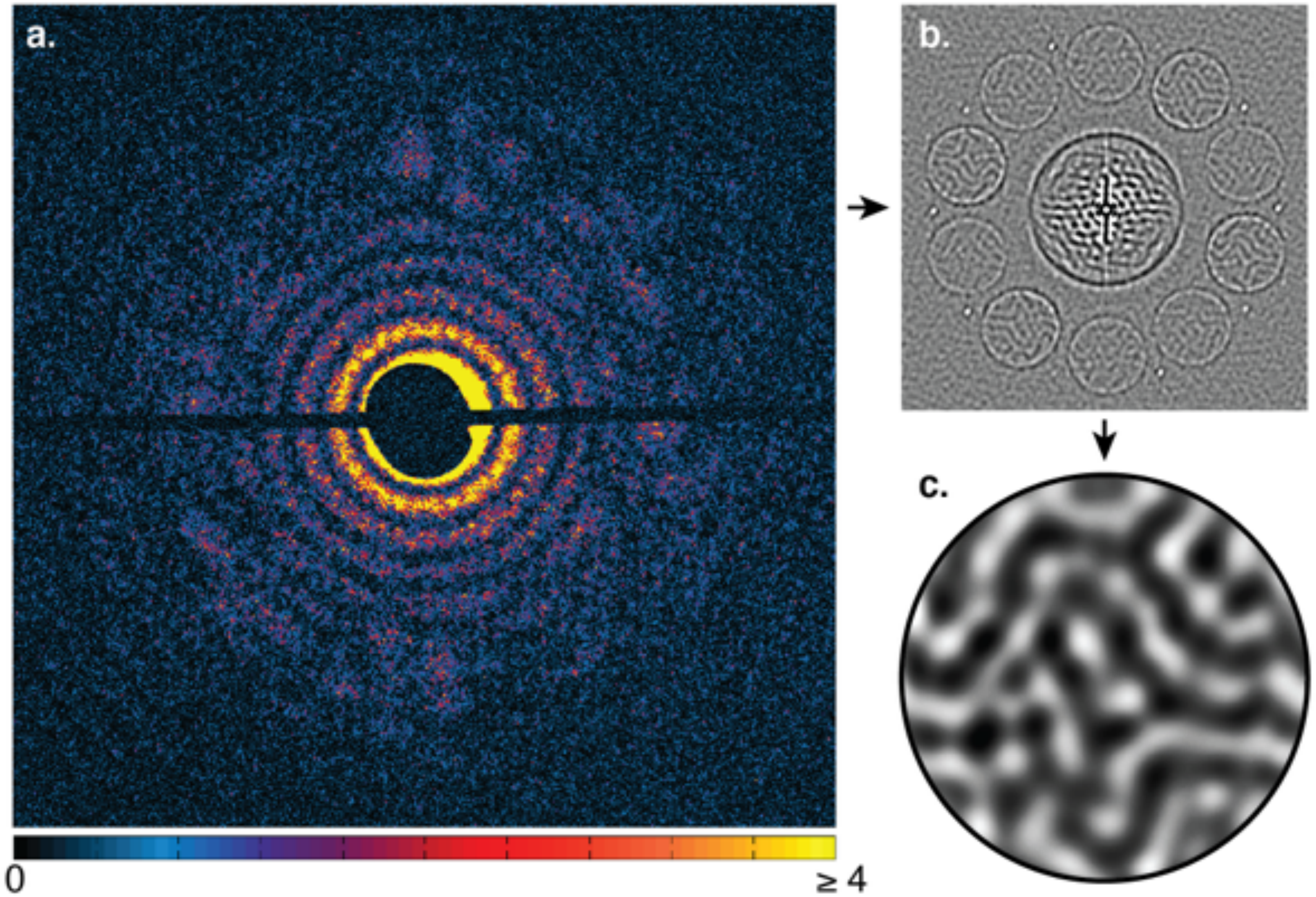

$1.5x10^5$ photons detected in a 80fs x-ray pulse
Spatial multiplexing to improve image quality by up to a factor 4 (15 ref.)

Combination of resonant enhancement, phase recording and spatial multiplexing

⇩

Imaging threshold as low as $5mJ/cm^2$

Wang, Zhu, Wu *et al.* PRL **108**, 267403 (2012)

Single Shot Holography

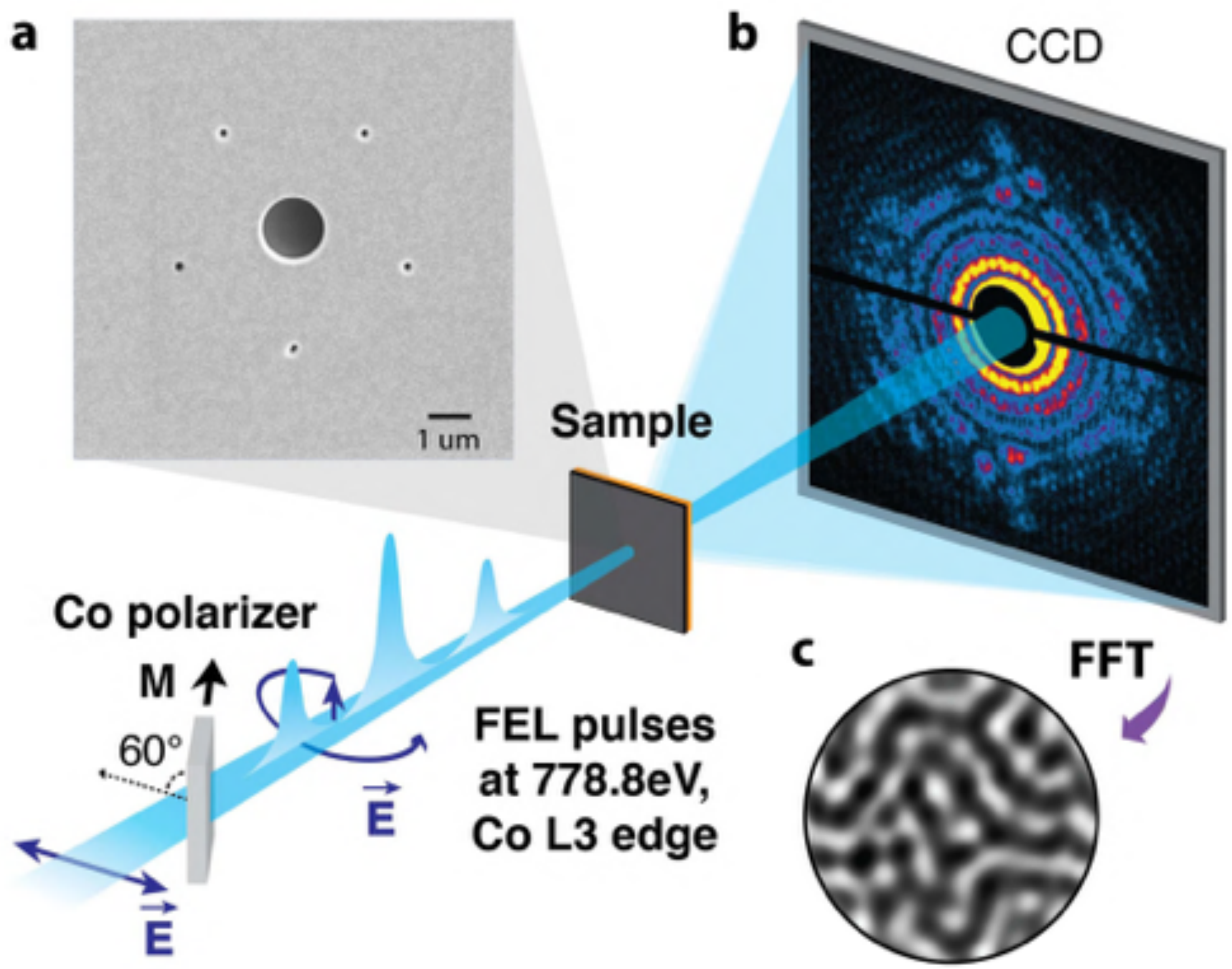

Wang, Zhu, Wu *et al*. PRL **108**, 267403 (2012)

- Using Fourier transform holography, obtain real-space image of magnetic domains.
- Diffraction from a single x-ray pulse (~5 mJ/cm^2).
- We can combine this with pump-probe techniques to make time-resolved movies!
- Attain high resolution in single shot:

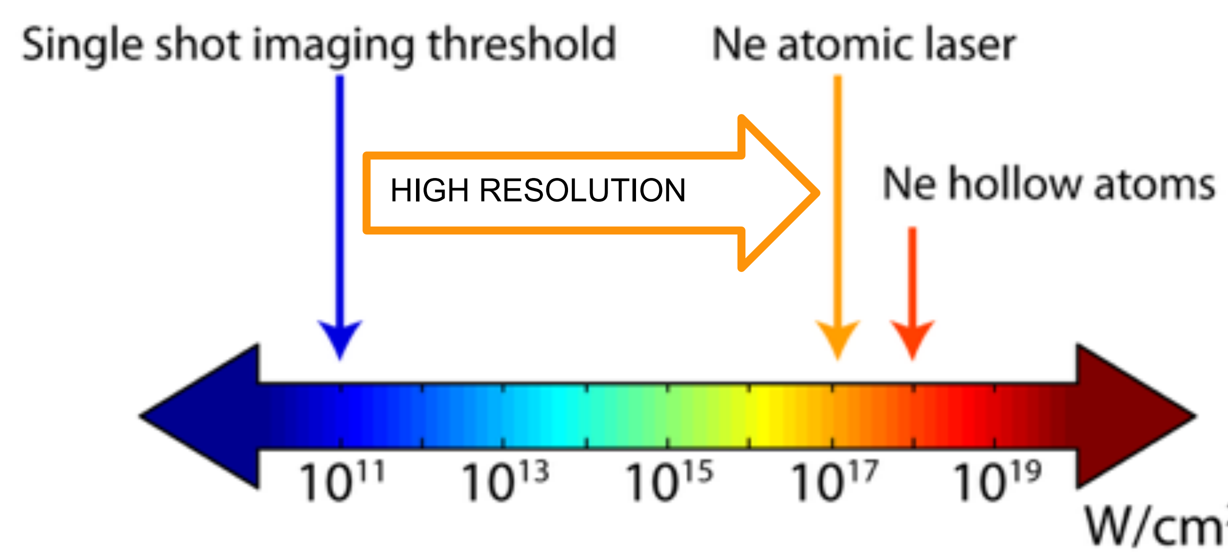

Critical time scale of stimulated x-ray processes

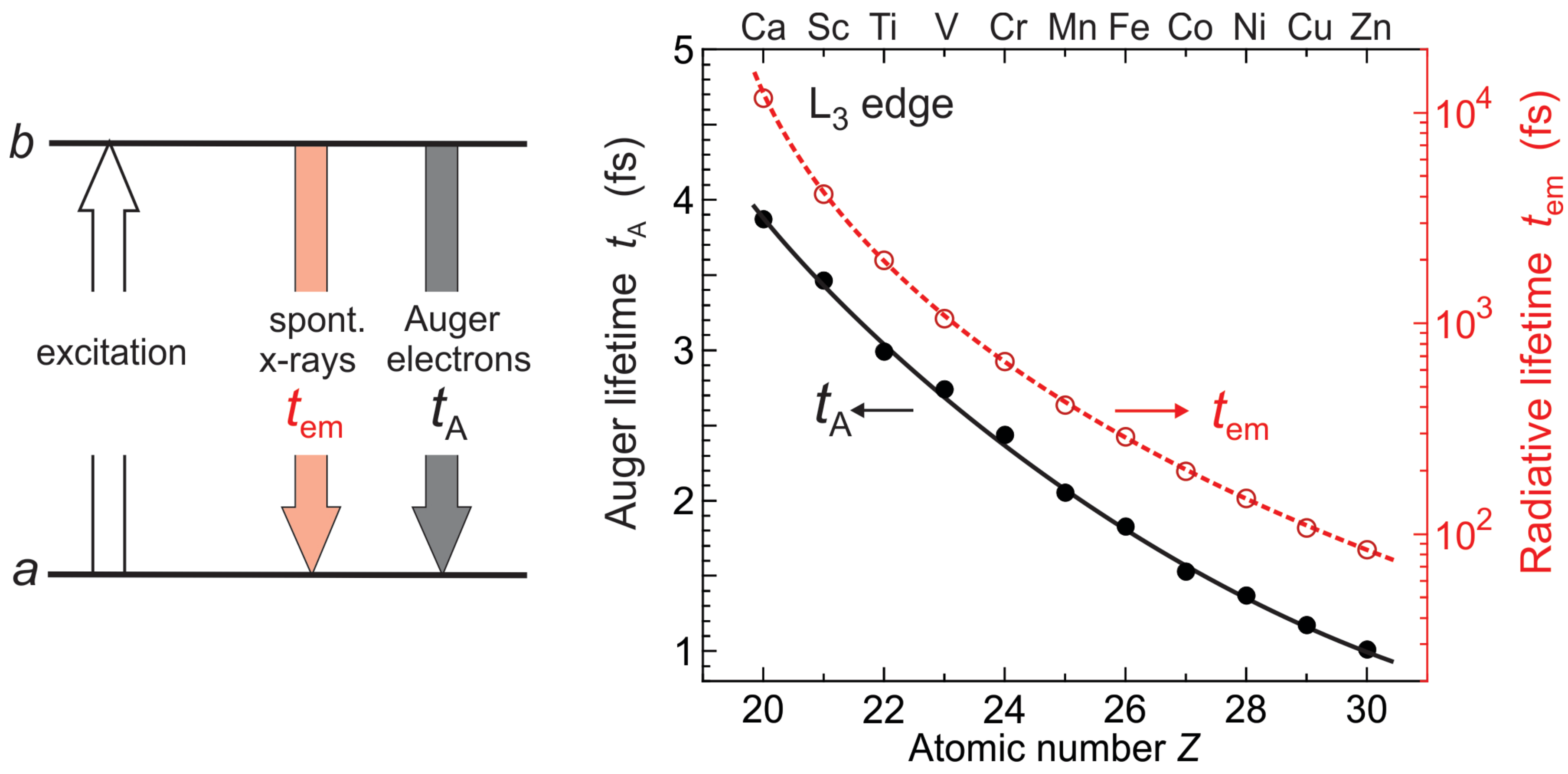

Stimulated processes must be triggered before spontaneous excited state decays

"atomic clock" = total decay time = a few femtoseconds

Amplified stimulated emission in a gas

LETTER

doi:10.1038/nature10721

Atomic inner-shell X-ray laser at 1.46 nanometres pumped by an X-ray free-electron laser

Nina Rohringer[1]†, Duncan Ryan[2], Richard A. London[1], Michael Purvis[2], Felicie Albert[1], James Dunn[1], John D. Bozek[3], Christoph Bostedt[3], Alexander Graf[1], Randal Hill[1], Stefan P. Hau-Riege[1] & Jorge J. Rocca[2]

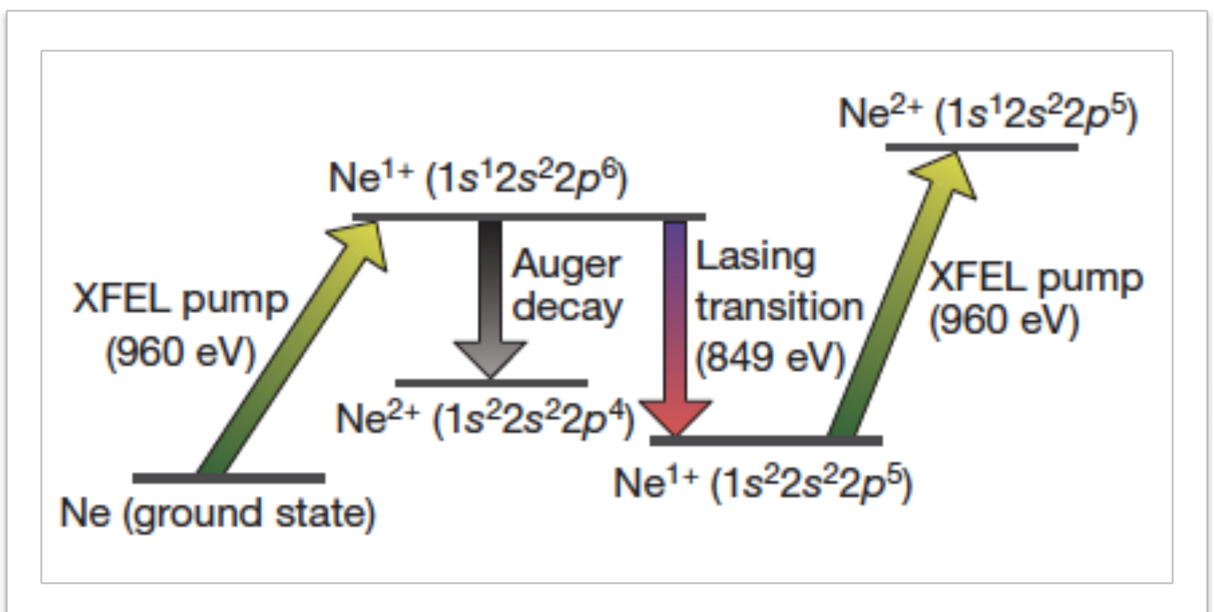

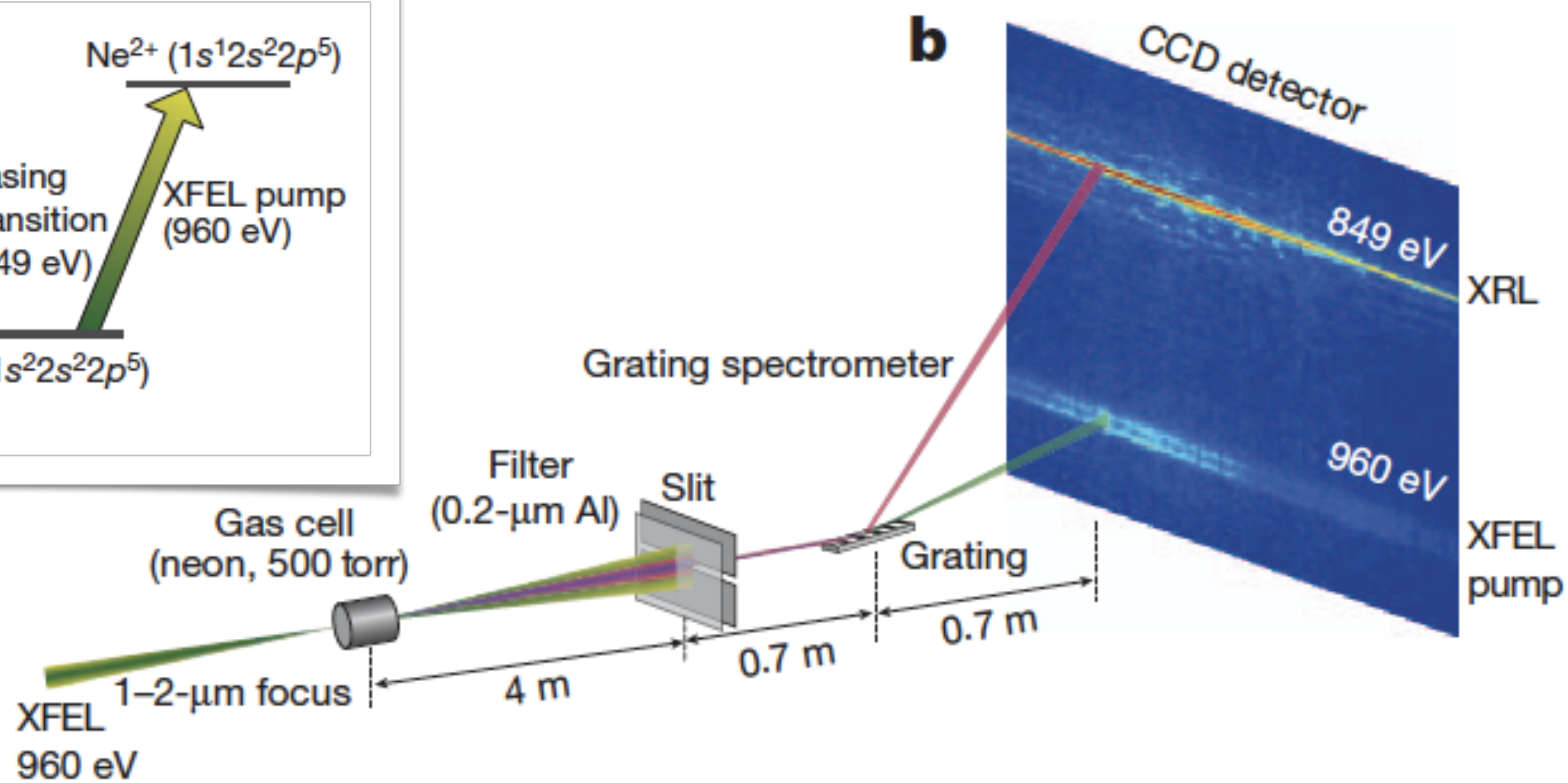

Pulse length 40-80 fs
Pulse energy < 0.27 mJ
Power density < $2*10^{17}$ W/cm²

Rohringer et al, Nature, 481, 488 (2012)

Atomic inner-shell X-ray laser

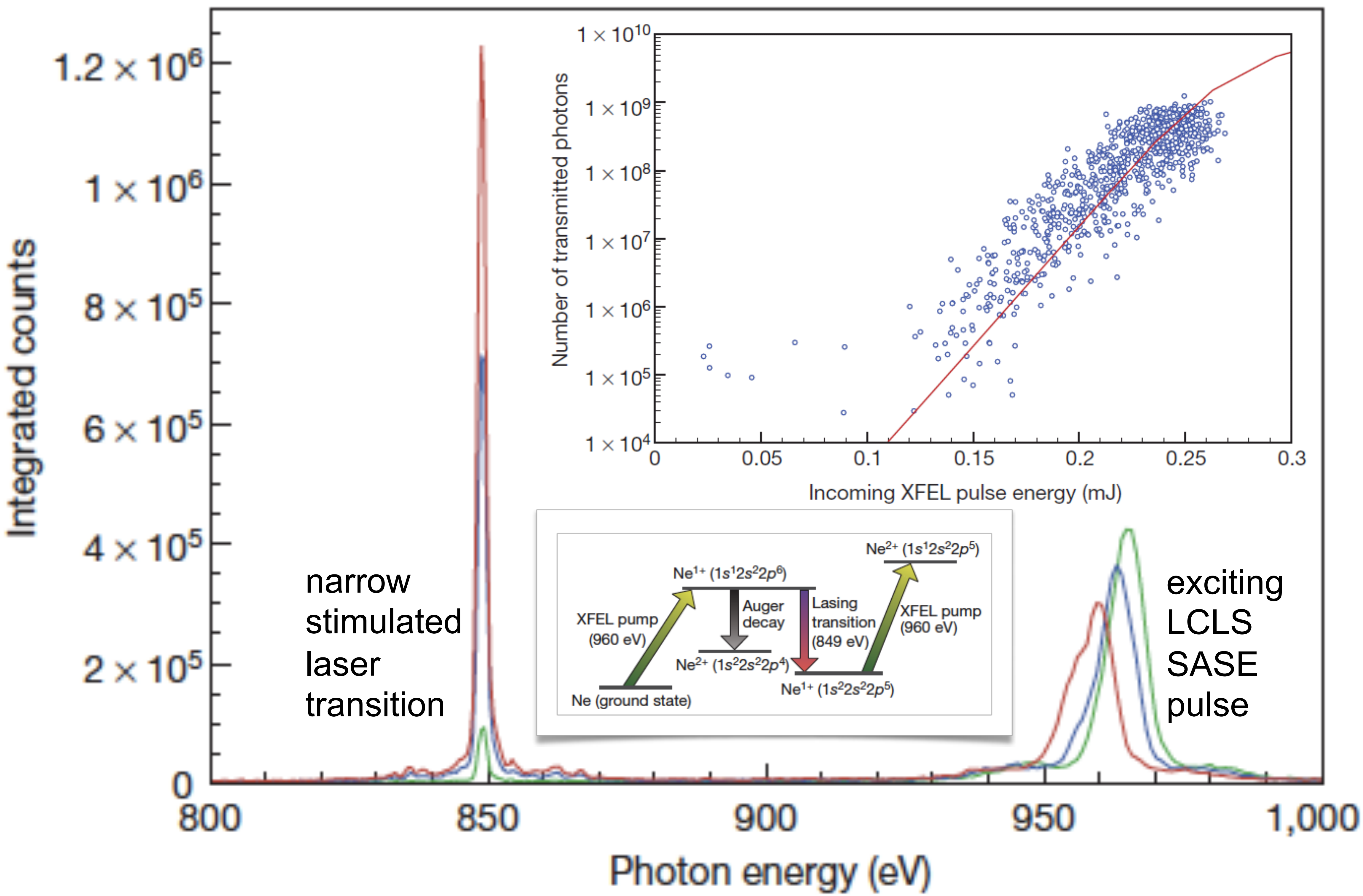

Rohringer et al, Nature, 481, 488 (2012)

Amplified stimulated emission in a solid

LETTER

doi:10.1038/nature12449

Stimulated X-ray emission for materials science

M. Beye[1], S. Schreck[1,2], F. Sorgenfrei[1,3], C. Trabant[1,2,4], N. Pontius[1], C. Schüßler-Langeheine[1], W. Wurth[3] & A. Föhlisch[1,2]

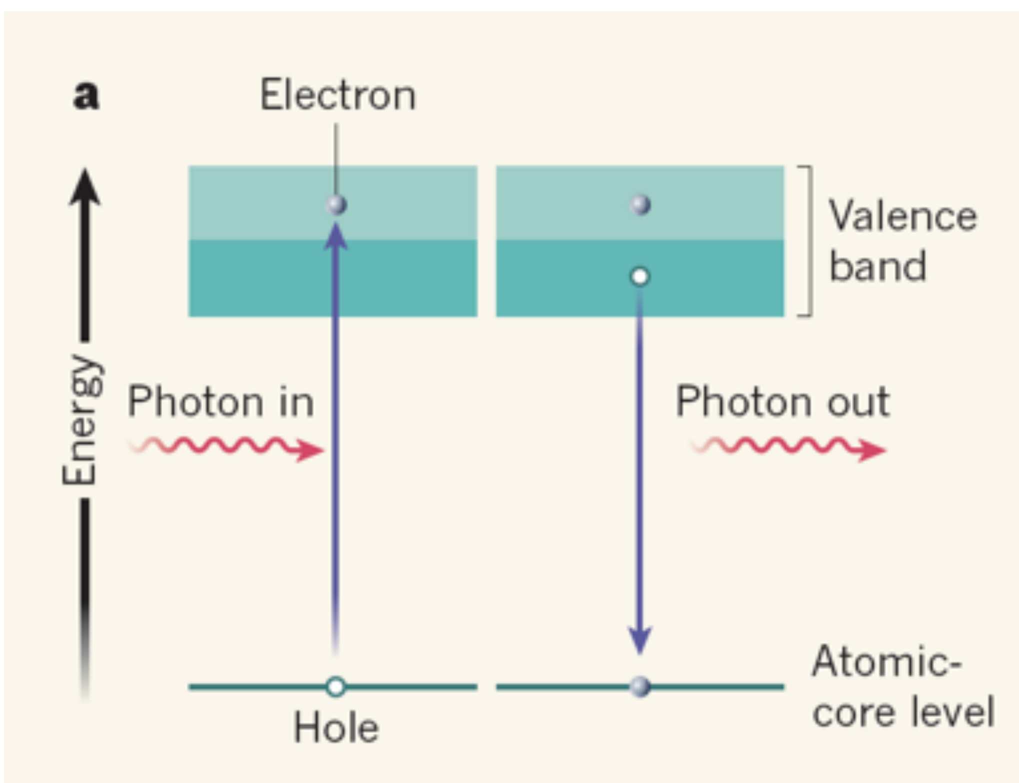

$$I = 1 \times 10^{16} \frac{\mathrm{W}}{\mathrm{cm}^2}$$

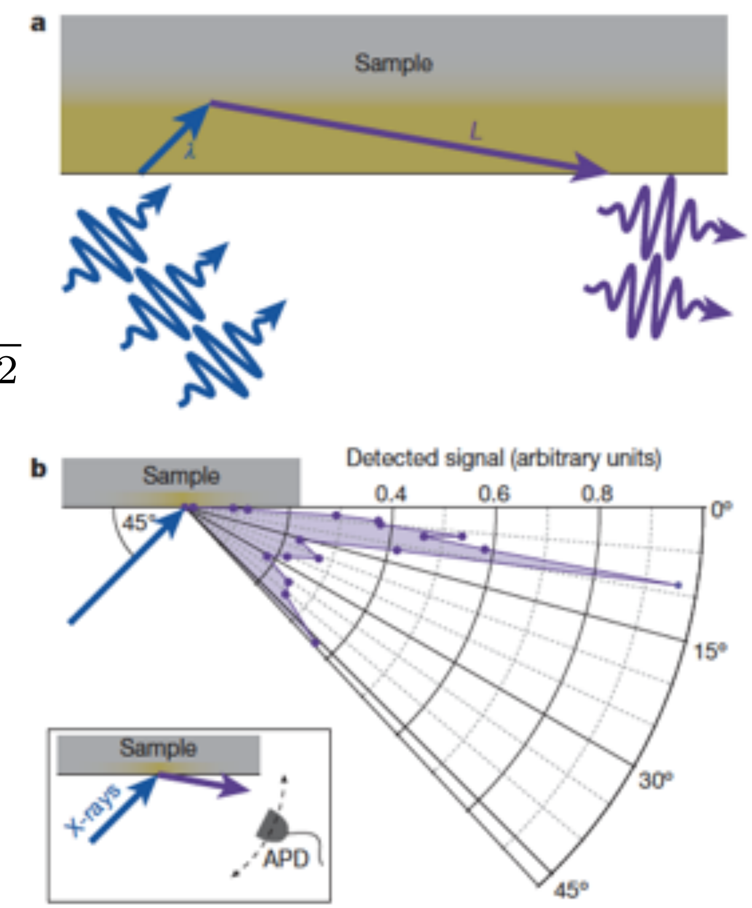

Detected conversion is 10-11, stimulation enhancement by a factor ~2

Single shot diffraction atomic versus electronic structure

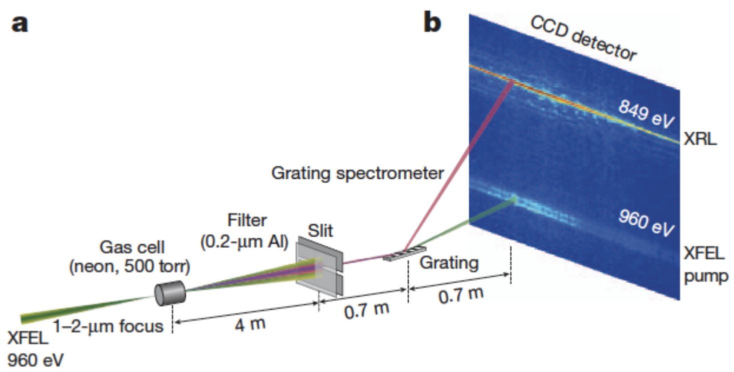

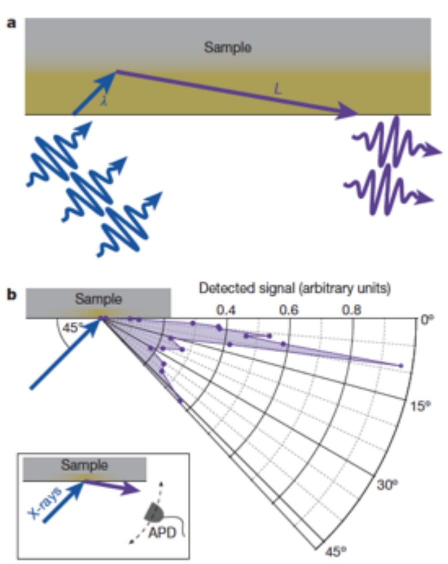

1 KJ/cm^2 ←

1 J/cm^2

← single shot magnetic imaging

1 mJ/cm^2

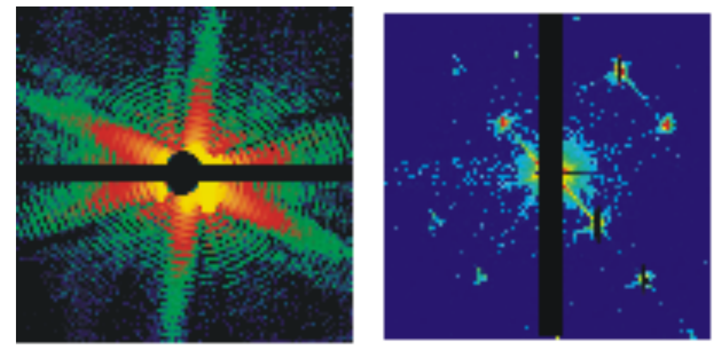

atomic structure:
single shot pattern of virus or crystal

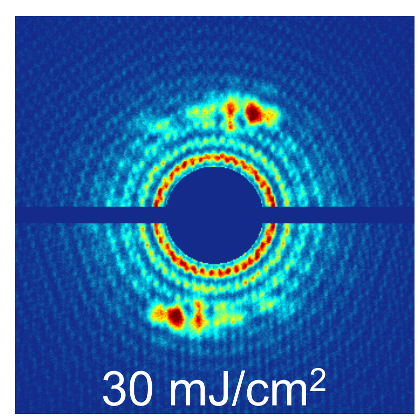

magnetic structure:
Co/Pt domains
50 fs pulses

Summary

Part 1 (Tuesday)

- Spectroscopy and Microscopy
- XFEL and SASE radiation
- Stimulated emission

Part 2 (Wednesday)

- Nonlinear absorption
- Three-wave mixing
- Four-wave mixing

NONLINEAR ABSORPTION

Extension to High Intensity Single Shots

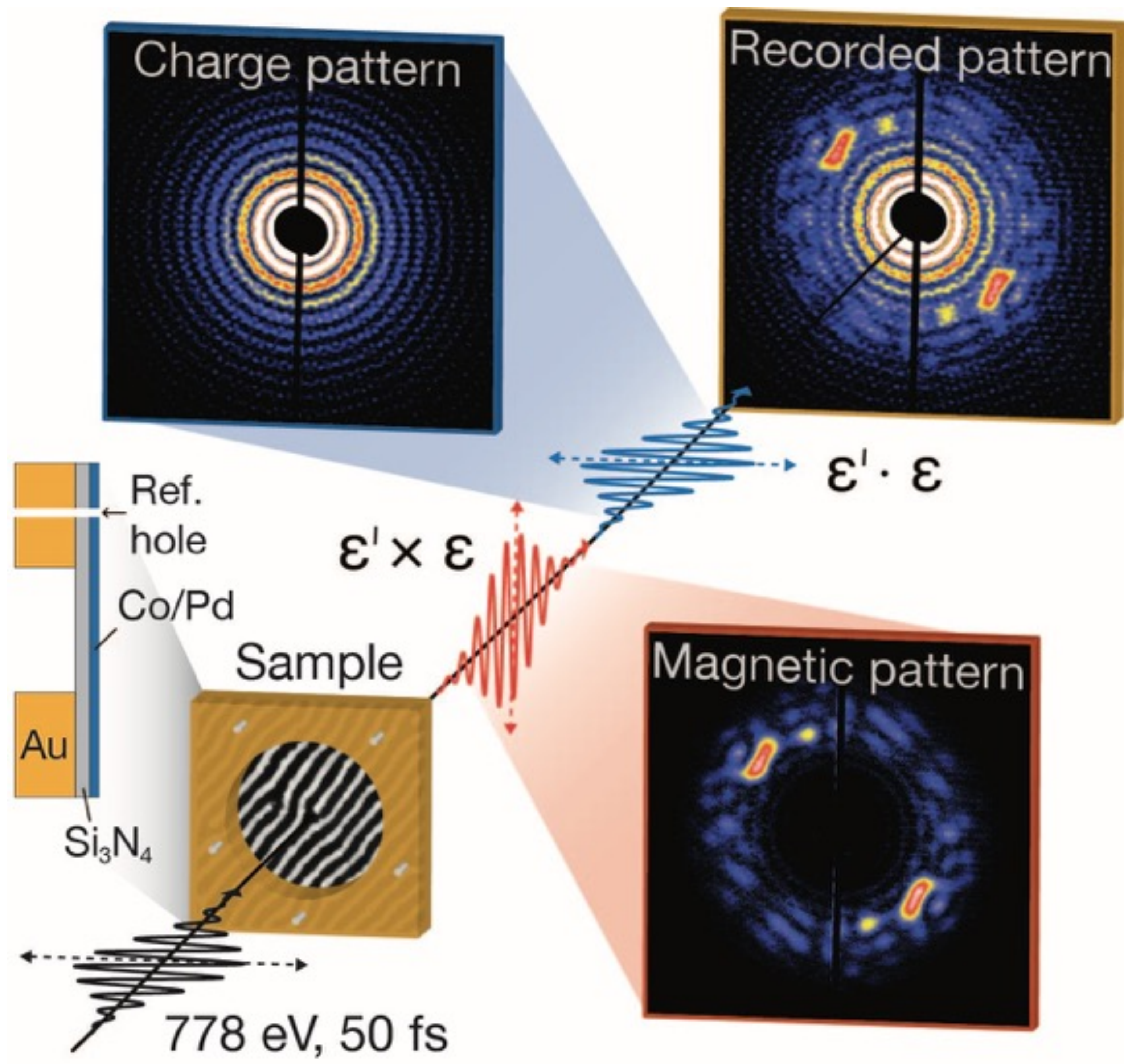

Wu *et al.* , PRL 117, 027401 (2016)

Intensity Dependent Diffraction

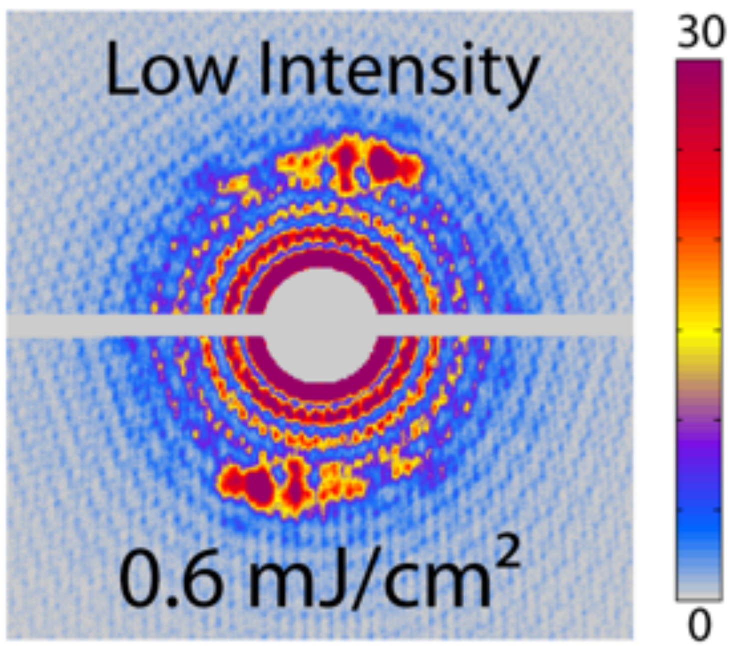

- If diffraction scales linearly with intensity:

High Intensity Pattern = Low Intensity Pattern x Intensity Ratio

Wu *et al.* , PRL 117, 027401 (2016)

Intensity Dependent Diffraction

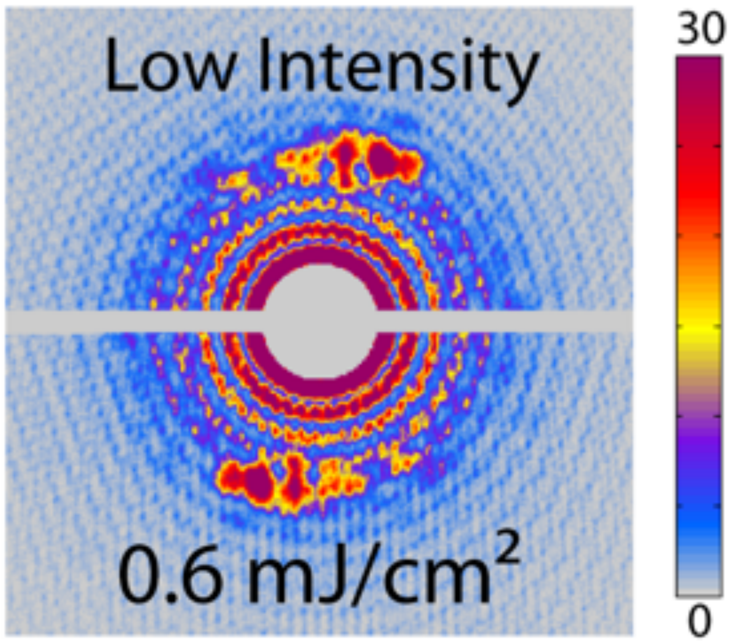

Increase intensity to ~300mJ/cm²

- If diffraction scales linearly with intensity:

High Intensity Pattern = Low Intensity Pattern x Intensity Ratio

Wu *et al.* , PRL 117, 027401 (2016)

Intensity Dependent Diffraction

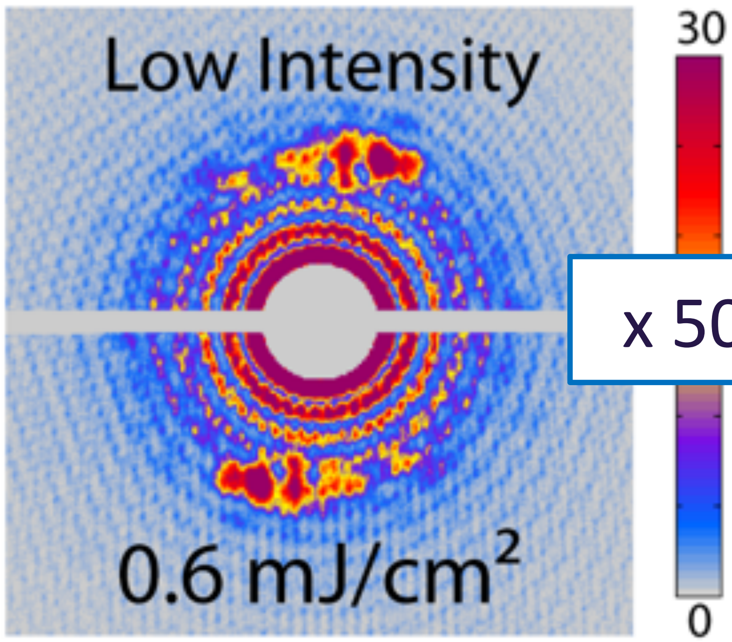

Increase intensity to ~300mJ/cm²

- If diffraction scales linearly with intensity:

High Intensity Pattern = Low Intensity Pattern x Intensity Ratio

Wu *et al.* , PRL 117, 027401 (2016)

Intensity Dependent Diffraction

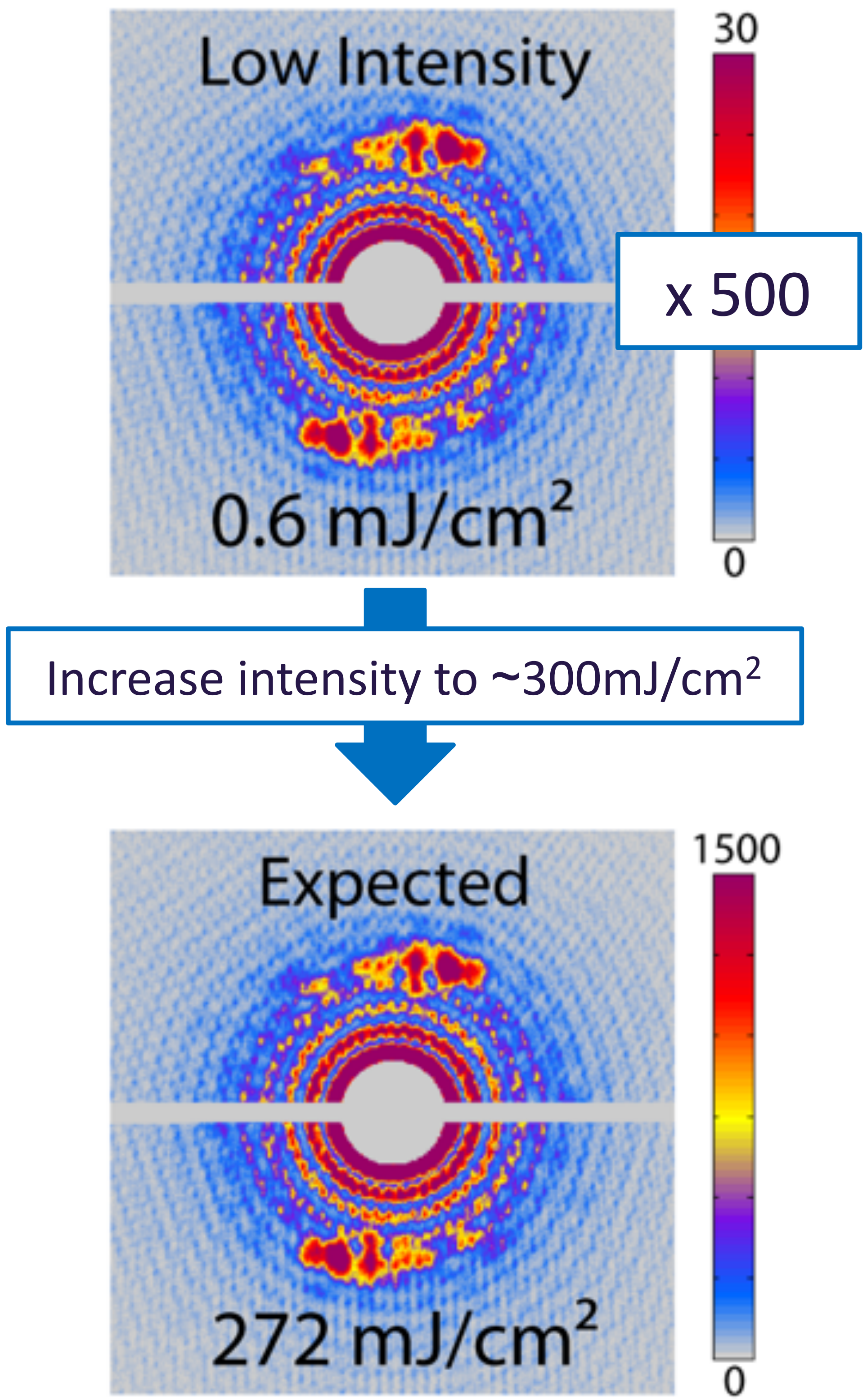

- If diffraction scales linearly with intensity:

High Intensity Pattern = Low Intensity Pattern x Intensity Ratio

Wu *et al.* , PRL 117, 027401 (2016)

Intensity Dependent Diffraction

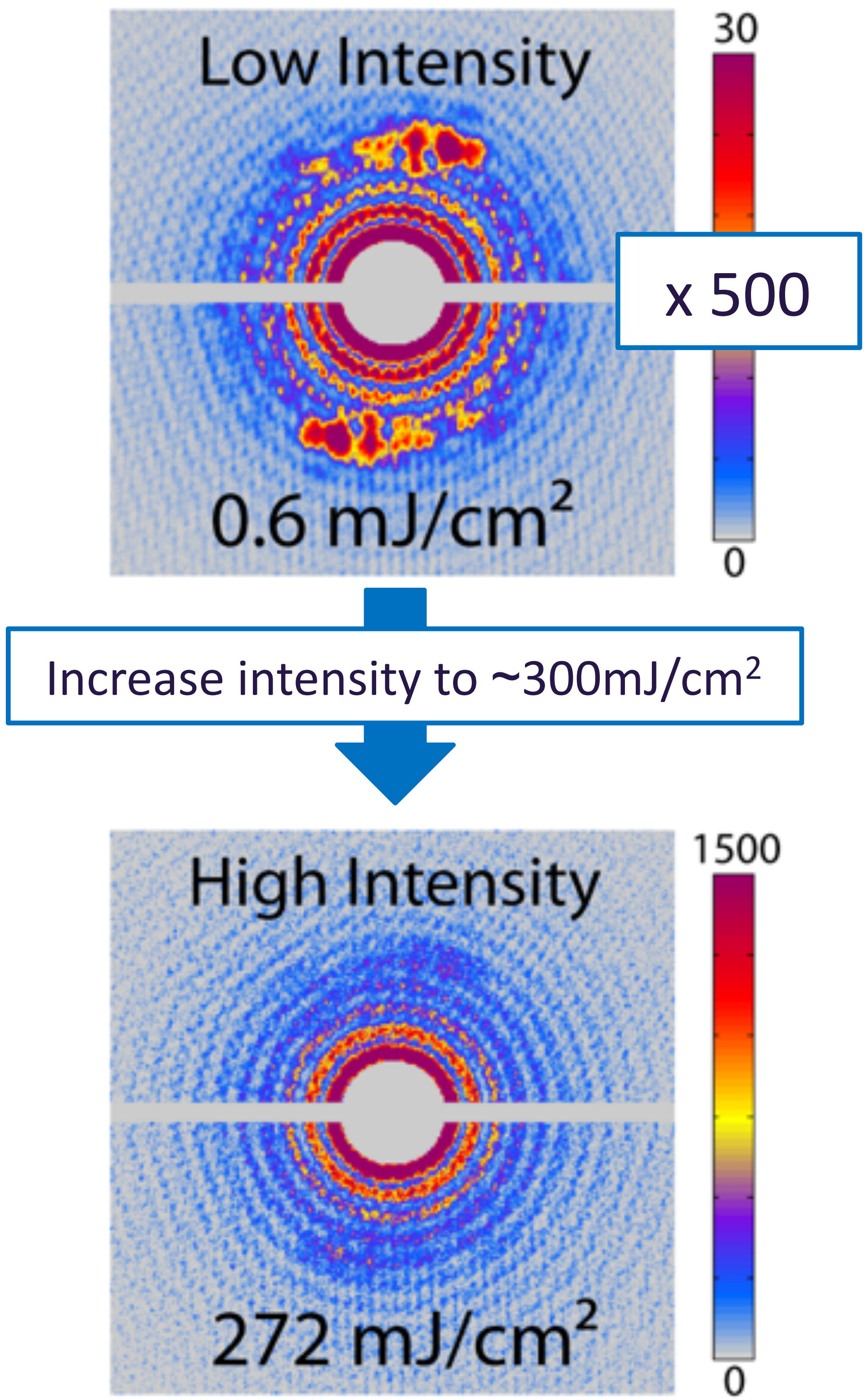

- If diffraction scales linearly with intensity:

High Intensity Pattern = Low Intensity Pattern x Intensity Ratio

Wu *et al.* , PRL 117, 027401 (2016)

Intensity Dependent Diffraction

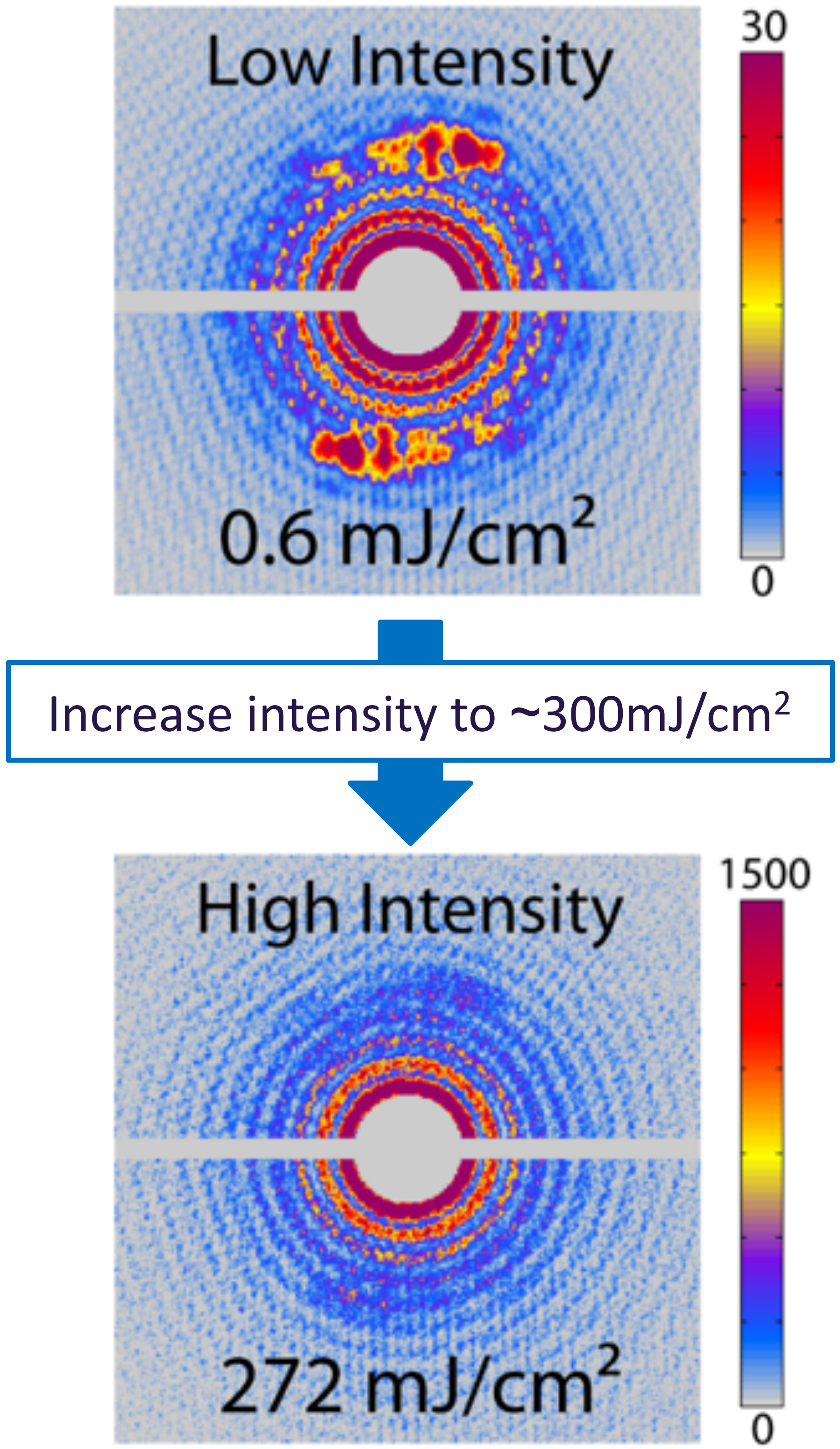

Two main observations:

1) Strong decrease in magnetic speckle intensity (loss of magnetic contrast)
2) Decrease in charge scattering

Wu *et al.* , PRL 117, 027401 (2016)

Intensity Dependent Diffraction

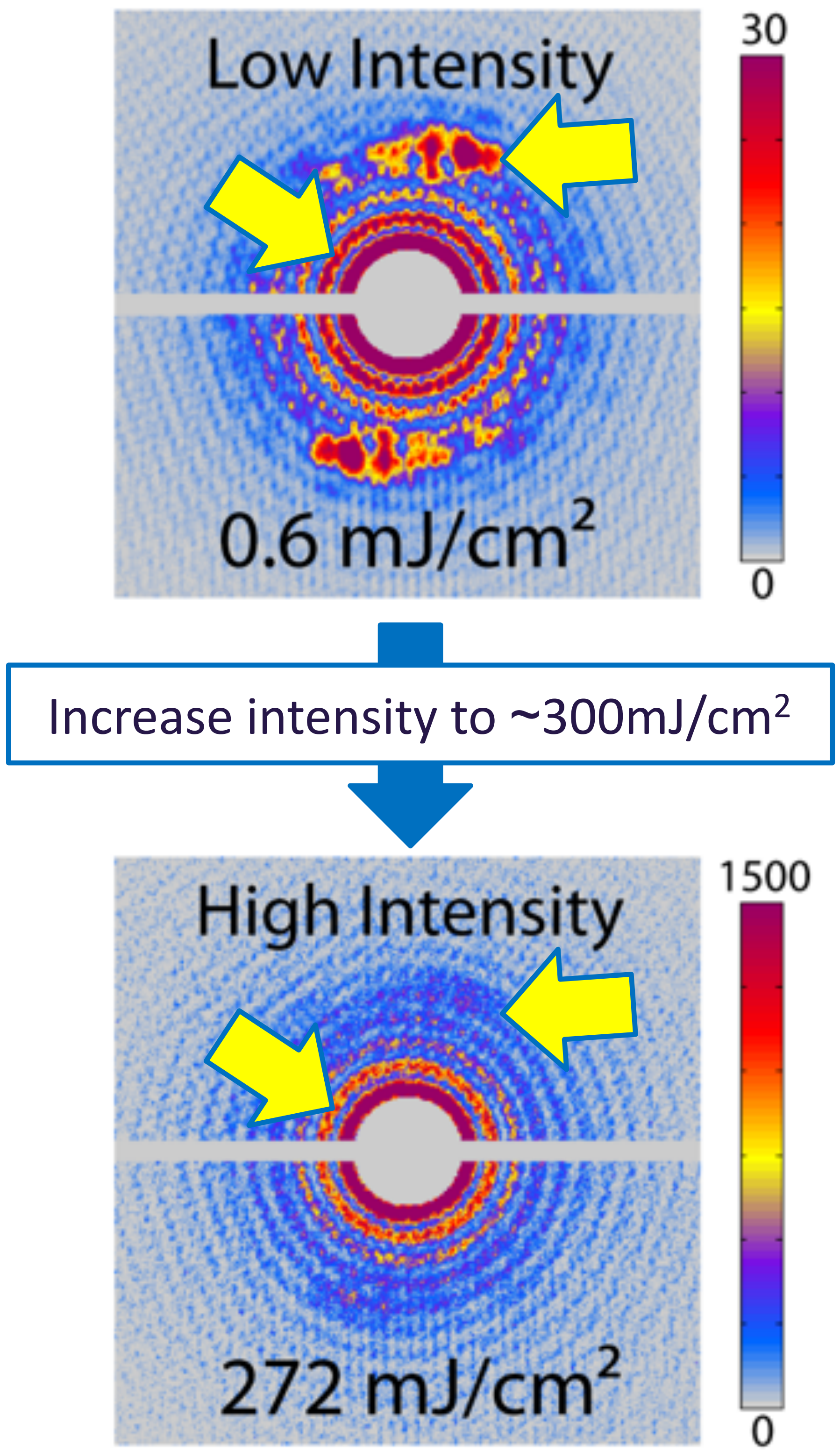

Two main observations:

1) Strong decrease in magnetic speckle intensity (loss of magnetic contrast)
2) Decrease in charge scattering

Wu *et al.* , PRL 117, 027401 (2016)

Intensity Dependent Diffraction

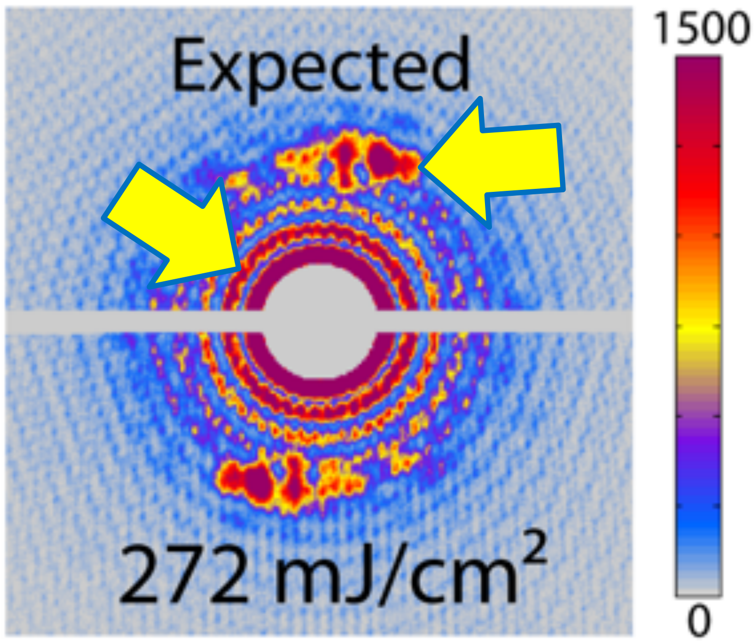

Increase intensity to ~300mJ/cm²

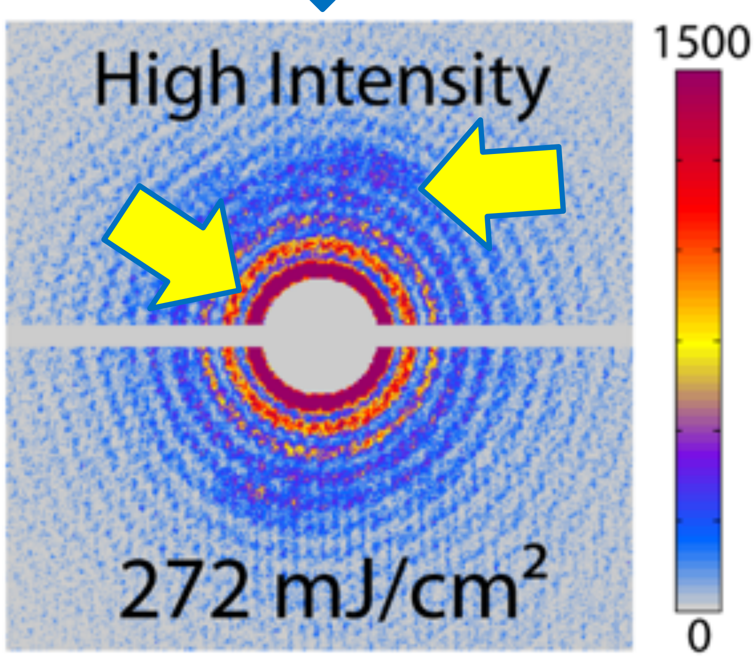

Two main observations:

1) Strong decrease in magnetic speckle intensity (loss of magnetic contrast)
2) Decrease in charge scattering

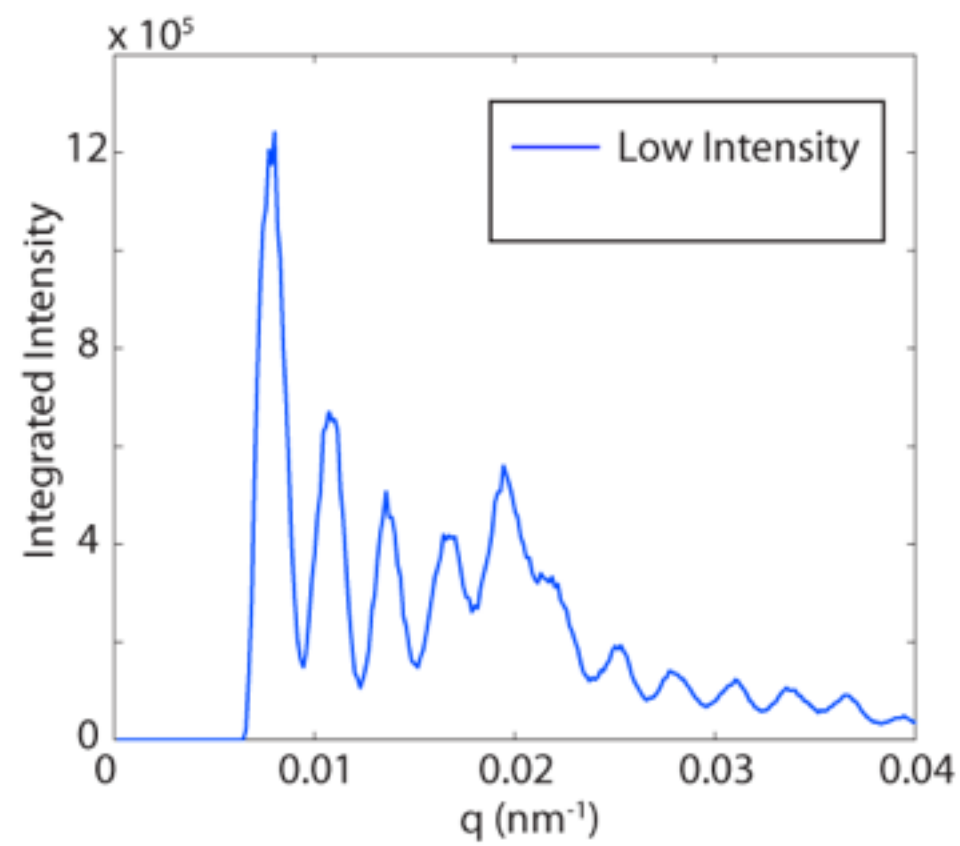

Wu *et al.* , PRL 117, 027401 (2016)

Intensity Dependent Diffraction

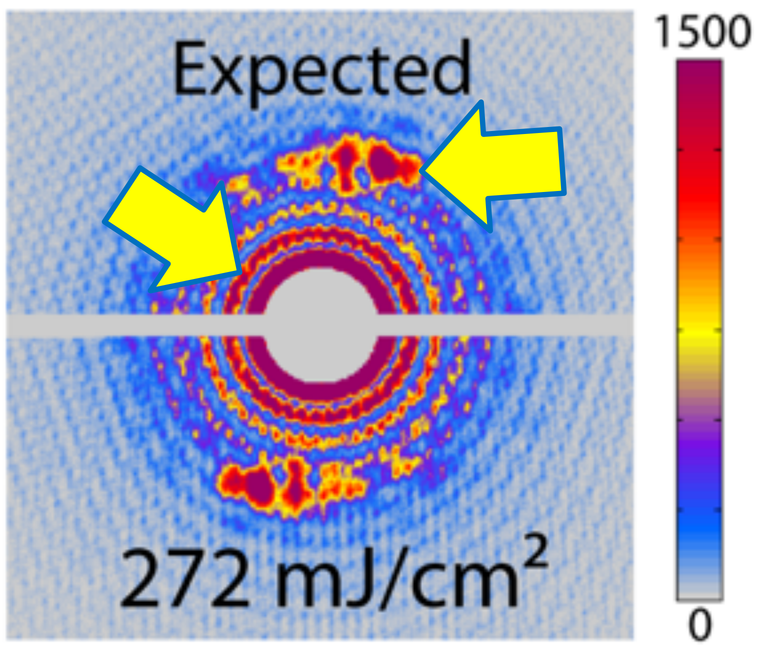

Increase intensity to ~300mJ/cm²

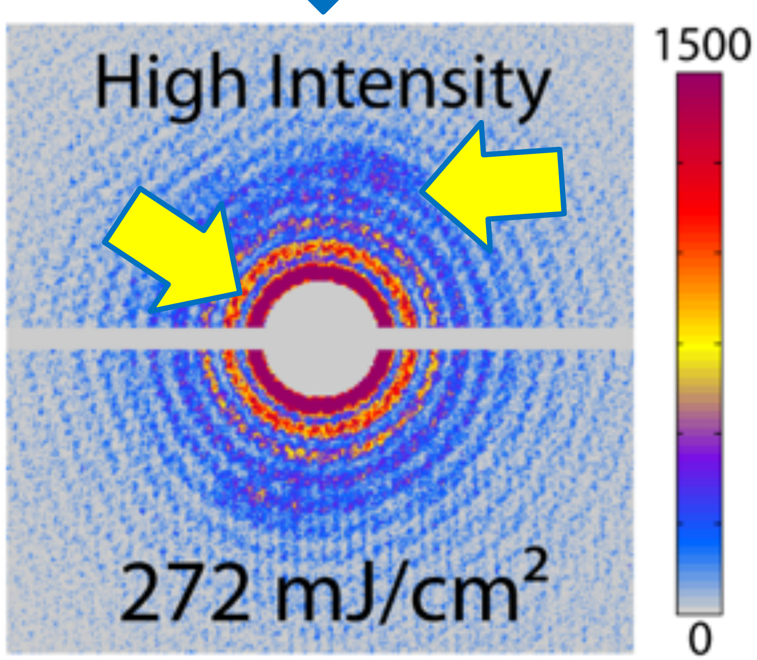

Two main observations:

1) Strong decrease in magnetic speckle intensity (loss of magnetic contrast)
2) Decrease in charge scattering

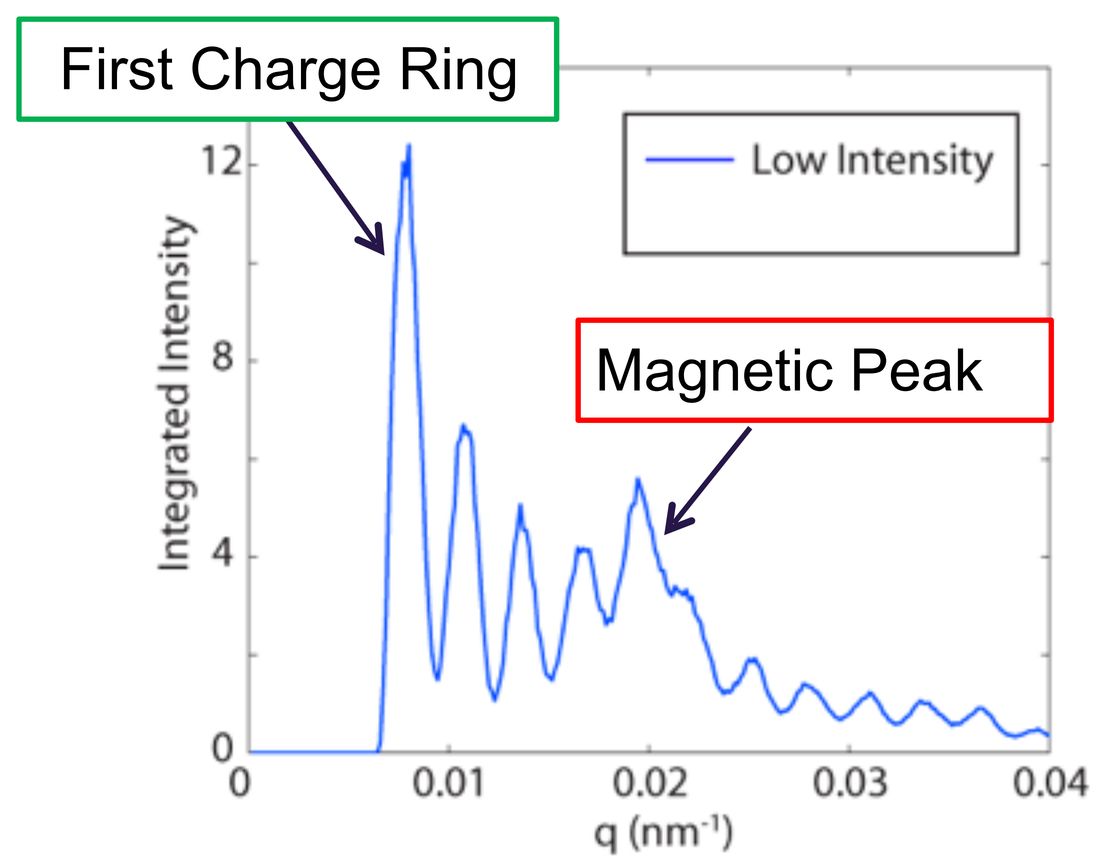

Wu *et al.* , PRL 117, 027401 (2016)

Intensity Dependent Diffraction

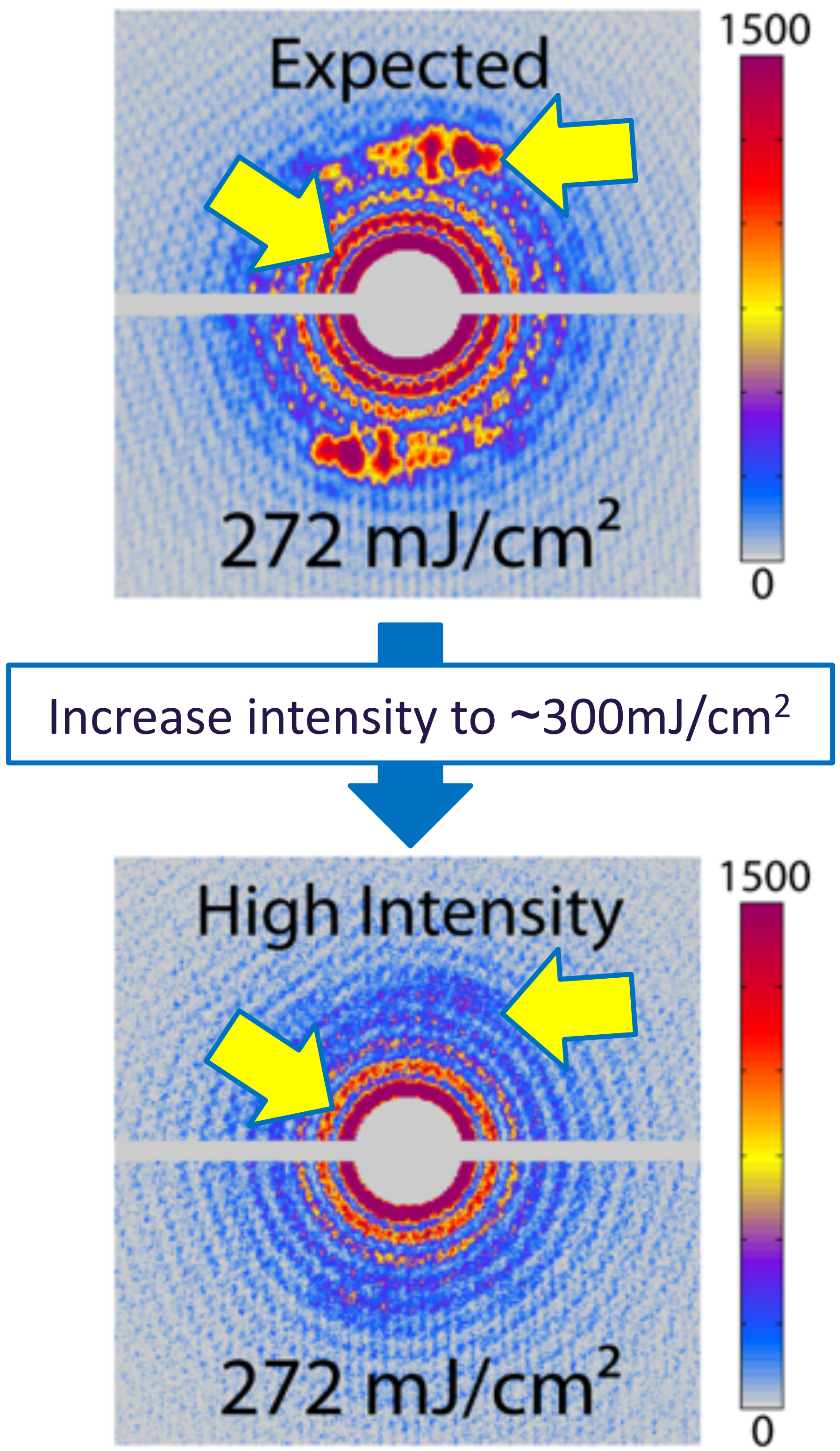

Two main observations:

1) Strong decrease in magnetic speckle intensity (loss of magnetic contrast)
2) Decrease in charge scattering

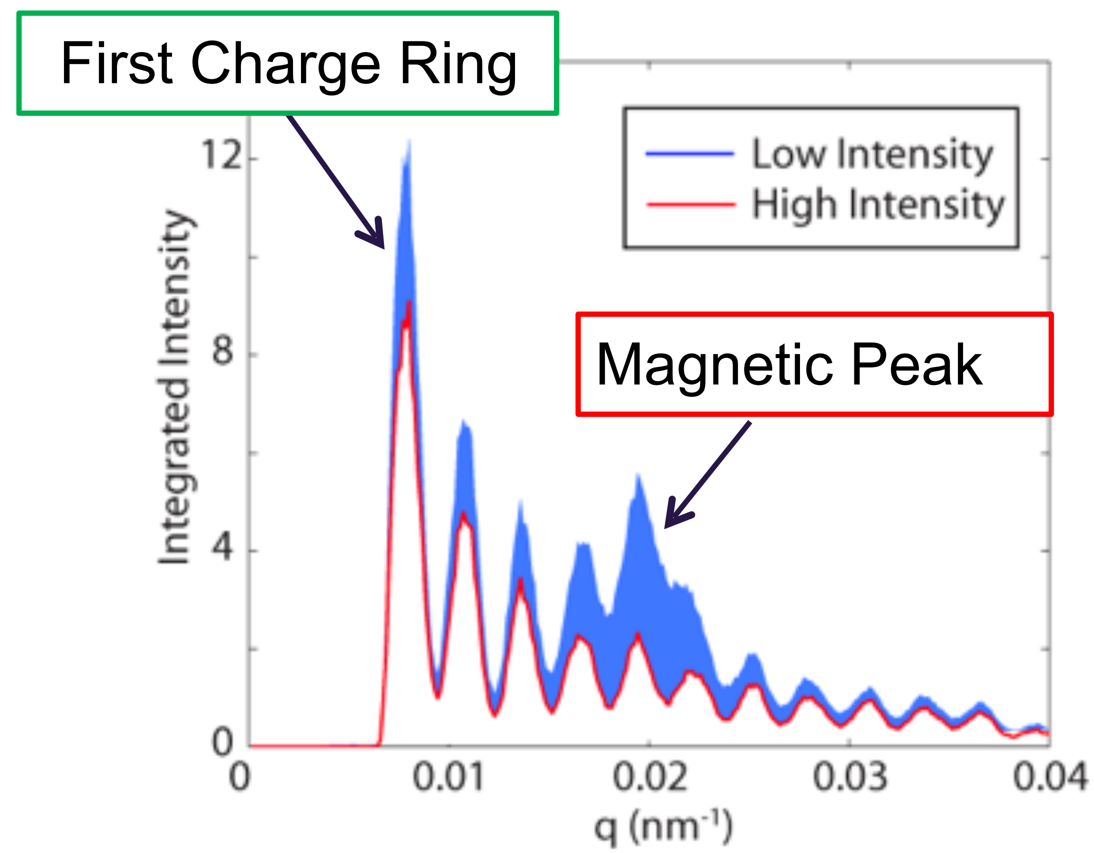

Wu *et al.* , PRL 117, 027401 (2016)

Single shot diffraction of atomic versus magnetic structure

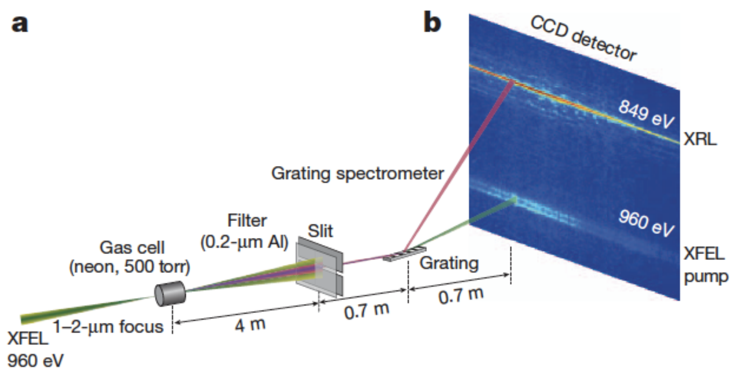

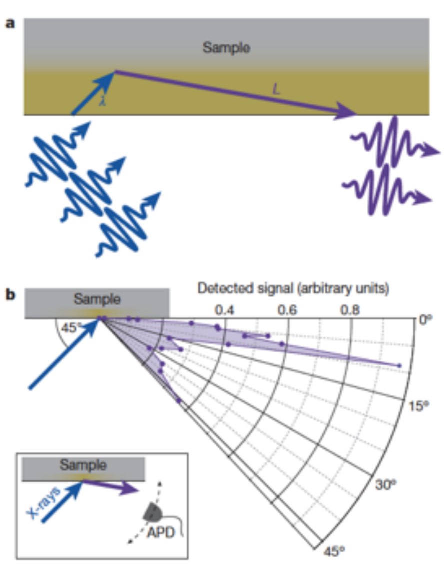

1 KJ/cm^2 ←

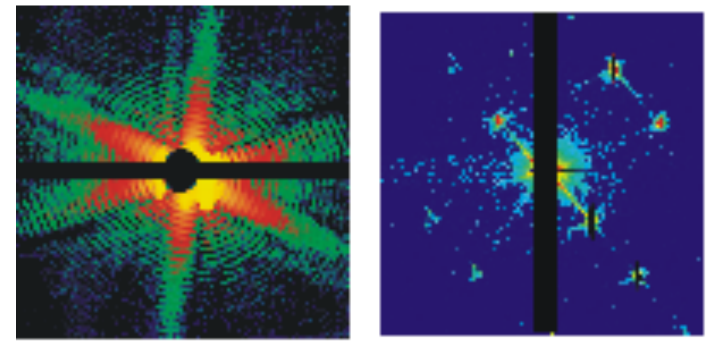

atomic structure:
single shot pattern of
virus or crystal

> 10^3 difference in fluence !

1 J/cm^2

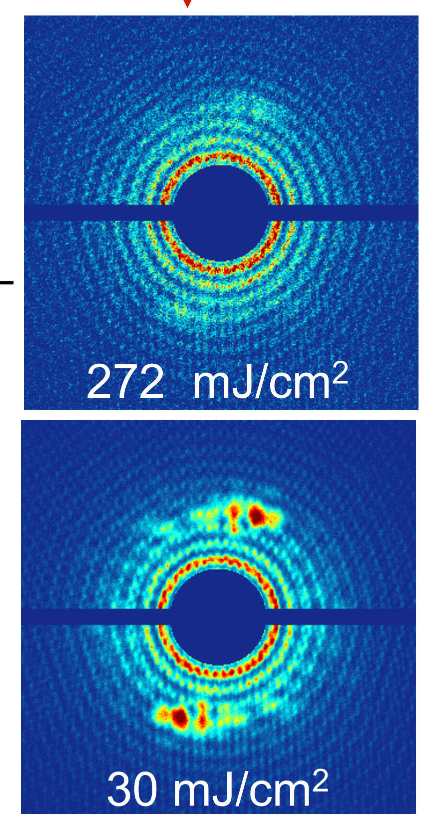

single shot
magnetic
imaging

1 mJ/cm^2

magnetic structure:
Co/Pt domains
50 fs pulses

Optical theorem

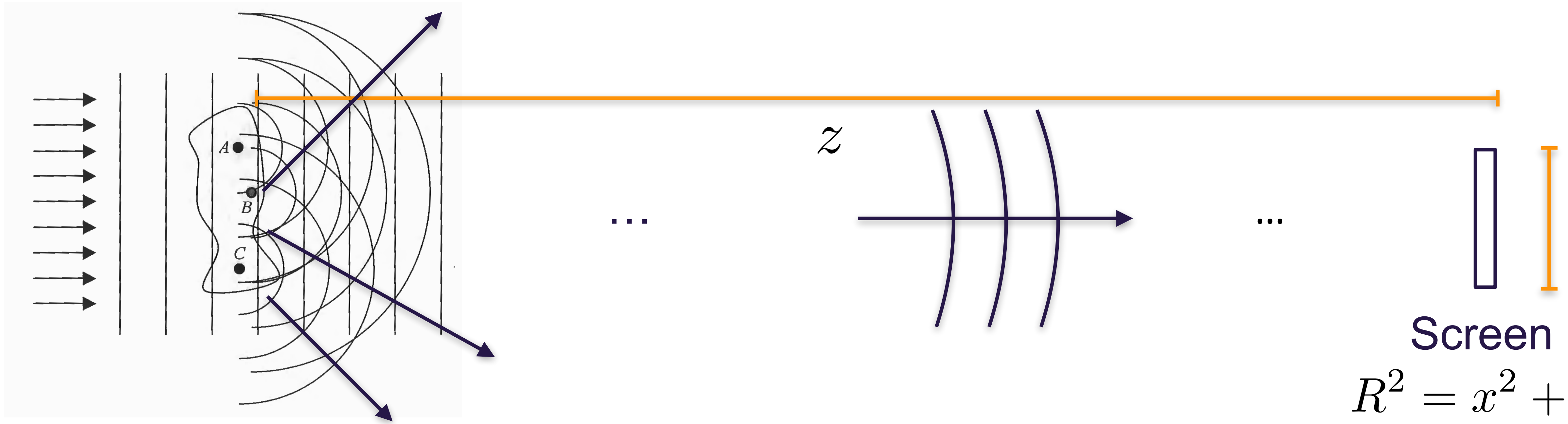

$$R^2 = x^2 + y^2$$

$$\psi_{\text{tot}}(r \simeq z) = \exp\left[ik_0 z\right] + \frac{\exp\left[i\boldsymbol{kr}\right]}{r} f(\boldsymbol{q}) \qquad \psi_{\text{tot}} \simeq \exp\left[ikz\right]\left\{1 + \frac{\exp\left[ik(x^2+y^2)/2z\right]}{z} f(\boldsymbol{q} \simeq 0)\right\}$$

in the forward direction we require $kR^2/z \gg 2\pi \text{ and } R/z \ll 1$

$$\Rightarrow \int ds|\psi_{\text{tot}}|^2 = \pi R^2 - \frac{4\pi}{k}\text{Im}\left\{f(q=0)\right\}$$

$$\sigma_{\text{sc}} = 4\pi(f'^2 + f''^2)$$

$$\frac{2\pi}{\lambda}\frac{\Gamma_{\text{tot}}}{\Gamma_x}\left(f'^{\,2} + f''^{\,2}\right) = f''(0)$$

$$\sigma_{\text{abs}} = \frac{\Gamma_A}{\Gamma} 2\lambda f''$$

R.G. Newton, Am. J. Phys. 44, 639 (1976)

Optical constants, response function and their relation to the atomic scattering length

Refractive index and electric susceptibility

$$n_\omega^2 = 1 + \chi(\omega) = 1 + \chi'(\omega) + i\chi''(\omega)$$

Optical constants

$$n_\omega = 1 - \delta_\omega + i\beta_\omega$$

Atomic scattering length

$$f(\omega) = r_0 Z + f'(\omega) - i f''(\omega)$$

$$\delta_\omega = \frac{2\pi}{k^2} N_{\text{at}} (r_0 Z + f'(\omega))$$

$$\beta_\omega = \frac{2\pi}{k^2} N_{\text{at}} f''(\omega)$$

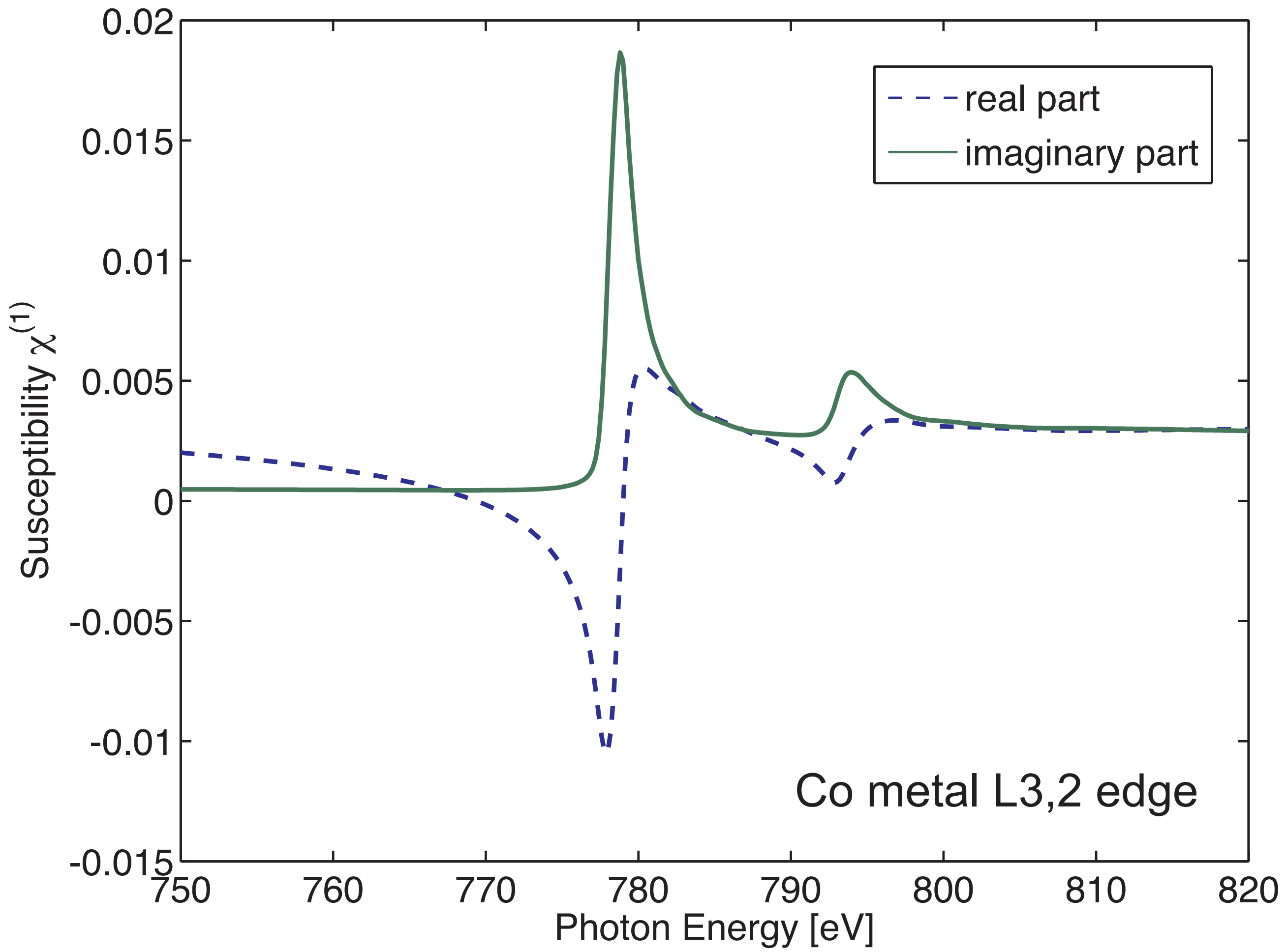

Kramers-Heisenberg vs. Bloch-Rabi

Stimulated resonant process

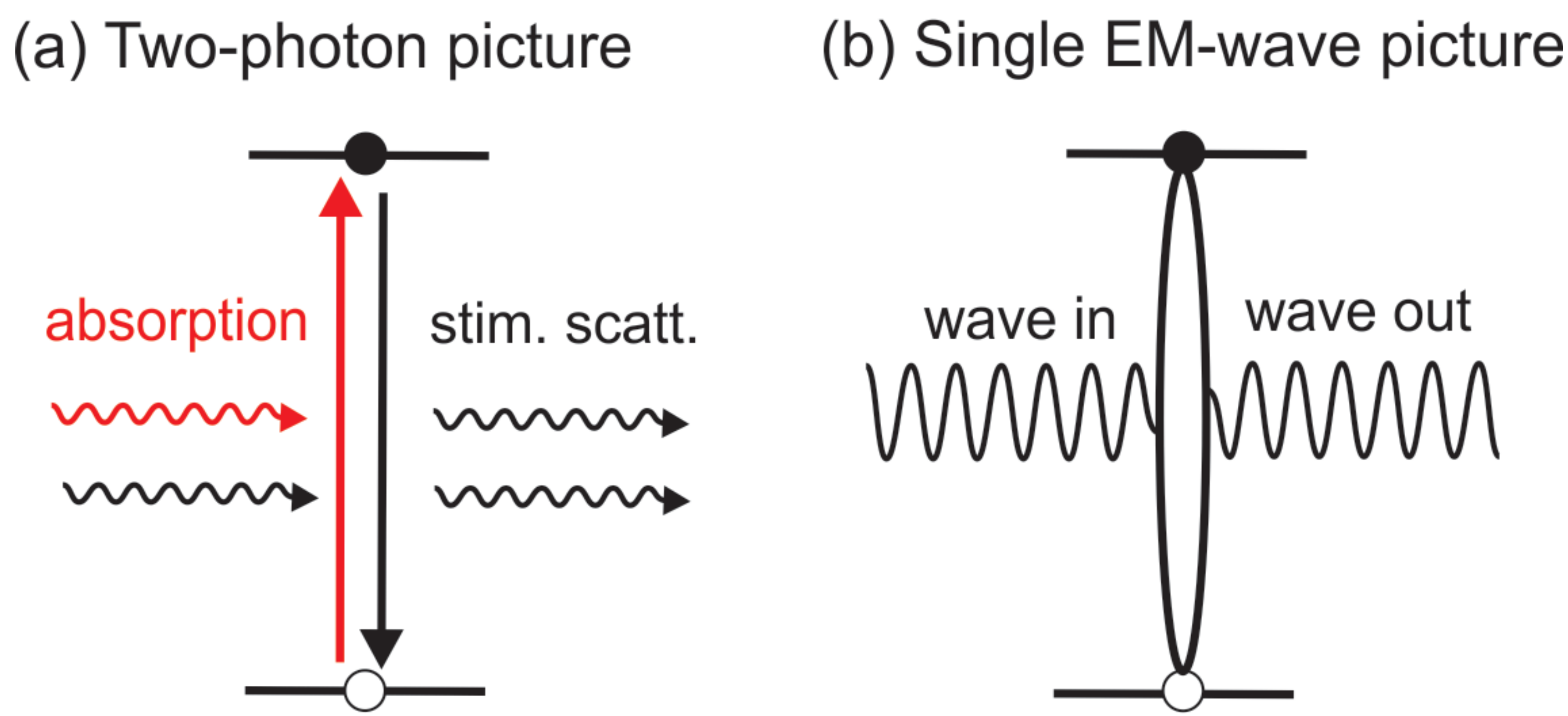

Polarisability and nonlinear media response
Estimate of higher order response

Polarisability

$$\boldsymbol{P}(t) = \varepsilon_0 \chi \boldsymbol{E}(t)$$

$$\boldsymbol{P}(t) = \varepsilon_0 \left(\chi^{(1)} + \chi^{(2)}\boldsymbol{E}(t) + \chi^{(3)}\boldsymbol{E}^2(t) + \cdots\right)\boldsymbol{E}(t)$$

$$\equiv \boldsymbol{P}^{(1)} + \boldsymbol{P}^{(2)} + \boldsymbol{P}^{(3)} + \cdots$$

$$\chi = \chi^{(1)} + \chi^{(2)}\boldsymbol{E}(t) + \chi^{(3)}\boldsymbol{E}^2(t) + \cdots$$

Polarisability and nonlinear media response
Estimate of higher order response

Polarisability

$$\boldsymbol{P}(t) = \varepsilon_0 \chi \boldsymbol{E}(t)$$

$$\boldsymbol{P}(t) = \varepsilon_0 \left(\chi^{(1)} + \chi^{(2)} \boldsymbol{E}(t) + \chi^{(3)} \boldsymbol{E}^2(t) + \cdots \right) \boldsymbol{E}(t)$$

$$\equiv \boldsymbol{P}^{(1)} + \boldsymbol{P}^{(2)} + \boldsymbol{P}^{(3)} + \cdots$$

$$\chi = \chi^{(1)} + \chi^{(2)} \boldsymbol{E}(t) + \chi^{(3)} \boldsymbol{E}^2(t) + \cdots$$

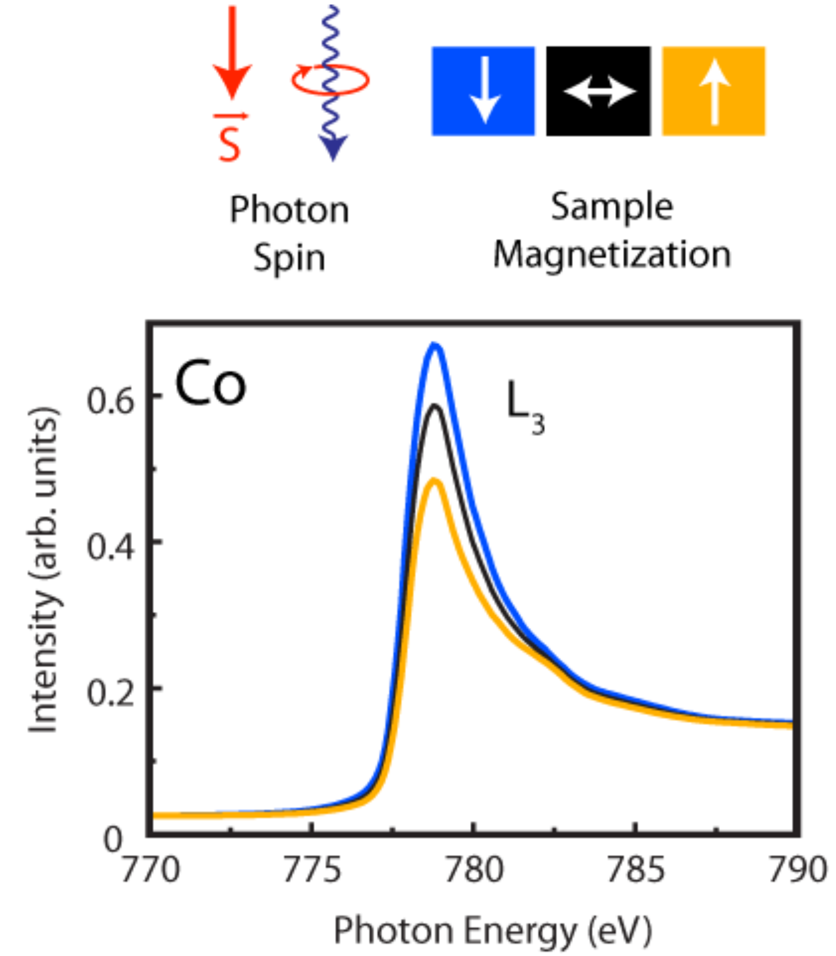

When NL terms compete with the linear term?

$$\chi^{(n)} = \chi^{(n-1)}/|\boldsymbol{E}| \simeq \chi^{(n-1)}/|\boldsymbol{E}_{\mathrm{atom}}|$$

$$\hbar\omega_{\mathrm{L23}} = \int_{2p}^{3d} \mathrm{d}r \, eE_{\mathrm{atom}} = eE_{\mathrm{atom}} |\mathcal{R}_{\mathrm{2p3d}}|$$

$$\mathcal{R}_{\mathrm{2p3d}} = 6.2 \times 10^{-3} \ \mathrm{e\,nm}$$

Polarisability and nonlinear media response
Estimate of higher order response

Polarisability

$$\boldsymbol{P}(t) = \varepsilon_0 \chi \boldsymbol{E}(t)$$

$$\boldsymbol{P}(t) = \varepsilon_0 \left(\chi^{(1)} + \chi^{(2)} \boldsymbol{E}(t) + \chi^{(3)} \boldsymbol{E}^2(t) + \cdots \right) \boldsymbol{E}(t)$$

$$\equiv \boldsymbol{P}^{(1)} + \boldsymbol{P}^{(2)} + \boldsymbol{P}^{(3)} + \cdots$$

$$\chi = \chi^{(1)} + \chi^{(2)} \boldsymbol{E}(t) + \chi^{(3)} \boldsymbol{E}^2(t) + \cdots$$

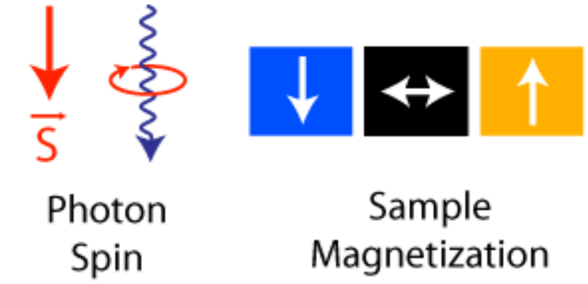

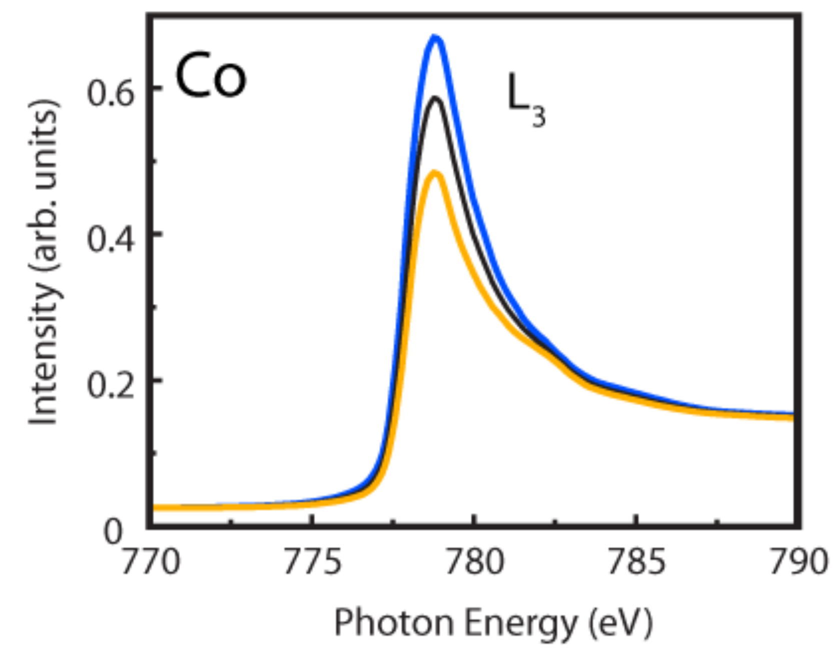

When NL terms compete with the linear term?

$$\chi^{(n)} = \chi^{(n-1)} / |\boldsymbol{E}| \simeq \chi^{(n-1)} / |\boldsymbol{E}_{\text{atom}}|$$

$$\hbar\omega_{\text{L23}} = \int_{2p}^{3d} \mathrm{d}r \, eE_{\text{atom}} = eE_{\text{atom}} |\mathcal{R}_{\text{2p3d}}|$$

$$\mathcal{R}_{\text{2p3d}} = 6.2 \times 10^{-3} \ \mathrm{e\,nm}$$

$$\Longrightarrow \quad E_{\text{atom}} = 1.3 \times 10^{12} \, \frac{\mathrm{V}}{\mathrm{cm}}$$

$$\chi^{(1)} \simeq 1 \times 10^{-3}$$

$$\chi^{(2)} = \chi^{(1)} / E_{\text{atom}} \simeq 0.8 \times 10^{-15} \ \frac{\text{cm}}{\text{V}}$$

$$\chi^{(3)} = \chi^{(1)} / E^2_{\text{atom}} \simeq 0.6 \times 10^{-27} \ \frac{\text{cm}^2}{\text{V}^2}$$

The classical anharmonic oscillator model off-resonant vs. resonant nonlinear response

$$U(x) = \frac{1}{2}m\omega_0^2 x^2 - \frac{1}{4}mbx^4$$

- Nonlinearity constant: $b = \dfrac{\omega_0^2}{d^2 a_0^2}$

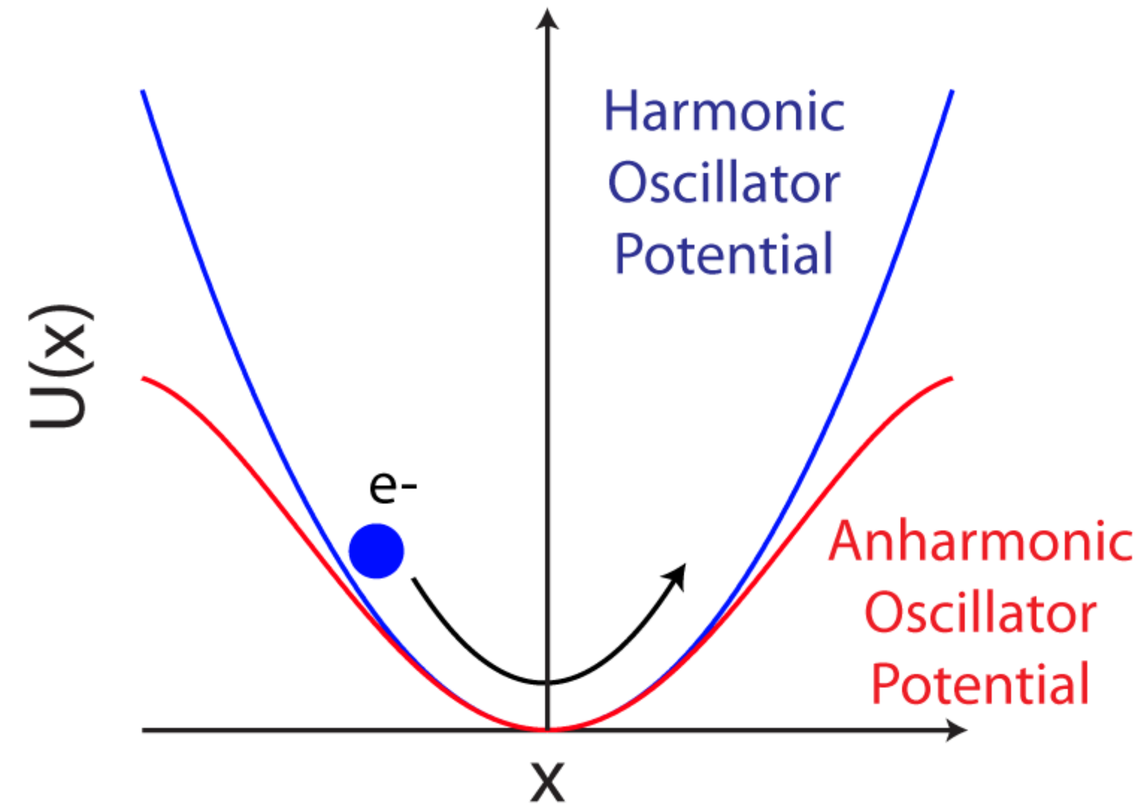

The classical anharmonic oscillator model off-resonant vs. resonant nonlinear response

$$U(x) = \frac{1}{2}m\omega_0^2x^2 - \frac{1}{4}mbx^4$$

- Nonlinearity constant: $b = \frac{\omega_0^2}{d^2a_0^2}$

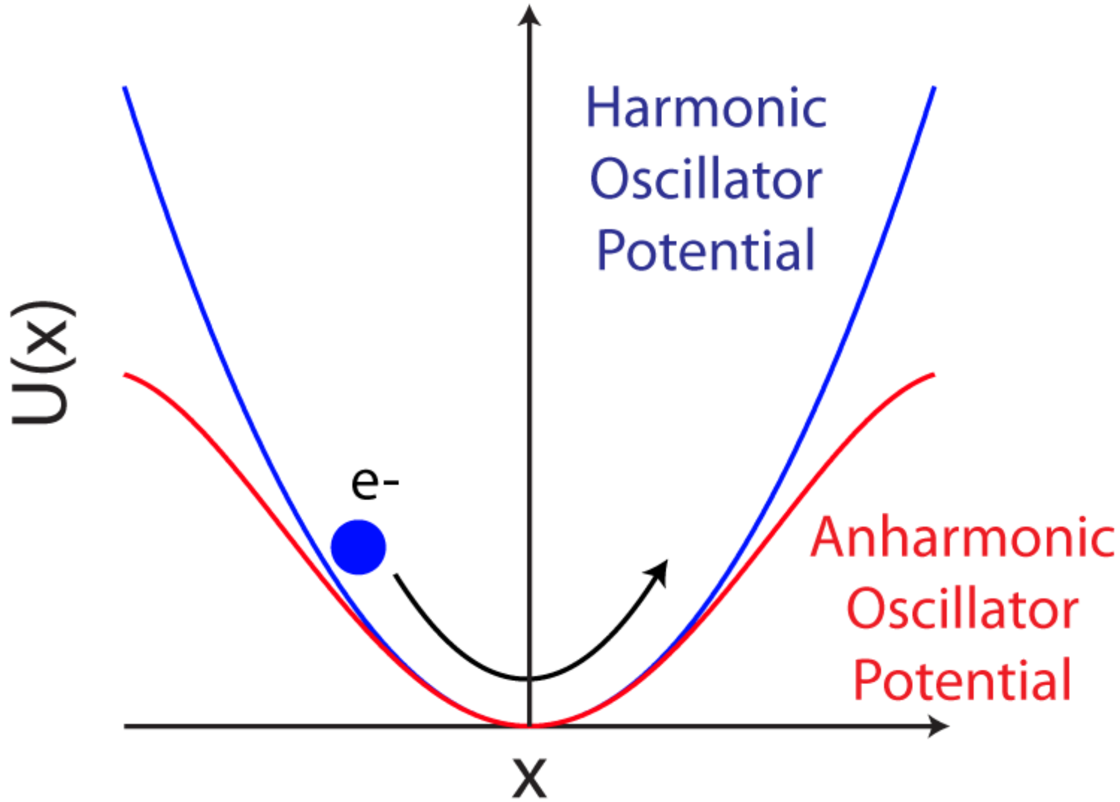

- Off-resonant Nonlinear response

⇨ $$\chi^{(3)}_{\text{off}}(\omega_0) = \frac{Ne^4}{\varepsilon_0 d^2 a_0^2 m^3 \omega_0^6}$$

The classical anharmonic oscillator model off-resonant vs. resonant nonlinear response

$$U(x) = \frac{1}{2}m\omega_0^2x^2 - \frac{1}{4}mbx^4$$

- Nonlinearity constant: $b = \frac{\omega_0^2}{d^2a_0^2}$

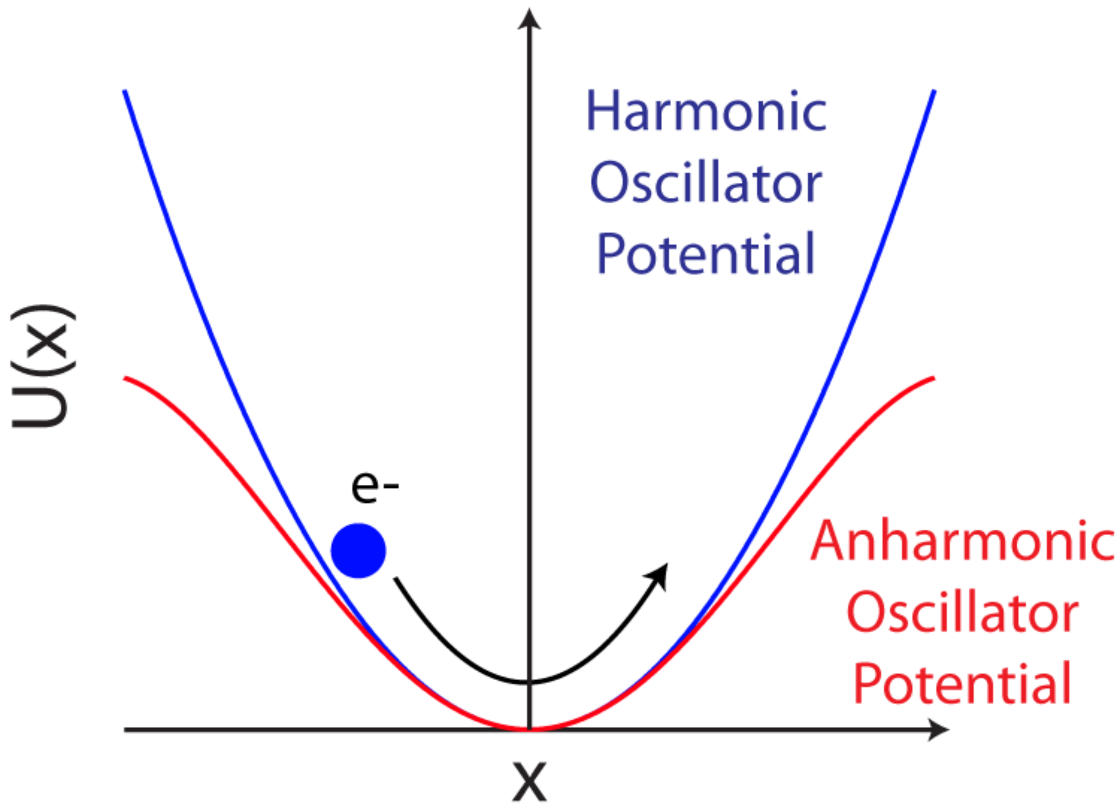

- Off-resonant Nonlinear response

$$\chi^{(3)}_{\text{off}}(\omega_0) = \frac{Ne^4}{\varepsilon_0 d^2 a_0^2 m^3 \omega_0^6}$$

- Resonant Nonlinear response

$$\chi^{(3)}_{\text{res}}(\omega_0) = \frac{Ne^4}{16\varepsilon_0 d^2 a_0^2 m^3 \omega_0^2 \gamma^4}$$

The classical anharmonic oscillator model off-resonant vs. resonant nonlinear response

$$U(x) = \frac{1}{2}m\omega_0^2 x^2 - \frac{1}{4}mbx^4$$

- Nonlinearity constant: $b = \frac{\omega_0^2}{d^2 a_0^2}$

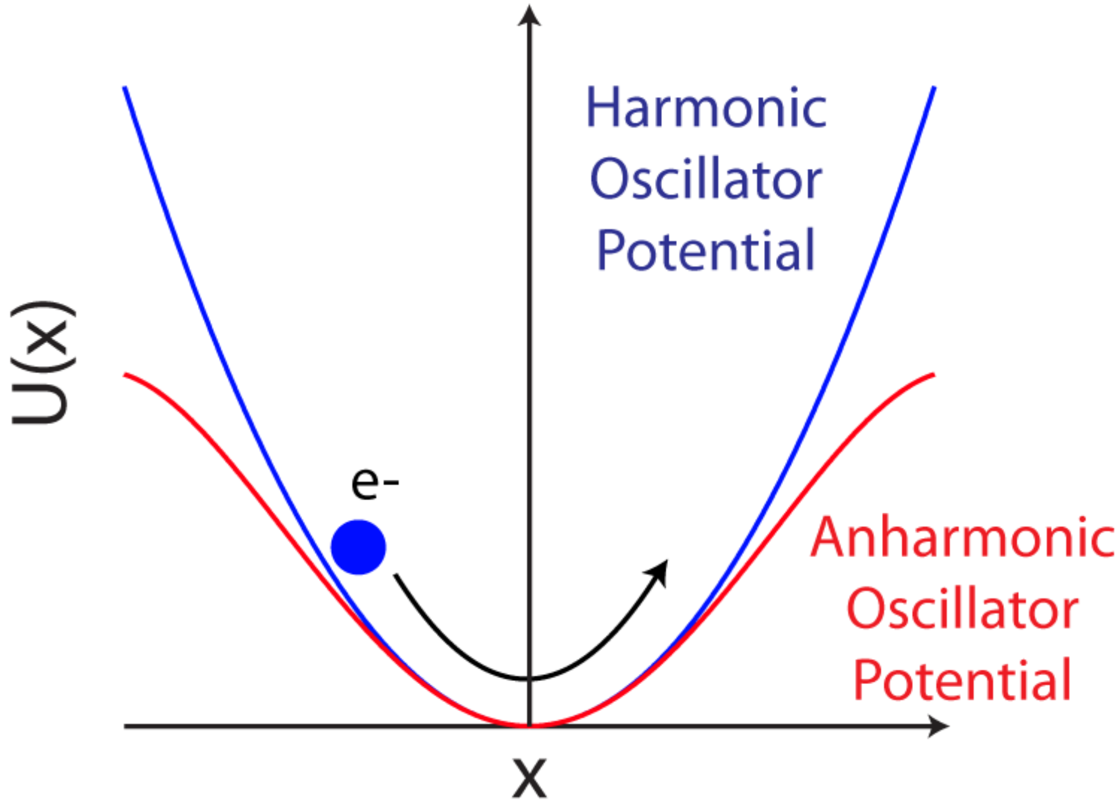

- Off-resonant Nonlinear response

$$\chi^{(3)}_{\text{off}}(\omega_0) = \frac{Ne^4}{\varepsilon_0 d^2 a_0^2 m^3 \omega_0^6}$$

- Resonant Nonlinear response

$$\chi^{(3)}_{\text{res}}(\omega_0) = \frac{Ne^4}{16\varepsilon_0 d^2 a_0^2 m^3 \omega_0^2 \gamma^4}$$

$$\chi^{(3)}_{\text{off}}(\omega_0) \simeq 1.1 \times 10^{-27} \frac{\text{cm}^2}{\text{V}^2}$$

$$\chi^{(3)}_{\text{res}}(\omega_0) \simeq 2 \times 10^{-20} \frac{\text{cm}^2}{\text{V}^2}$$

- Co metal

$N = 90$ at./nm^3

$d = 2.4$ in units of the Bohr radius a_0

$\gamma \simeq 0.4$ eV

The classical anharmonic oscillator model off-resonant vs. resonant nonlinear response

$$U(x) = \frac{1}{2}m\omega_0^2 x^2 - \frac{1}{4}mbx^4$$

- Nonlinearity constant: $b = \frac{\omega_0^2}{d^2 a_0^2}$

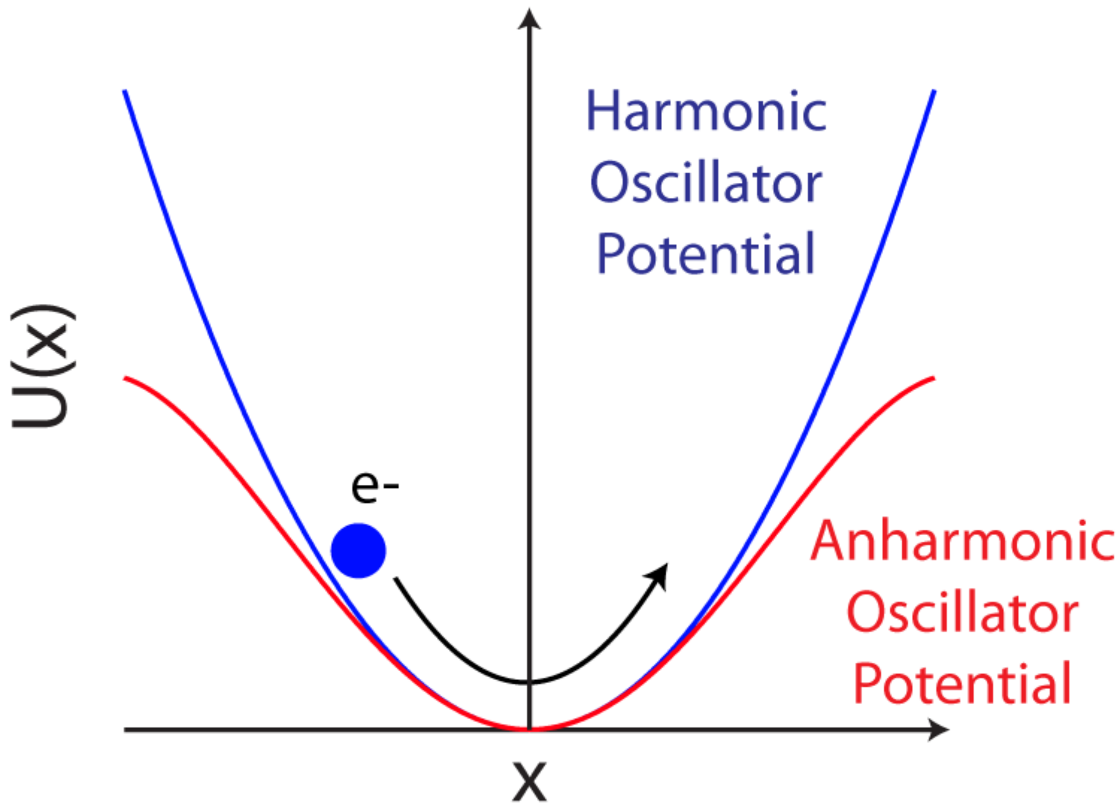

Off-resonant Nonlinear response

$$\chi^{(3)}_{\text{off}}(\omega_0) = \frac{Ne^4}{\varepsilon_0 d^2 a_0^2 m^3 \omega_0^6}$$

Resonant Nonlinear response

$$\chi^{(3)}_{\text{res}}(\omega_0) = \frac{Ne^4}{16\varepsilon_0 d^2 a_0^2 m^3 \omega_0^2 \gamma^4}$$

$$\chi^{(3)}_{\text{off}}(\omega_0) \simeq 1.1 \times 10^{-27}\,\frac{\text{cm}^2}{\text{V}^2}$$

$$\chi^{(3)}_{\text{res}}(\omega_0) \simeq 2 \times 10^{-20}\,\frac{\text{cm}^2}{\text{V}^2}$$

$$\chi^{(3)}_{\text{off}}(\text{optical}) \sim 1 \times 10^{-18}\,\frac{\text{cm}^2}{\text{V}^2}$$

Nonlinear term at soft x-ray resonances becomes almost as large as the nonlinear term at optical wavelengths

Optical Bloch equations of a two-level system

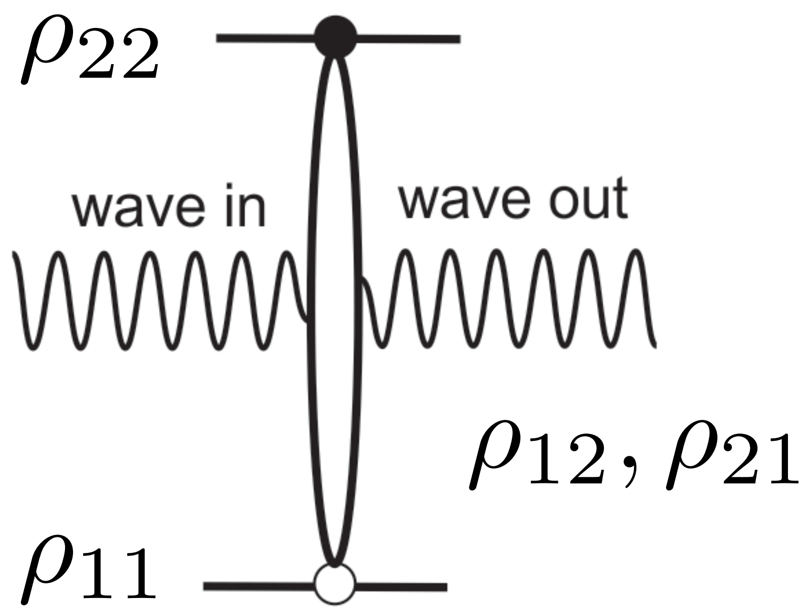

$$\Gamma = \Gamma_x + \Gamma_a$$

$$\gamma = \frac{1}{2}\Gamma_x + \frac{1}{2}\Gamma_a + \gamma_{el}$$

Equation of motion for state populations and coherences

$$\frac{\mathrm{d}}{\mathrm{d}t}\Delta\rho_{21} = -\Gamma\left(\Delta\rho_{21} - \Delta\rho_{21}^{\mathrm{eq}}\right) - \frac{2i}{\hbar}\left(V_{21}\rho_{12} - \rho_{21}V_{12}\right)$$

$$\dot{\rho}_{21} = -\left(i\omega_{21} + \gamma\right)\rho_{21} + \frac{i}{\hbar}V_{21}\Delta\rho_{21}$$

$$V_{21} = -\mu_{21}E(t) = -e\left\langle 1\right|\epsilon r\left|2\right\rangle E\mathrm{e}^{-i\omega t}$$

Excited state population in the Bloch picture

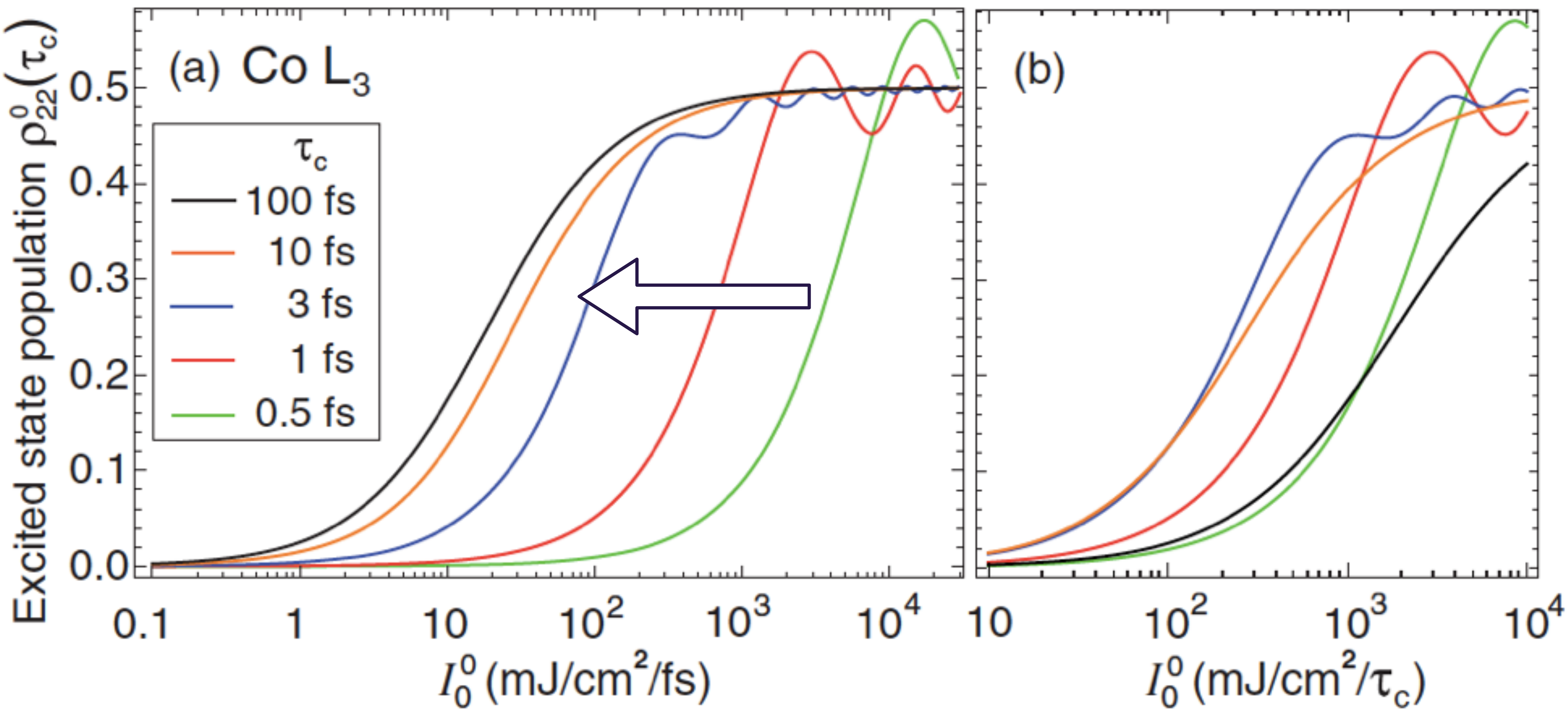

For $\tau_c \gg \hbar/\Gamma_A = 1.5\text{fs}$ (Auger decay time)

Equilibrium excited state population:

Stöhr, Scherz, PRL 115, 107402 (2015)

Steady state response of the two level system

Polarisability

$$P = \chi\varepsilon_0 E = n_a \mathrm{tr}\,(\rho\mu) = n_a(\rho_{12}\mu_{21} + \rho_{21}\mu_{12})$$

Susceptibility

$$\chi = \frac{n_a|\mu_{21}|^2(\omega - \omega_{21} - i\gamma)\Delta\rho_{21}^{\mathrm{eq}}}{\varepsilon_0\hbar\left[(\omega - \omega_{21})^2 + \gamma^2 + 4\gamma/\Gamma\mathcal{V}^2\right]}$$

Rabi Frequency

$$\mathcal{V} = |\mu_{21}|\,|E|/\hbar \qquad \Gamma_x = \frac{4\pi^2}{\varepsilon_0\hbar\lambda^3}|\mu_{21}|^2 = \frac{4\pi^2\hbar}{\varepsilon_0\lambda^3}\boxed{\frac{\mathcal{V}^2}{|E|^2}}$$

Nonlinear atomic scattering length

$$\chi = \chi^{(1)} \boxed{\frac{1}{1 + \mathcal{G}\frac{\Gamma_x \gamma}{\Delta^2+\gamma^2}\langle n_x \rangle}} = \chi^{(1)} \mathcal{B}_{\mathrm{NL}} \qquad \mathcal{V}^2 = \frac{1}{4}\mathcal{G}\Gamma_x \Gamma \langle n \rangle$$

$$\chi^{(1)} = \frac{n_a \lambda^3}{4\pi^2} \frac{\Gamma_x(\Delta - i\gamma)}{\Delta^2 + \gamma^2} \Delta\rho_{21}^{\mathrm{eq}}$$

atomic scattering length

$$f' = -\frac{\lambda}{4\pi} \frac{\Gamma_x \Delta}{\Delta^2 + \gamma^2} \Delta\rho_{21}^{\mathrm{eq}} \mathcal{B}_{\mathrm{NL}} - r_0 Z = f_0' \mathcal{B}_{\mathrm{NL}} - r_0 Z$$

$$f'' = -\frac{\lambda}{4\pi} \boxed{\frac{\Gamma_x \gamma}{\Delta^2 + \gamma^2}} \Delta\rho_{21}^{\mathrm{eq}} \mathcal{B}_{\mathrm{NL}} = f_0'' \mathcal{B}_{\mathrm{NL}}$$

$$\boxed{\mathcal{B}_{\mathrm{NL}} = \frac{1}{1 + \frac{4\pi}{\lambda} f_0'' \mathcal{G} \langle n \rangle}}$$

European XFEL

Single pole approximation

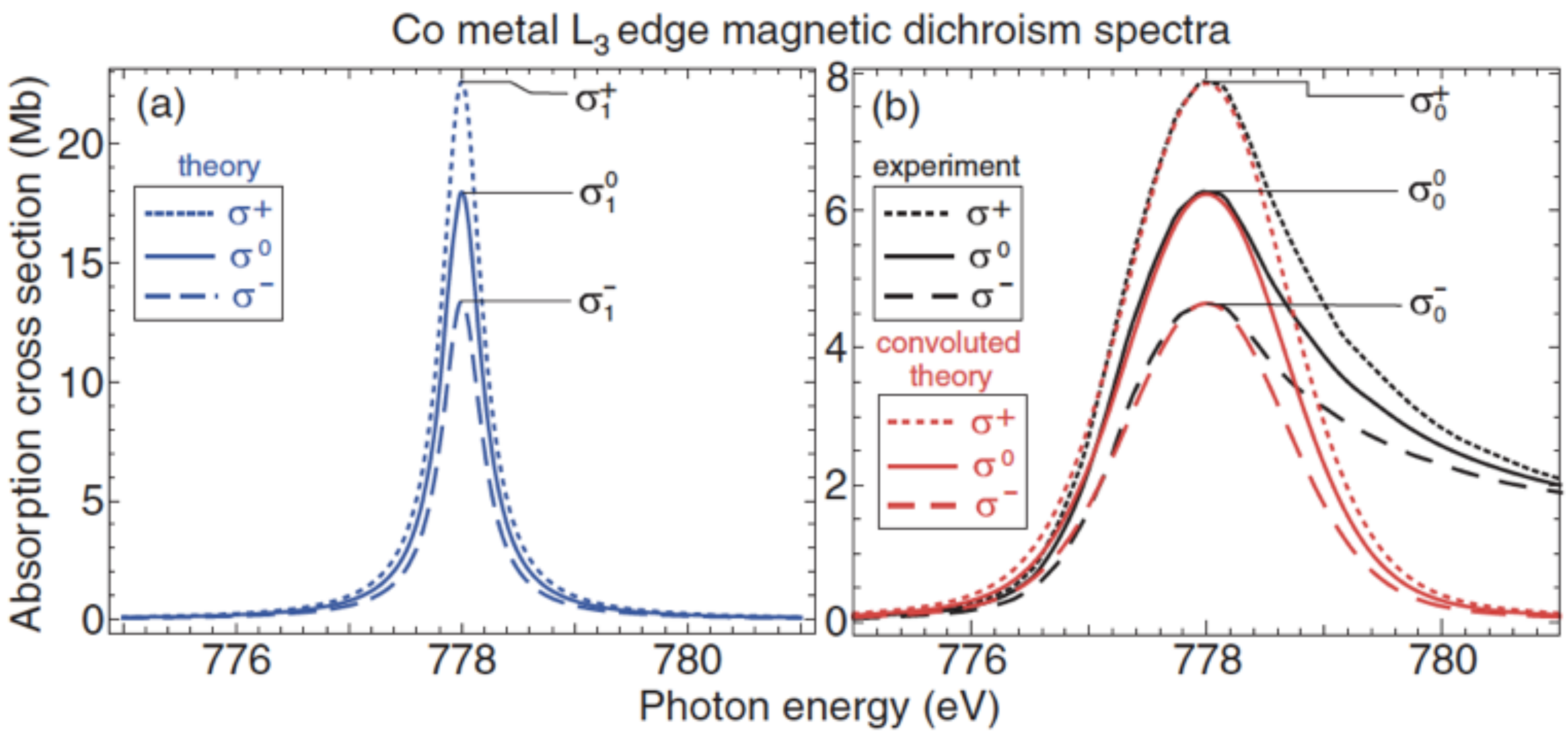

TABLE I. Polarization dependent parameters for the L_3 resonances of Fe, Co, and Ni metals. Listed are the atomic number densities ρ_a, the resonance energies and wavelengths, and the polarization dependent ($q = 0, \pm$) peak experimental cross sections σ_0^q (1 Mb $= 10^{-4}$ nm^2), assuming propagation along the magnetization direction. Γ_x^q is the polarization dependent dipole transition width which includes the number of valence holes N_h, and Γ is the natural decay energy width [15].

	ρ_a [atoms/nm^3]	$\mathcal{E}_0$ [eV]	λ_0 [nm]	σ_0^+ [Mb]	σ_0^0 [Mb]	σ_0^- [Mb]	Γ_x^+ [meV]	Γ_x^0 [meV]	Γ_x^- [meV]	Γ [eV]
Fe	84.9	707	1.75	8.8	6.9	5.0	1.37	1.08	0.78	0.36
Co	90.9	778	1.59	7.9	6.25	4.65	1.208	0.96	0.715	0.43
Ni	91.4	853	1.45	5.1	4.4	3.7	0.675	0.575	0.48	0.48

Stöhr, Scherz, PRL 115, 107402 (2015)

Onset of nonlinear contributions

High intensity $$\mathcal{B}_{\mathrm{NL}} = \frac{1}{1 + \frac{4\pi}{\lambda} f_0'' \mathcal{G} \langle n \rangle}$$

Med intensity $$\mathcal{B}_{\mathrm{NL}} \simeq 1 - \frac{4\pi}{\lambda} \mathcal{G} f_0'' \langle n \rangle$$

$$f' = f_0' - \frac{4\pi}{\lambda} f_0' f_0'' \mathcal{G} \langle n \rangle$$

$$f'' = f_0'' - \frac{4\pi}{\lambda} f_0''^{\,2} \mathcal{G} \langle n \rangle$$

Low intensity $\mathcal{B}_{\mathrm{NL}} \simeq 1 \quad f_0', \; f_0''$

Stöhr, Scherz, PRL 115, 107402 (2015)

First and third order response function

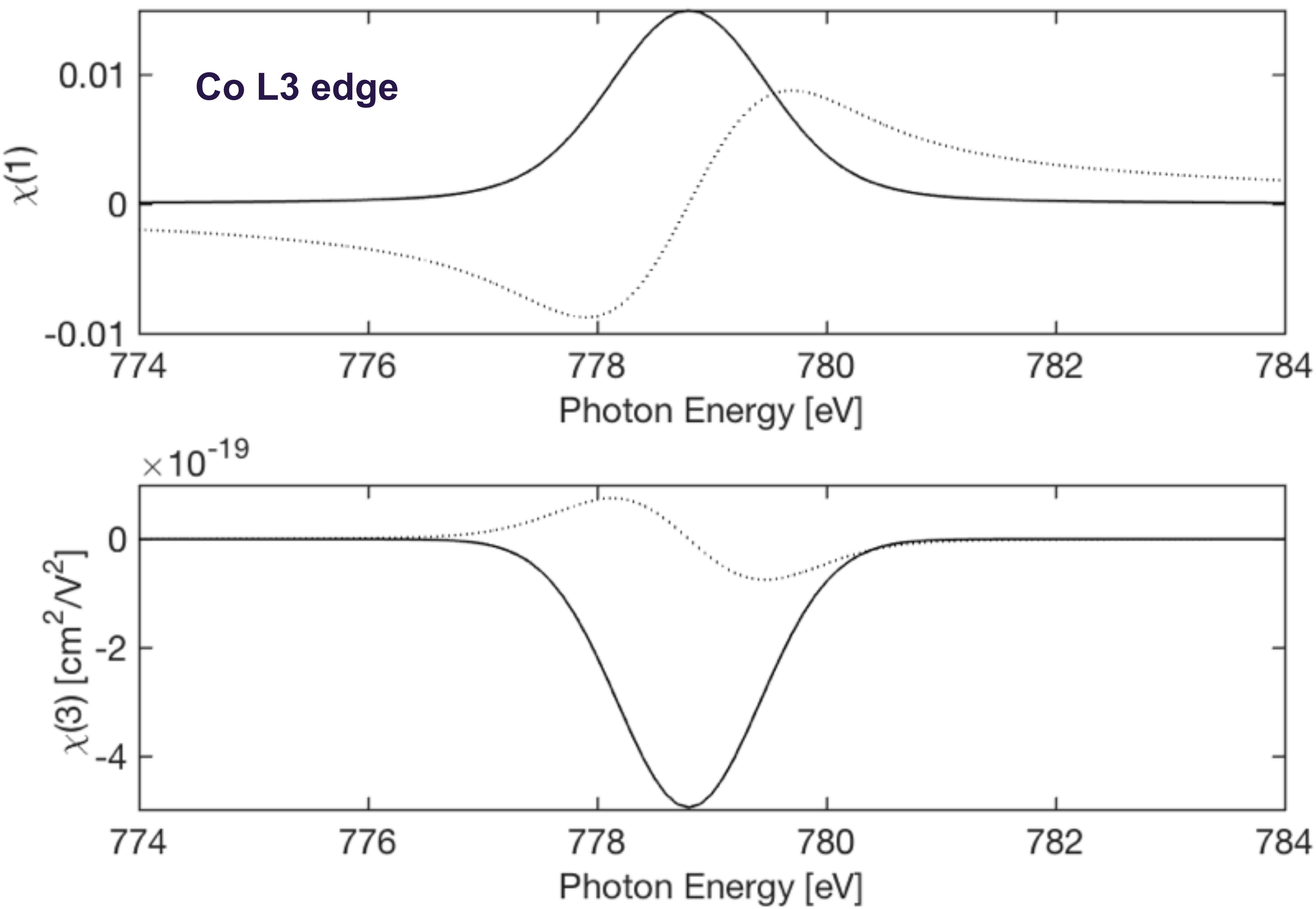

Gain Factor by coherent forward scattering

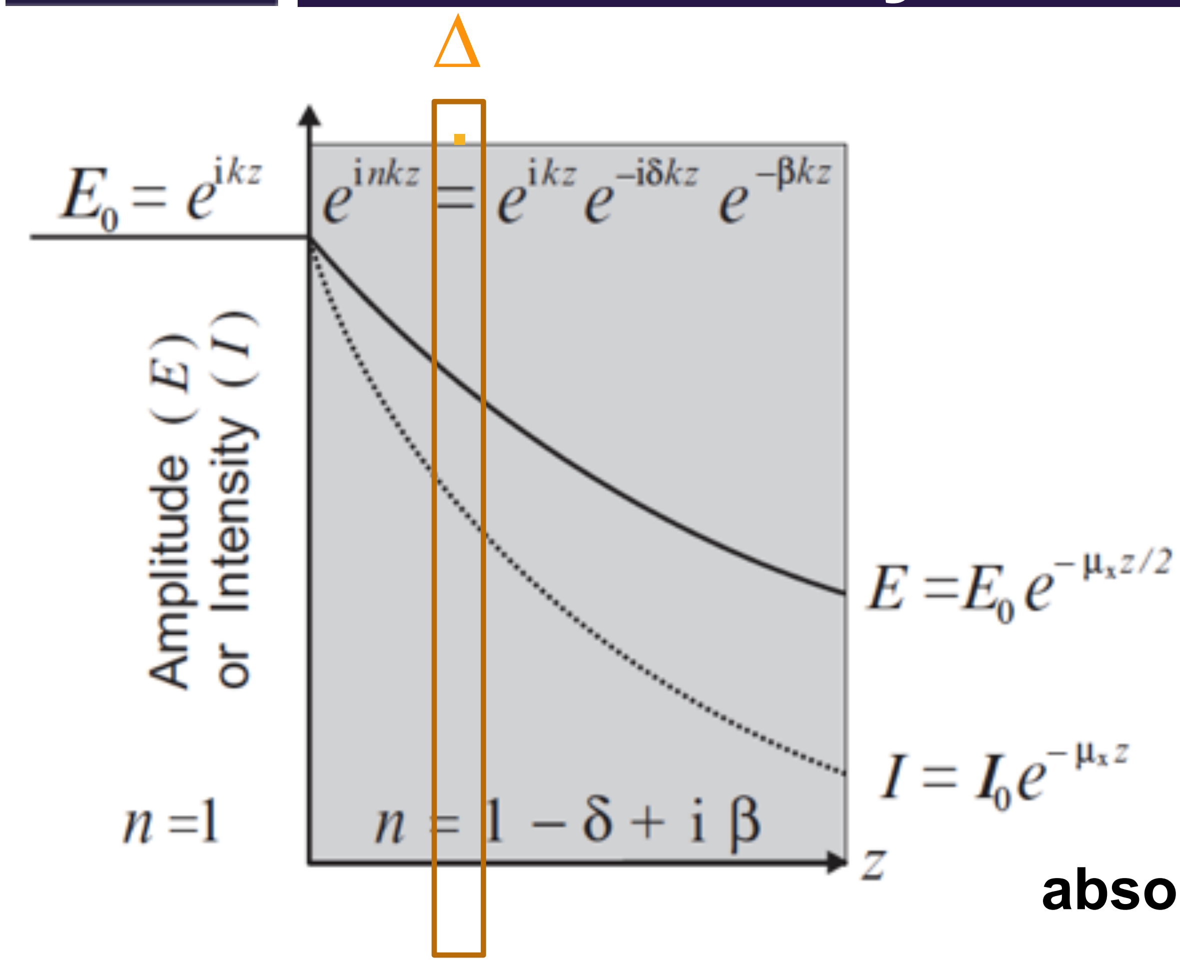

$$f' = f'_0 - \frac{4\pi}{\lambda} f'_0 f''_0 \mathcal{G} \langle n \rangle$$

$$f'' = f''_0 - \frac{4\pi}{\lambda} f''^2_0 \mathcal{G} \langle n \rangle$$

absorption loss **coherent forward scattering gain**

$$I_{\mathrm{FW}} = |E|^2 \simeq I_0 \left[1 - 2\lambda n_a \Delta f'' + 2\lambda^2 n_a^2 \Delta^2 f''^2\right]$$

$$I_{\mathrm{FW}} \simeq I_0 \left[1 - 2\lambda n_a \Delta f''_0 + 2\lambda^2 n_a^2 \Delta^2 f''^2_0 (1 + \frac{4\pi}{\lambda^2 n_a \Delta} \mathcal{G} \langle n \rangle)\right]$$

Gain factor: $\mathcal{G} = \dfrac{\lambda^2 N_a}{4\pi A}$

Saturable X-ray absorption

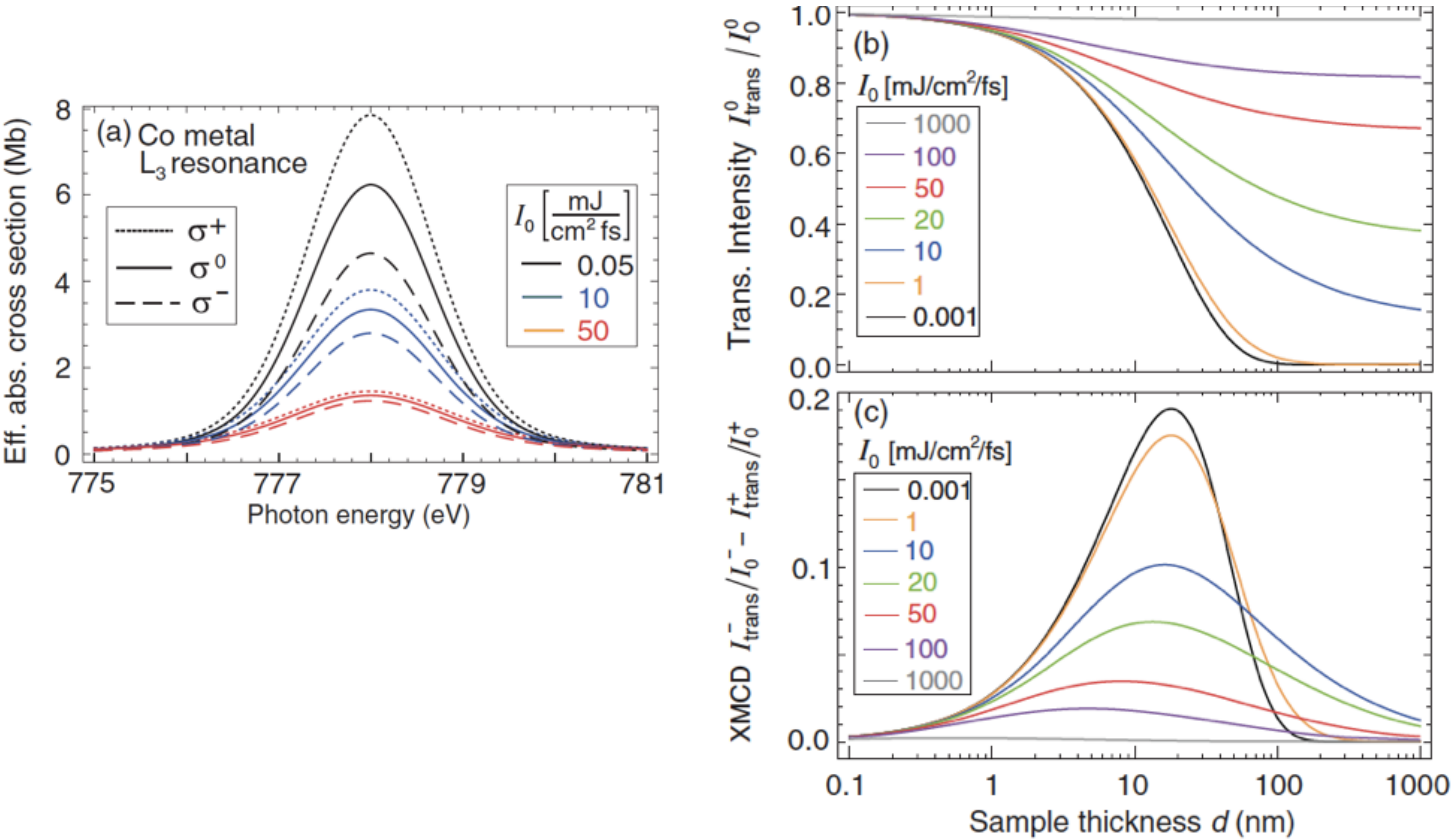

Stöhr, Scherz, PRL 115, 107402 (2015)

Experiment vs Theory

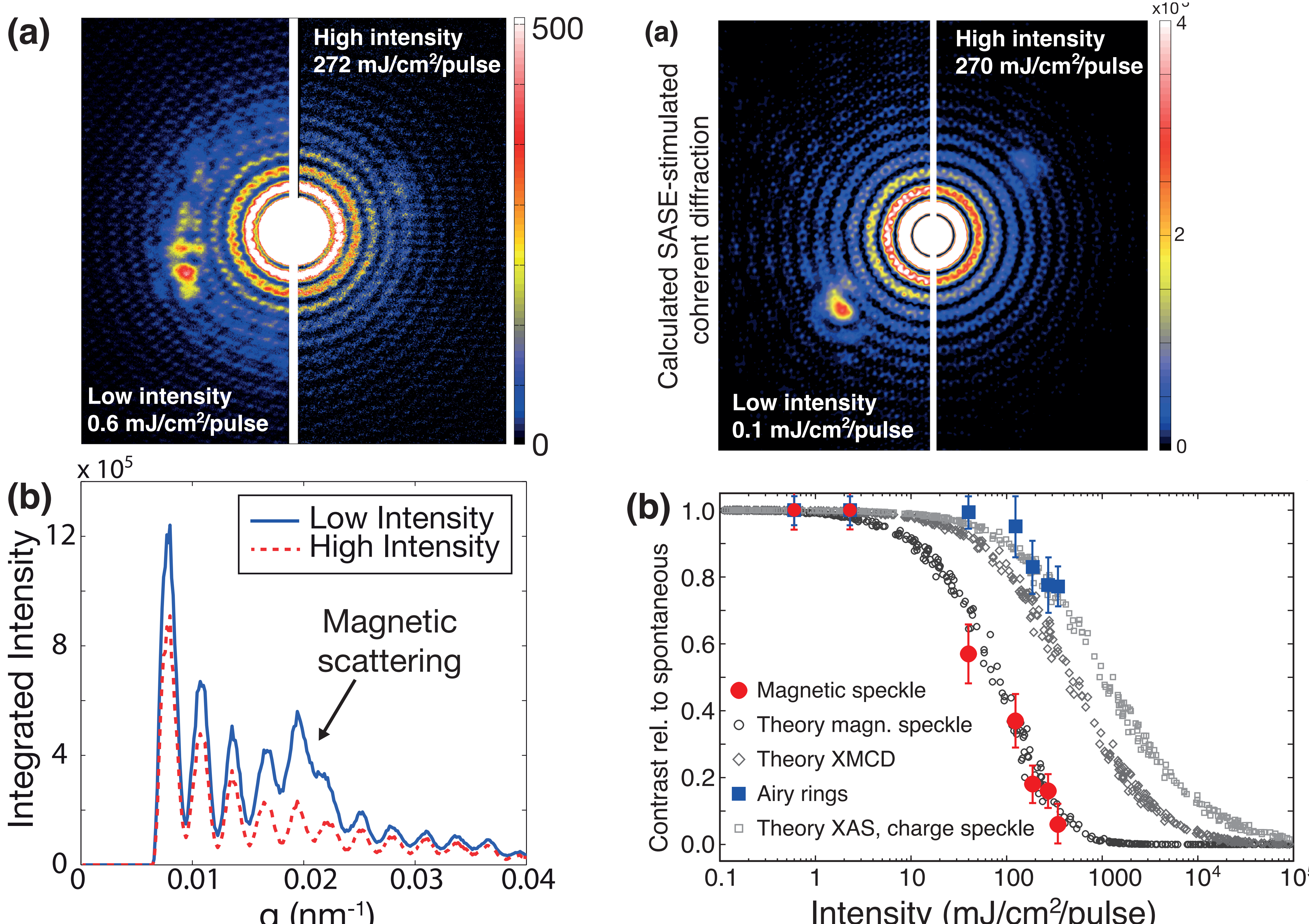

Wu *et al.* , PRL 117, 027401 (2016)

Optical theorem

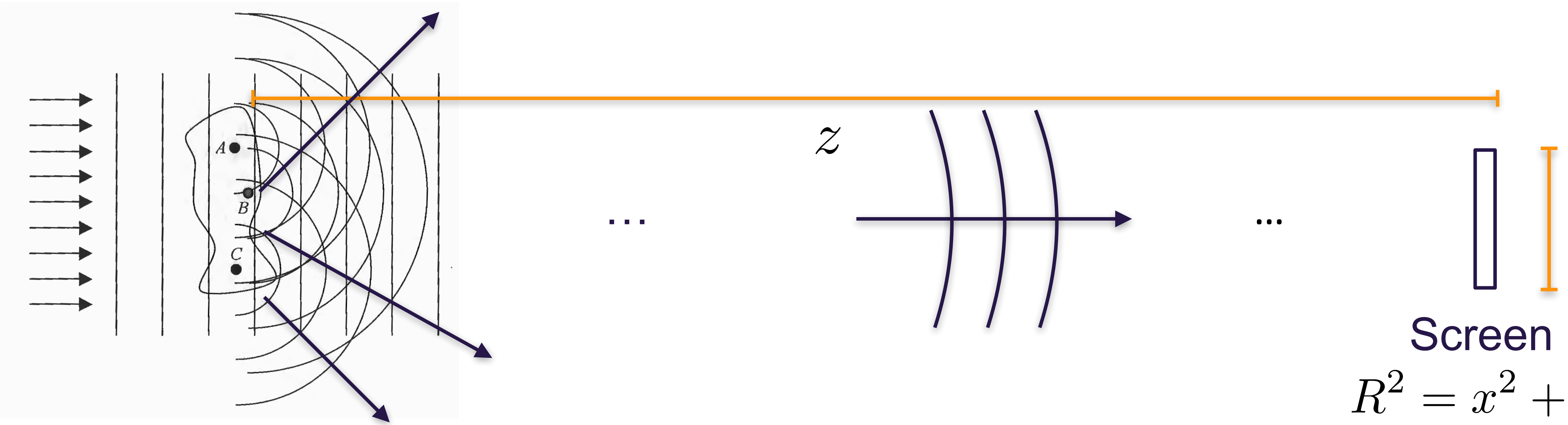

$$R^2 = x^2 + y^2$$

$$\psi_{\text{tot}}(r \simeq z) = \exp\left[ik_0 z\right] + \frac{\exp\left[i\boldsymbol{kr}\right]}{r} f(\boldsymbol{q}) \qquad \psi_{\text{tot}} \simeq \exp\left[ikz\right]\left\{1 + \frac{\exp\left[ik(x^2+y^2)/2z\right]}{z} f(\boldsymbol{q} \simeq 0)\right\}$$

in the forward direction we require $kR^2/z \gg 2\pi \text{ and } R/z \ll 1$

⇒ $$\int ds|\psi_{\text{tot}}|^2 = \pi R^2 - \frac{4\pi}{k}\text{Im}\left\{f(q=0)\right\}$$

$$\sigma_{\text{tot}} = \sigma_{\text{sc}} + \sigma_{\text{abs}} = \sigma_{\text{ex}} = \frac{4\pi}{k}\text{Im}f(0)$$

$$\sigma_{\text{sc}} = 4\pi(f'^2 + f''^2)$$

$$\sigma_{\text{abs}} = \frac{\Gamma_A}{\Gamma} 2\lambda f''$$

R.G. Newton, Am. J. Phys. 44, 639 (1976)

THREE-WAVE MIXING
FOUR-WAVE MIXING

Wave mixing in response theory

$$\boldsymbol{P}(t) = \varepsilon_0 \left(\chi^{(1)} + \chi^{(2)} \boldsymbol{E}(t) + \chi^{(3)} \boldsymbol{E}^2(t) + \cdots \right) \boldsymbol{E}(t)$$

$$P^{(1)}(\omega_2) = \varepsilon_0 \chi^{(1)}(\omega_2 = \pm\omega_1) E(\omega_1)$$

Wave mixing in response theory

$$\boldsymbol{P}(t) = \varepsilon_0 \left(\chi^{(1)} + \chi^{(2)} \boldsymbol{E}(t) + \chi^{(3)} \boldsymbol{E}^2(t) + \cdots \right) \boldsymbol{E}(t)$$

$$P^{(1)}(\omega_2) = \varepsilon_0 \chi^{(1)}(\omega_2 = \pm\omega_1) E(\omega_1)$$

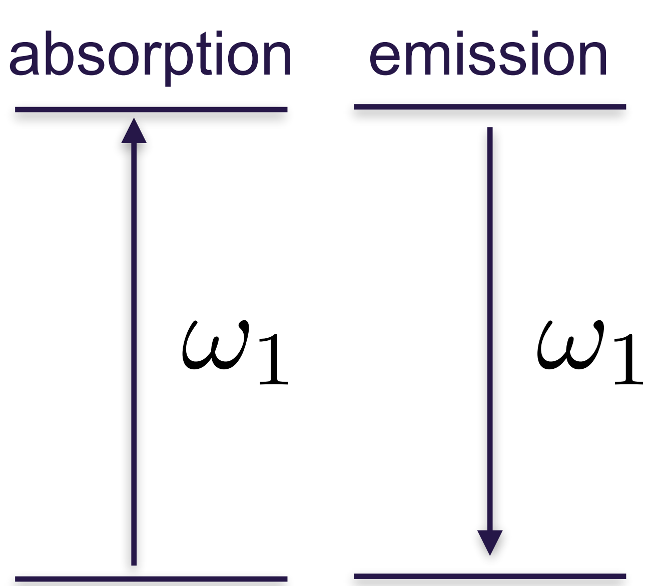

Wave mixing in response theory

$$\boldsymbol{P}(t) = \varepsilon_0 \left(\chi^{(1)} + \chi^{(2)} \boldsymbol{E}(t) + \chi^{(3)} \boldsymbol{E}^2(t) + \cdots \right) \boldsymbol{E}(t)$$

$$P^{(1)}(\omega_2) = \varepsilon_0 \chi^{(1)}(\omega_2 = \pm\omega_1) E(\omega_1)$$

$$P^{(2)}(\omega_3) = \varepsilon_0 \chi^{(2)}(\omega_3, \pm\omega_2, \pm\omega_1) E(\omega_2) E(\omega_1)$$

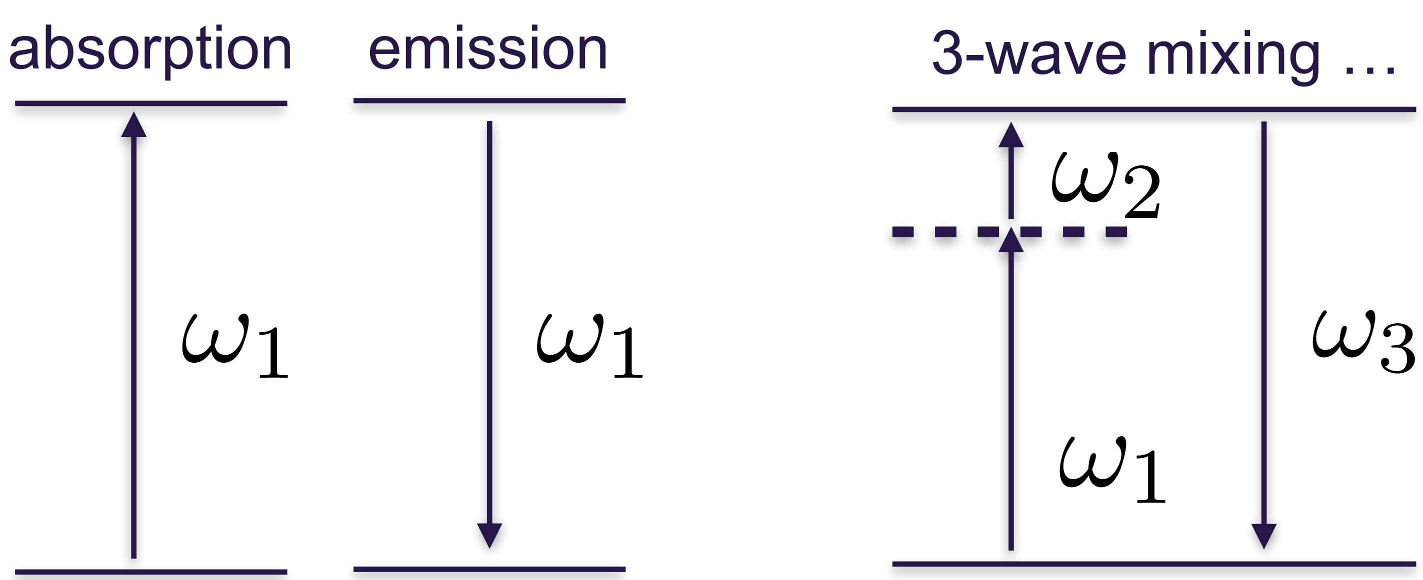

Wave mixing in response theory

$$\boldsymbol{P}(t) = \varepsilon_0 \left(\chi^{(1)} + \chi^{(2)} \boldsymbol{E}(t) + \chi^{(3)} \boldsymbol{E}^2(t) + \cdots \right) \boldsymbol{E}(t)$$

$$P^{(1)}(\omega_2) = \varepsilon_0 \chi^{(1)}(\omega_2 = \pm\omega_1) E(\omega_1)$$

$$P^{(2)}(\omega_3) = \varepsilon_0 \chi^{(2)}(\omega_3, \pm\omega_2, \pm\omega_1) E(\omega_2) E(\omega_1)$$

$$P^{(3)}(\omega_4) = \varepsilon_0 \chi^{(3)}(\omega_4, \omega_3\pm, \omega_2\pm, \omega_1\pm) E(\omega_3) E(\omega_2) E(\omega_1)$$

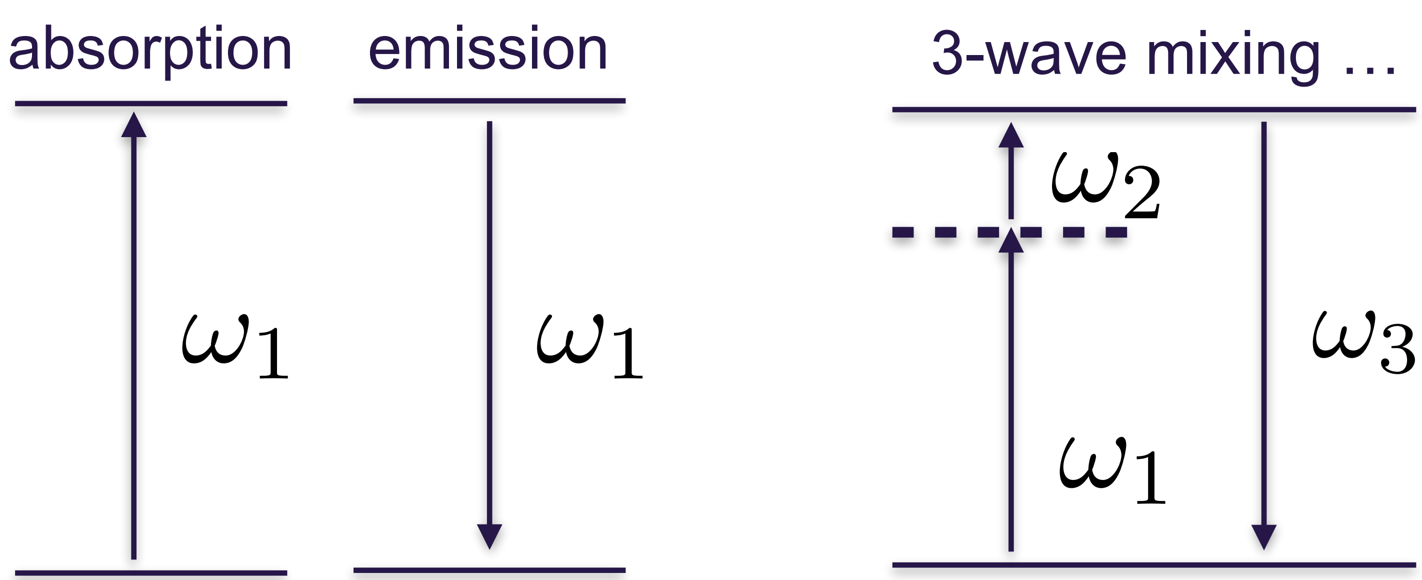

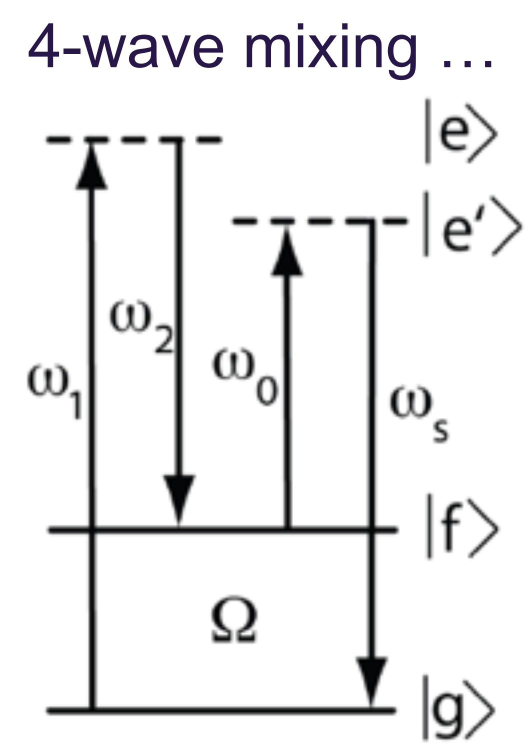

Three wave mixing: Second harmonic generation in diamond

PRL **112**, 163901 (2014) PHYSICAL REVIEW LETTERS week ending 25 APRIL 2014

X-Ray Second Harmonic Generation

S. Shwartz,[1,2,*] M. Fuchs,[3,4] J. B. Hastings,[5] Y. Inubushi,[6] T. Ishikawa,[6] T. Katayama,[7] D. A. Reis,[3,8] T. Sato,[6] K. Tono,[7] M. Yabashi,[6] S. Yudovich,[1] and S. E. Harris[2]

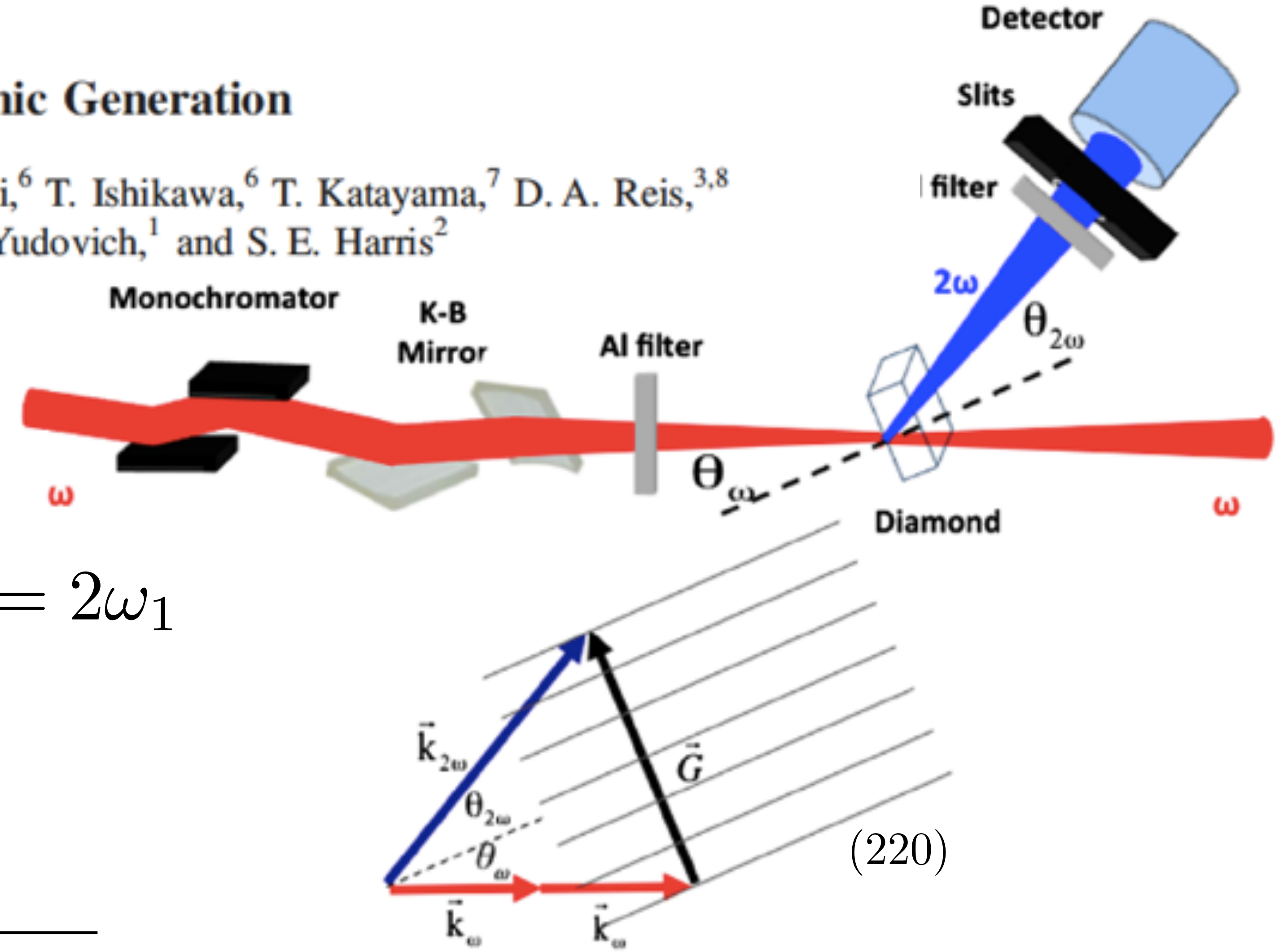

$$I = 1 \times 10^{16} \frac{\mathrm{W}}{\mathrm{cm}^2}$$

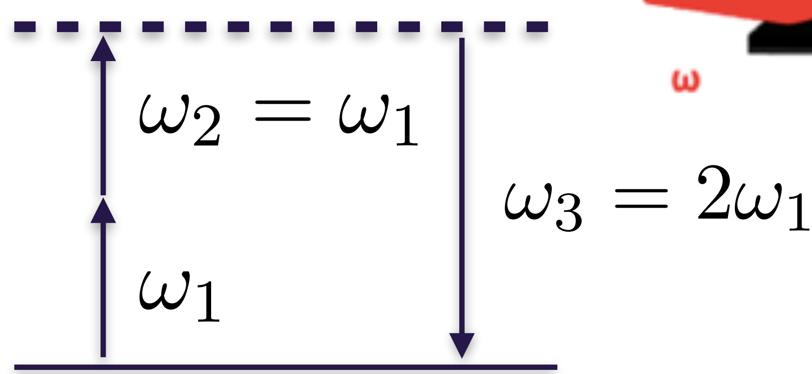

$$\chi^2(7.3\mathrm{keV}) \approx \sqrt{\nu_{\mathrm{eff}}}/E_{\omega 1} = \sqrt{\frac{I_{\mathrm{SHG}}}{I_{\omega 1}}}/E_{\omega 1}$$

$$= 5.8 \times 10^{-11}/2.5 \times 10^9 \frac{\mathrm{V}}{\mathrm{cm}} = 2.3 \times 10^{-20} \frac{\mathrm{cm}}{\mathrm{V}}$$

Four wave mixing (FWM)

General four wave mixing scheme

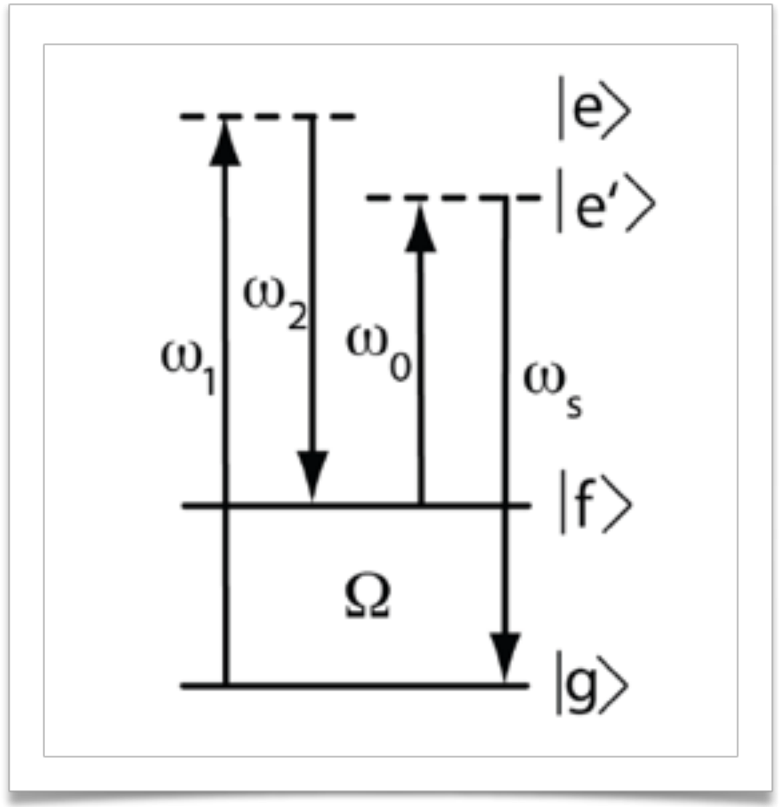

Transient grating spectroscopy

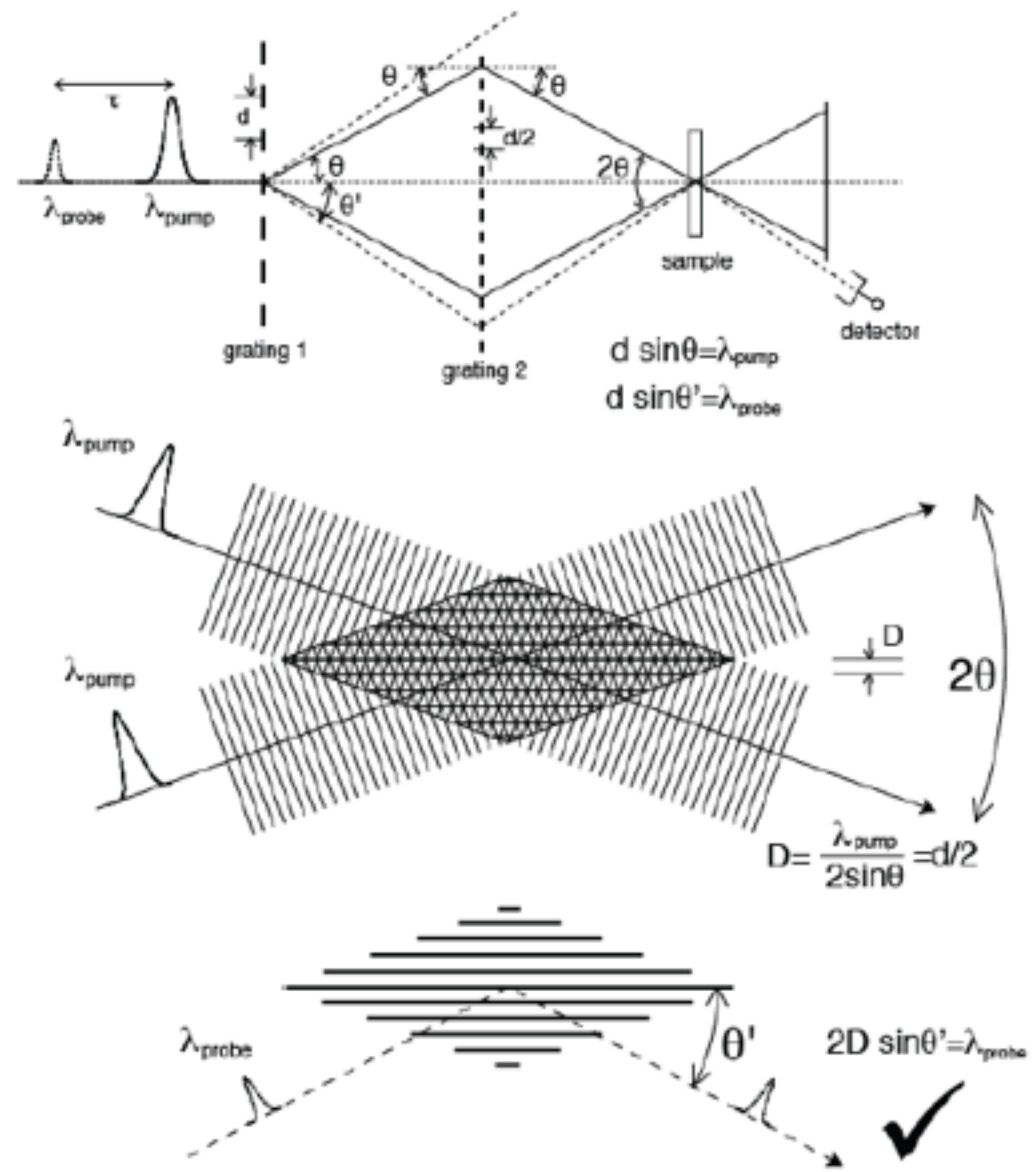

d) resonance Raman scattering (RIXS)

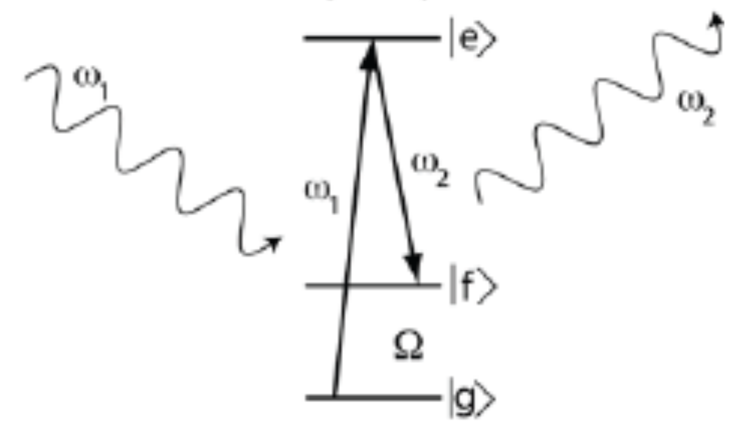

e) stimulated Raman scattering

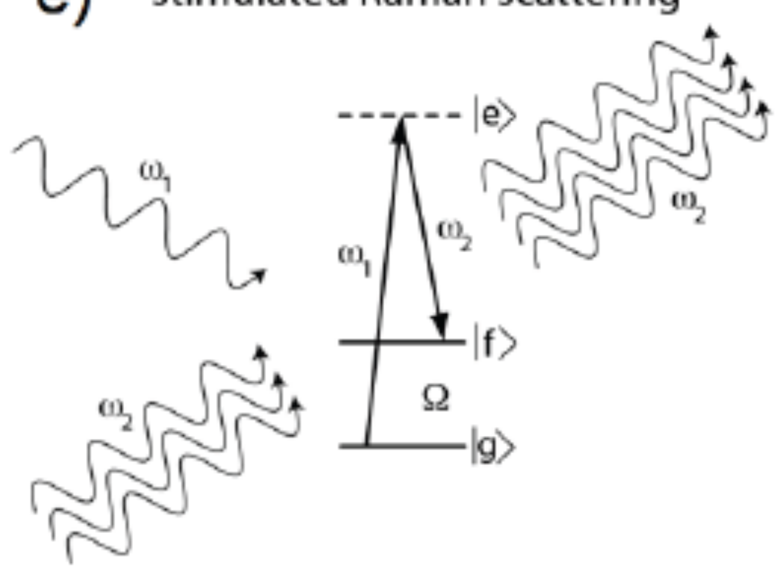

Bruce Patterson, SLAC-TN-10-026 (2010)

Transient grating spectroscopy at XUV wavelengths

LETTER

doi:10.1038/nature14341

Four-wave mixing experiments with extreme ultraviolet transient gratings

F. Bencivenga[1], R. Cucini[1], F. Capotondi[1], A. Battistoni[1,2], R. Mincigrucci[1,3], E. Giangrisostomi[1,2], A. Gessini[1], M. Manfredda[1], I. P. Nikolov[1], E. Pedersoli[1], E. Principi[1], C. Svetina[1,2], P. Parisse[1], F. Casolari[1], M. B. Danailov[1], M. Kiskinova[1] & C. Masciovecchio[1]

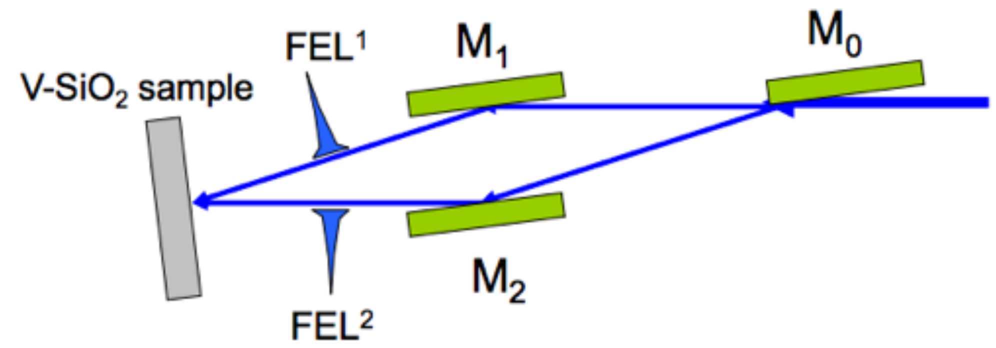

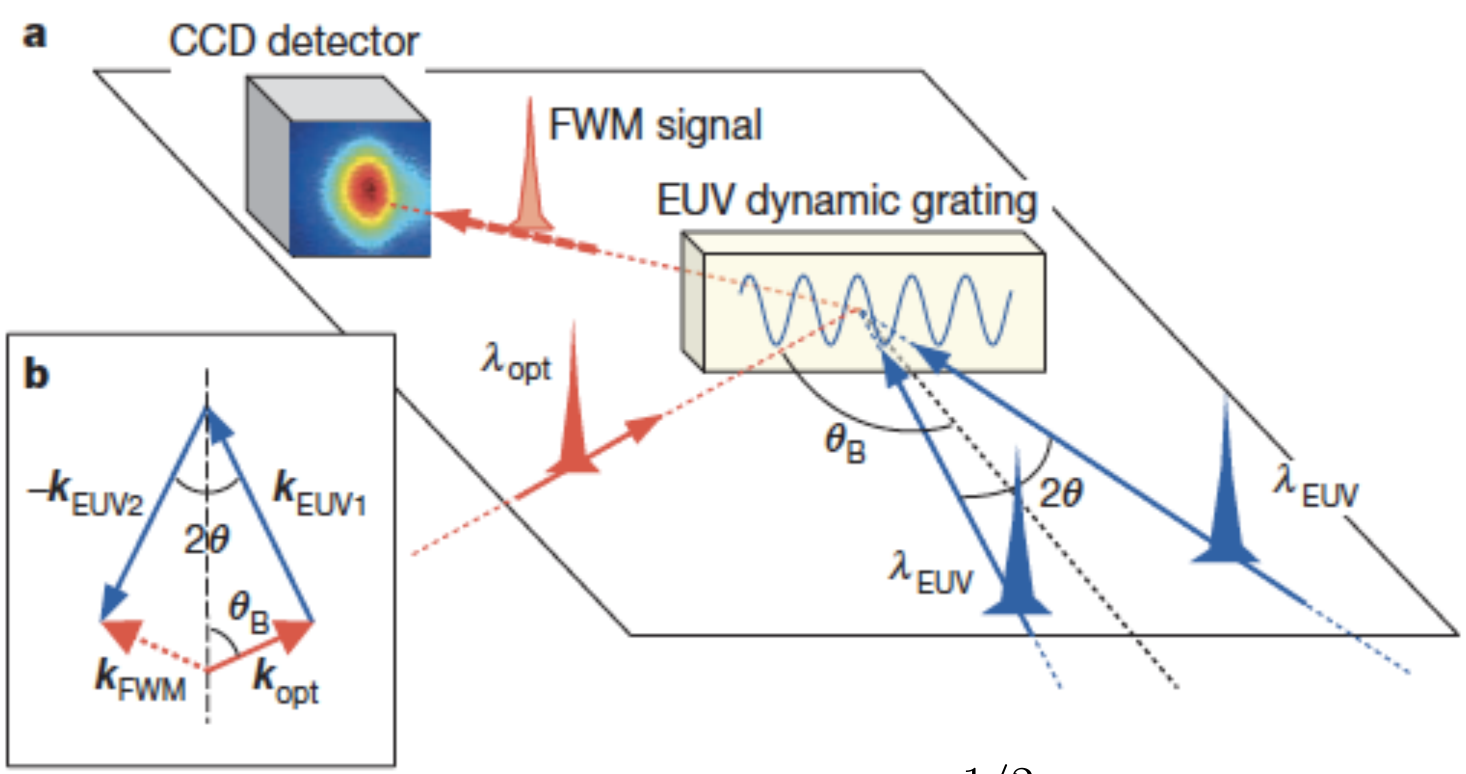

Permanent gratings on SiO_2 (after 1000's shots @ FEL flux > 50 mJ/cm^2)

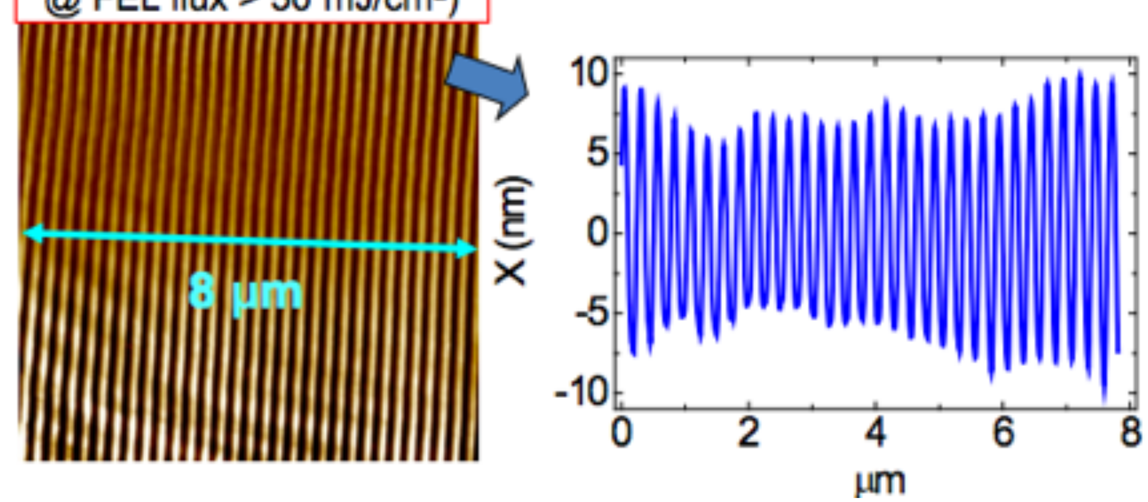

$$\chi^{(3)} = \left(\frac{I_{\rm FWM}}{I_0}\right)^{1/2} / (E_{\rm EUV1} E_{\rm EUV2}) \approx 6 \times 10^{-22} \rm m^2 V^{-2}$$

Impulsively-driven coherent lattice dynamics

Transient Grating Experiments on V-SiO_2

Elettra Sincrotrone Trieste

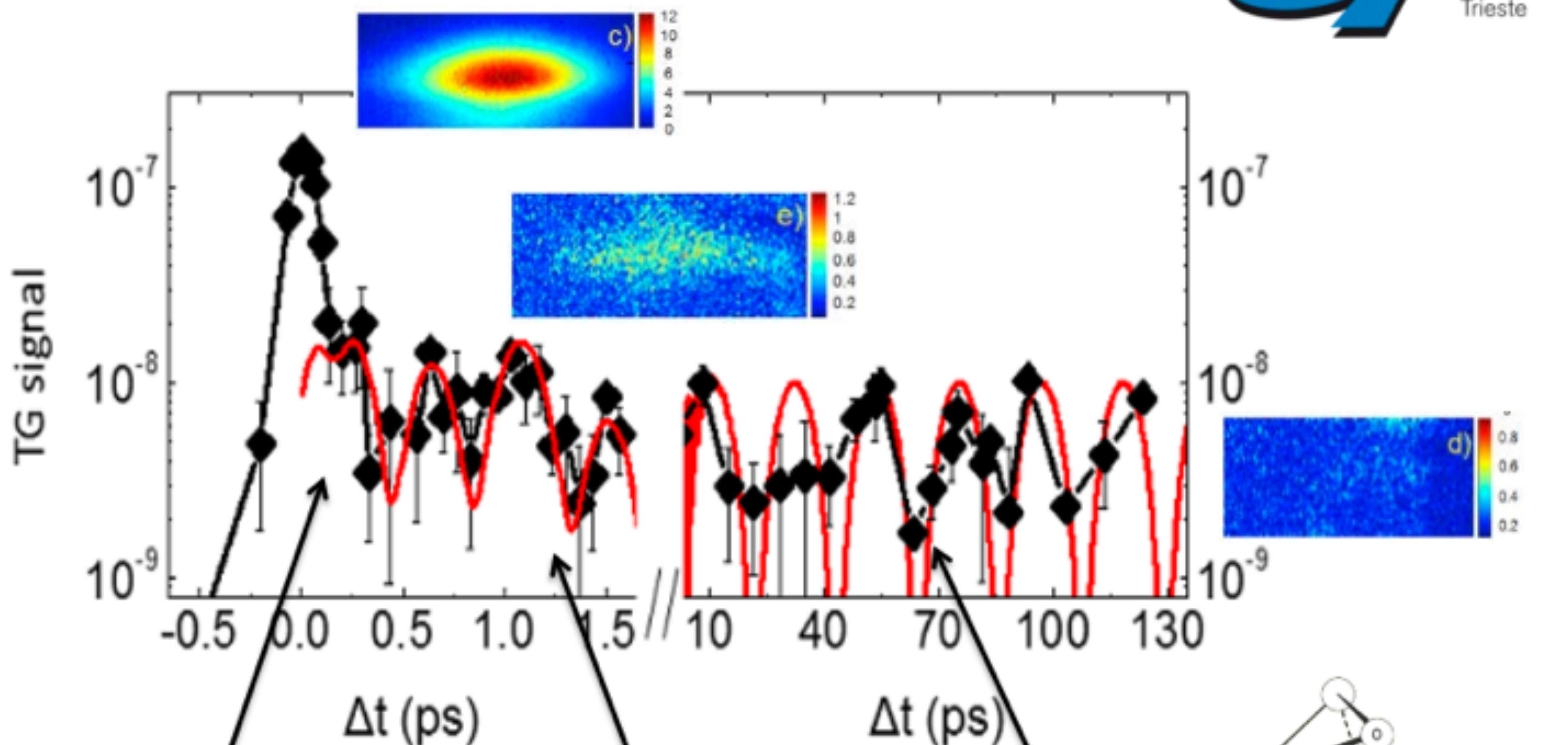

Hyper - Raman modes due to coupled tetrahedral rotations $\nu_2 \approx 4.1$ THz

Raman modes due to tetrahedral bending $\nu_1 \approx 1.2$ THz

Acoustic-like excitations

Courtesy C. Masciovecchio

Two colour pulses schemes at XFEL's

Multicolor at FERMI

Elettra Sincrotrone Trieste

nature COMMUNICATIONS

E. Allaria et al.,(2013)

Received 24 May 2013 | Accepted 21 Aug 2013 | Published 18 Sep 2013 DOI: 10.1038/ncomms3476 OPEN

Two-colour pump-probe experiments with a twin-pulse-seed extreme ultraviolet free-electron laser

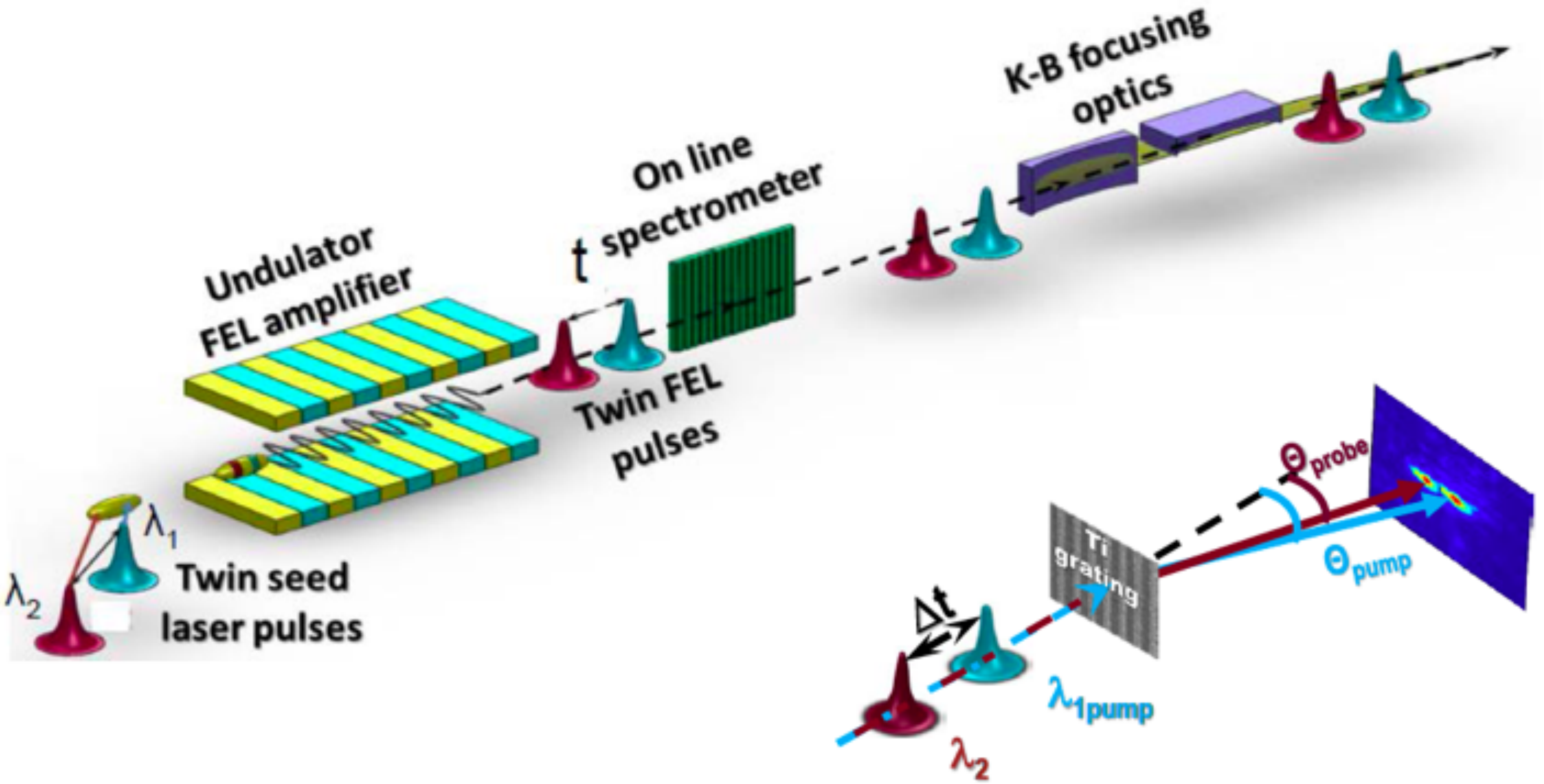

Courtesy C. Masciovecchio

CARS scheme using two-colour pulses from the machine and a x-ray split & delay line

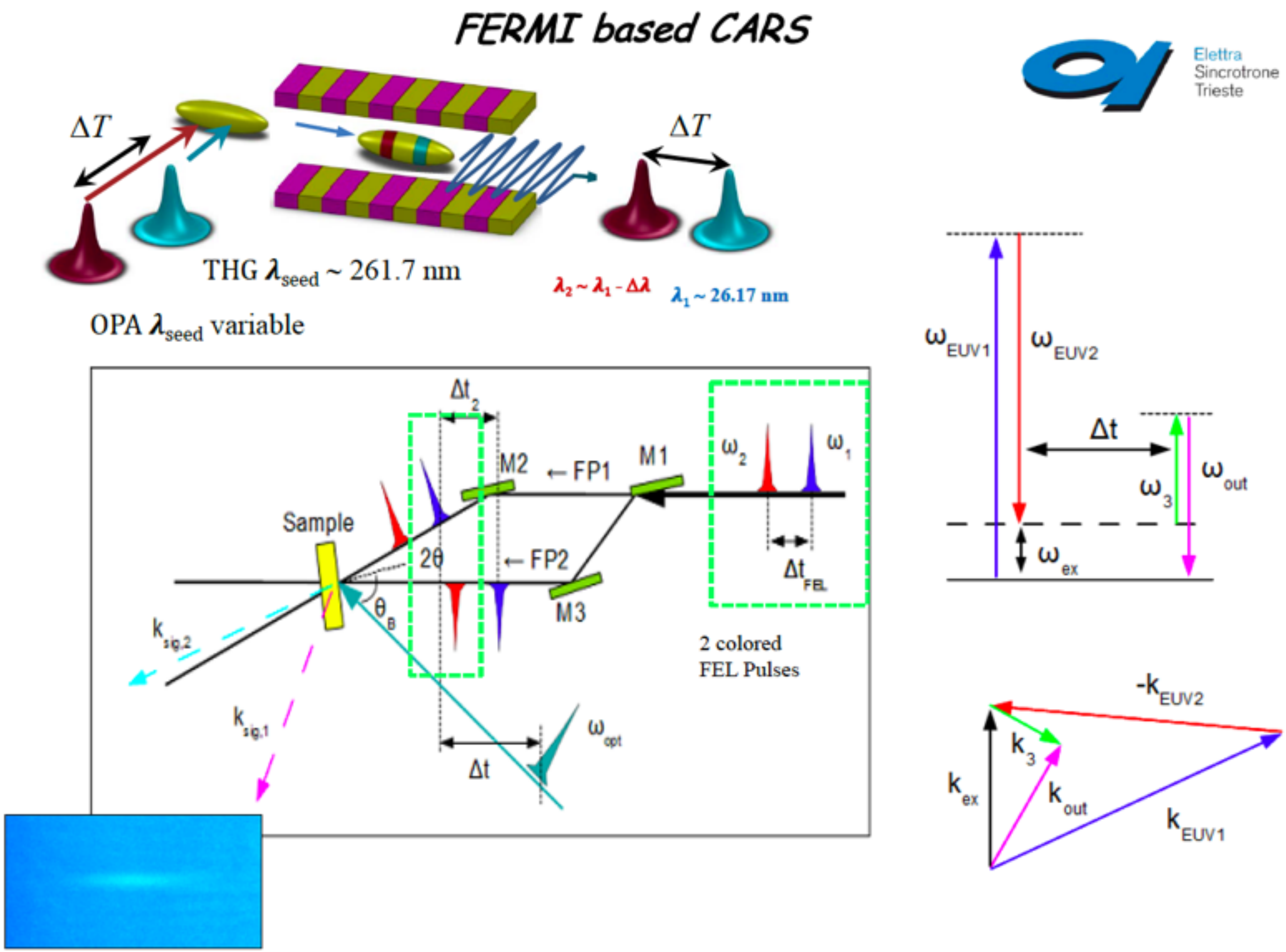

Courtesy C. Masciovecchio

Beyond CARS
Coherent X-ray Raman spectroscopy

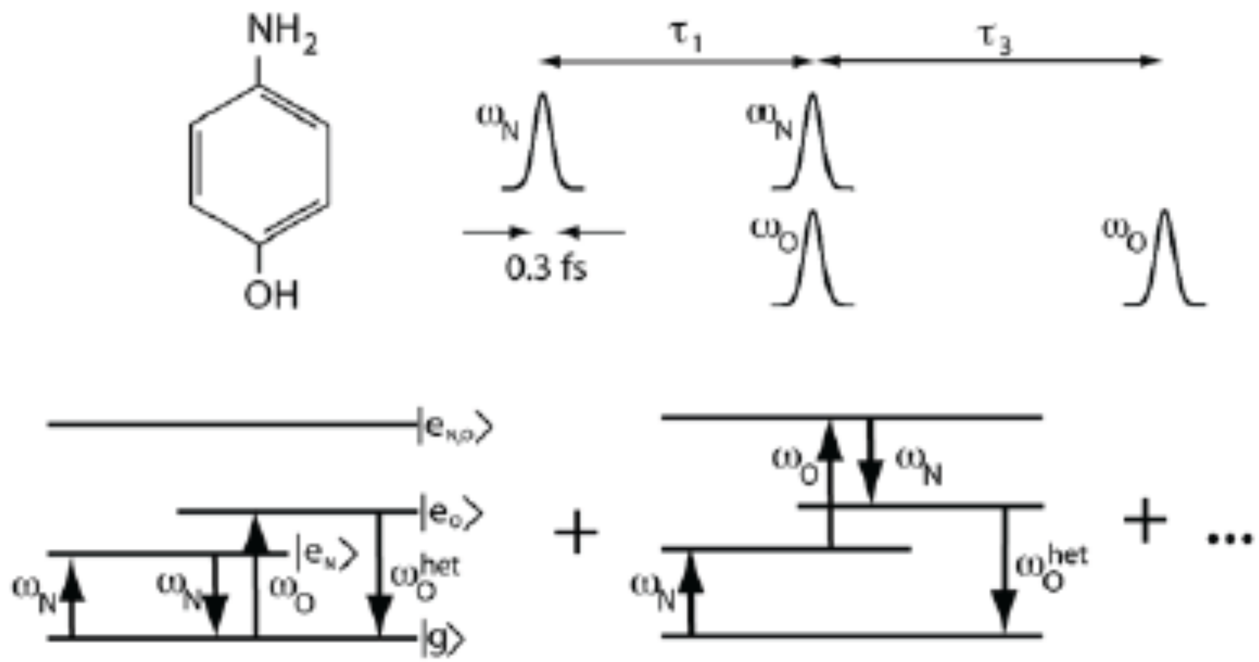

$$S(\Omega_1,\Omega_3) = \int d\tau_1 e^{i\Omega_1\tau_1} \int d\tau_3 e^{i\Omega_3\tau_3} I_O^{het}(\tau_1,\tau_3)$$

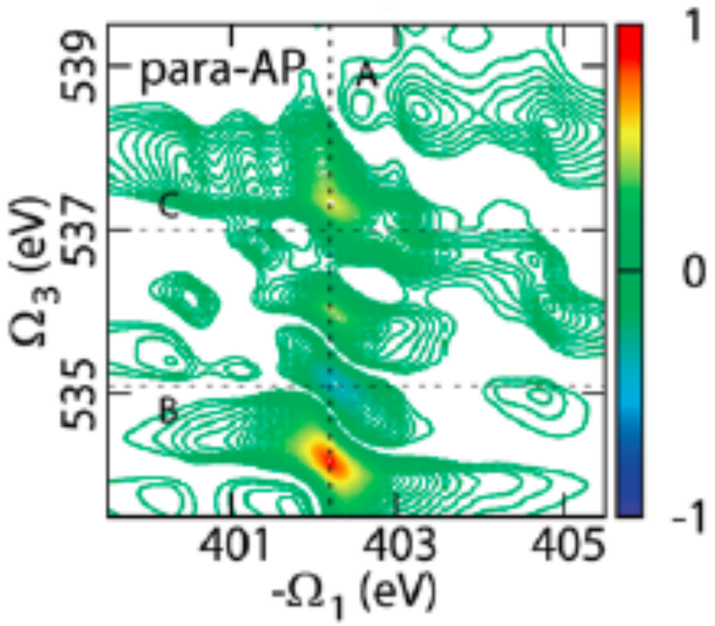

Tanaka, Mukamel, PRL 89, 043001

Acknowledgement

SCS team

Robert Carley
SCS Instrument Scientist

Carsten Broers
SCS Technician

Jan Torben Delitz
SCS Instrument Engineer

Manuel Izquierdo
SCS Instrument Scientist

Loic Le Guyader
Peter Paul Ewald fellowship
VolkswagenStiftung

Komal Khandelwal
SCS Student assistant

Justine Schlappa
SCS Instrument Scientist

Alexander Sorin
SCS Student assistant

Alexander Yaroslavtsev
SCS Staff Scientist

Summary

Part 1 (Tuesday)

- Spectroscopy and Microscopy
- XFEL and SASE radiation
- Stimulated emission
- nonlinear response at x-ray energies

Part 2 (Wednesday)

- Nonlinear absorption
- Three-wave mixing
- Four-wave mixing

END